Application of green nanoscience to olive polyphenols: Formulation design and biological evaluation of oleuropein-loaded nanostructured lipid carriers.

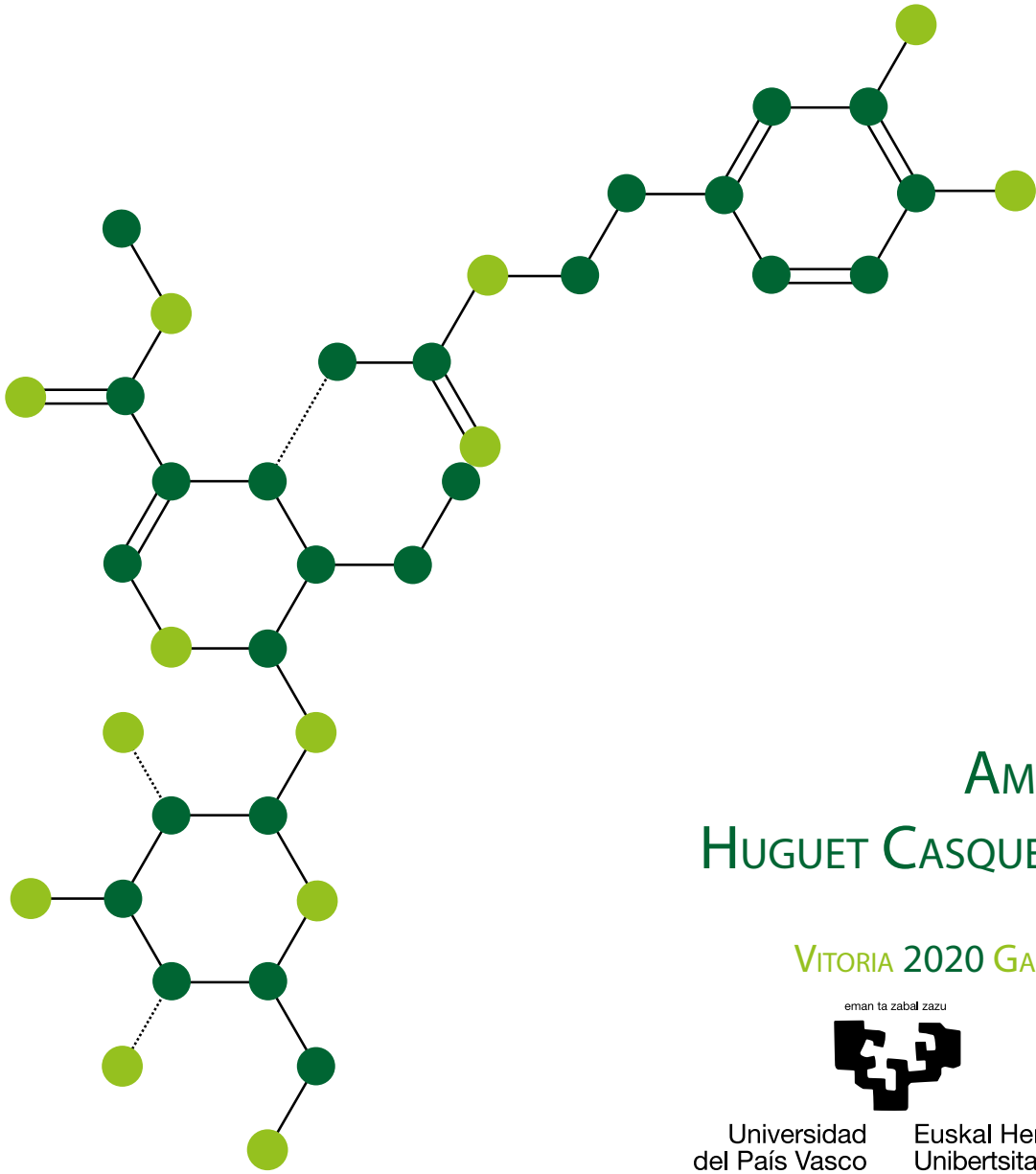

Amaia Huguet Casquero

Vitoria 2020 Gasteiz

eman ta zabal zazu

Universidad del País Vasco

Euskal Herriko Unibertsitatea

Universidad del País Vasco Euskal Herriko Unibertsitatea

NAZIOARTEKO BIKAINTASUN CAMPUSA
CAMPUS DE EXCELENCIA INTERNACIONAL

Application of Green Nanoscience to olive polyphenols: Formulation design and biological evaluation of oleuropein-loaded nanostructured lipid carriers

Amaia Huguet Casquero

Vitoria-Gasteiz, 2020

NanoBioCel
Micro and Nano technologies, Biomaterials and Cells Research Group

NanoBioCel group

Laboratory of Pharmaceutics, School of Pharmacy

University of the Basque Country (UPV/EHU)

BIOSASUN

Biosasun S.A.

Research & Development department

Agradecimientos

Parece mentira lo rápido que pueden pasar cuatro años, diría que fue ayer cuando me llamaron para darme la noticia de que nos habían concedido la ayuda para hacer el Doctorado Industrial y el vértigo que me dio pensar en cómo podría asumir todo lo que me venía por delante. Pero al fin, más pronto que tarde y con una pandemia en el último tramo… ¡lo hemos conseguido!

Y digo "hemos" porque hasta aquí una no llega sola.

En primer lugar, quiero agradecer el apoyo que he recibido por parte de mi familia. A mi madre, porque me animaste a adentrarme en esta aventura y me has apoyado desde el principio hasta el final. Porque siempre me has transmitido que con esfuerzo y empeño se puede llegar muy lejos. A mi padre, que junto con mi madre habéis apostado fuerte por la educación de vuestros hijos y gracias a ello hemos llegado tanto Álvaro como yo hasta donde estamos. A mi hermanico, Álvaro, por estar siempre ahí. A Estíbaliz, Germán, Vero y Mikel mi familia en Gasteiz. Mikel, por supuesto, gracias por aceptar sin pensarlo el diseñarme la portada ¡en tiempo record! A ti, Josu, mi compañero de viaje, porque al fin y al cabo eres el que ha sufrido mis idas y venidas con la tesis 365 días al año durante todo este tiempo, y siempre me has mostrado tu ilusión porque me convierta en la "doctora Huguet". A todos, ¡gracias!

Por supuesto, también quiero dar las gracias al el equipo de Biosasun, a todo el grupo de investigación Nanobiocel y el Departamento de Farmacia y Ciencias de los Alimentos. A mis directores de tesis por haberme guiado en la realización de este trabajo. Eusebio, todavía recuerdo con cariño el primer día que nos reunimos para hablar sobre mis posibles prácticas de máster. Ahí empezó todo. Me acogiste con los brazos abiertos para colaborar en un proyecto y gracias a ello me adentré en el mundo de la investigación. A Jose Luis, por acogerme en el Grupo Nanobiocel, por la comprensión y apoyo que he recibido de tu parte durante todo este tiempo.

Gracias también a todas mis compañeras y compañeros del laboratorio, amigas y amigos. Claudia, hemos ido en paralelo en esta aventura y nos hemos apoyado mucho la una en la otra. María, por todas esas horas en cultivos celulares… ¡volviéndonos locas ajustando tiempos entre ensayos! Tania, ¡mi fiel compañera de congresos! por transmitirme ese entusiasmo que tienes por la ciencia y la investigación y toda esa energía positiva que desprendes! Aiala, Sara, Itxaso… por los descansitos en la cafe. Enara, gracias por tu apoyo, comprensión y ayuda durante todos estos años en los que he tenido que combinar los proyectos en los que colaborábamos junto con la tesis. Ya te lo he dicho muchas veces, y es que trabajar contigo es un lujo, hemos formado un gran equipo y nos hemos dado apoyo la una a la otra cuando

lo hemos necesitado. Gracias también por haberme puesto en contacto con Ana Beloqui, y apoyarme para que me fuera de estancia. Precisamente gracias también a Ana Beloqui, por haberme acogido en su grupo de laboratorio del LDRI y haberme guiado y ayudado durante los tres meses que pasé allí en Bruselas, ¡a pesar de que estabas ya embarazadísima! Thank you to all the people that I met there. Yining, thank you for your help during my worst day at the lab… without Ana and you the last day of the in vivo would have been a disaster! Nikos, Elia and Xiao… my lunch team! Y aunque llegaste en mi último mes de estancia… gracias Cecilia fuiste un chute de energía, felicidad y… chocolate! Gracias también a mi "spanish group" fuera del laboratorio, Angye, Bárbara, Sara, Jaime, Doua…. Las escapadas de fin de semana, montarnos en un tren sin tener claro dónde iba… Tres meses es poco tiempo pero traigo muy buenos recuerdos! A big thank you also to my "family" from Brussels. Nathalie, my sister (and landlord!) there, it was such a discovery to meet you and your friends! Anne et André, merci pour votre aide. À bientôt!

Gracias a mi cuadrilla de Tudela, las de siempre, Leire S, Gartz, Eguz, Itzi, Olaia, Leire Kai... que aunque algunas todavía no sabéis exactamente a qué me dedico se que os esforzáis por saberlo! A mi gente de Gasteiz, a los que os tengo por Iruña (Ana, Iratxe, Vio…), por Barcelona (Alberto…), a todos los que me habéis seguido de alguna forma en este proyecto.

¡MUCHAS GRACIAS1

ESKERRIK ASKO!

THANK YOU!

MERCI BEAUCOUP!

ACKNOWLEDGEMENTS TO THE FINANCIAL SUPPORT

Amaia Huguet Casquero gratefully acknowledges the Spanish and Competitiveness for the Industrial Doctorate fellowship grant (DI-15-07513). This thesis was conducted under the R&D projects of BIOSASUN and supported by the University of the Basque Country (UPV/EHU) and the Basque Country Government (Consolidated Groups, No. IT907-16).

ACKNOWLEDGEMENTS TO THE EDITORIALS

Authors would like to thank the editorials for granting permission to reuse the published articles in this thesis. The published articles can be accessed at the following links:

Huguet-Casquero et al. Green Chem., 2020,22, 3495-3505

https://doi.org/10.1039/D0GC00965B

Huguet-Casquero et al. Pharmaceutics. 2020; 12(5):429.

https://doi.org/10.3390/pharmaceutics12050429

Huguet-Casquero et al. Int J Pharm. 2020 Jun 13;586:119515

https://doi.org/10.1016/j.ijpharm.2020.119515

The introduction chapter "*Towards green nanoscience: from extraction to nanoformulation*" has been already submitted to Biotechnological Advances (Manuscript ID JBA-D-20-00449).

A mis padres, Mariuca y Carlos,
a mi hermano, Álvaro y a ti, Josu.

"Defiende tu derecho a pensar, porque incluso pensar de manera errónea es mejor que no pensar"

Hipatia de Alejandría

Glossary

ABAP	2,2′-azobis (2-amidinopropane)
Abs	absorbance
ACN	acetonitrile
ANOVA	analysis of variance
BCA	bicinchoninic acid assay
BEBM	bronchial epithelial cell growth basal medium
BEGM	bronchial epithelial growth medium
BSA	bovine serum albumin
CCK-8	cell counting kit 8
CD	Crohn's disease
CFTR	cystic fibrosis transmembrane conductance regulator
CI	crystallinity index
DAD	diode array detector
DCF	dichlorofluorescein
DCFH-DA	2′,7′-dichlorodihydrofluorescein diacetate
DDS	drug delivery systems
DES	deep eutectic solvents
DLS	dynamic light scattering
DMSO	dimethyl sulfoxide
DPBS	Dulbecco's phosphate buffered saline
DPPH	2,2-diphenyl-1-picrylhydrazyl
DSC	differential scanning calorimetry
DSS	dextran sulfate sodium
EAT	Environmental Assessment Tool
EDTA	ethylenediaminetetraacetic acid
EE	encapsulation efficiency
EFSA	European Food Safety Authority
EGCG	epigallocatechin gallate
EGP	egg phosphatidylcholine
EMA	European Medicines Agency
EVOO	extra virgin olive oil
EVOO-ph	extra virgin olive oil rich in polyphenols
FBS	fetal bovine serum
FDA	Food and Drug Administration
FU	fluorescent intensity units
GIT	gastrointestinal tract
GRAS	generally recognized as safe
H_2O	water
H_2O_2	hydrogen peroxide

HDPE	high density polyethylene
HEPES	n-2-hydroxyethylpiperazine-n-2-ethane sulfonic acid
HME	hot melt emulsification
HPH	high pressure homogenization
HPLC	high performance liquid chromatography
HPMC	hydroxypropylmethylcellulose
HTAB	hexadecyltrimethylammonium bromide
IBD	inflammatory bowel diseases
IL-1β	interleukin-1β
IL-17	interleukin-17
IL-6	interleukin-6
k'	capacity factor
LNC	lipid nanocapsule
LOD	limit of detection
LOQ	limit of quantification
LPS	lipopolysaccharide
MCT	medium chain triglycerides
MeOH	methanol
MPO	myeloperoxidase
MWCO	molecular weight cut-off
N	number of theoretical plates
NaCas	sodium caseinate
NF-κB	nuclear factor κb
NLC	nanostructured lipid carrier
NLC-OLE	oleuropein loaded nanostructured lipid carrier
NP	nanoparticle
OLE	oleuropein
OVA	ovalbumin
PBS	phosphate buffered saline
PDI	polydispersity index
PEF	pulsed electric fields
PEG	polyethylene glycol
PEST	penicillin-streptomycin
PIT	phase inversion temperature
PLA	poly (d-l-lactic acid)
PLGA	poly(glycolic acid)
PVDF	polyvinylidene fluoride
r^2	regression coefficient
ROS	reactive oxygen species
RPMI 1640	Roswell park memorial institute 1640 medium
Rs	resolution

RSD	relative standard deviation
R_T	retention time
RP-HPLC-DAD	reverse phase high performance liquid chromatography coupled with diode array detector
RSD	relative standard deviation
SAA	supercritical assisted atomization
SAILA	supercritical assisted injection in a liquid antisolvent
SAS	supercritical antisolvent
$ScCO_2$	supercritical carbon dioxide
SCF	supercritical fluid
SD	standard deviation
SEDS	solution-enhanced dispersion by supercritical fluids
SEM	standard error of the mean
SLN	solid lipid nanoparticle
T	tailing factor
T80	tween 80
T20	twee 20
TA	tannic acid
TEM	transmission electron microscope
TNF-α	tumor necrosis factor-alpha
TPGS	α-tocopheryl polyethylene glycol 1000 succinate
TPP	tripolyphosphate
UC	ulcerative colitis

Index

Experimental section

Chapter 1

Development and validation of an eco-friendly HPLC-DAD method for the determination of oleuropein and its applicability to several matrices: olive oil, olive leaf extracts and nanostructured lipid carriers

Green Chemistry, 2020,22, 3495-3505.

DOI: https://doi.org/10.1039/D0GC00965B

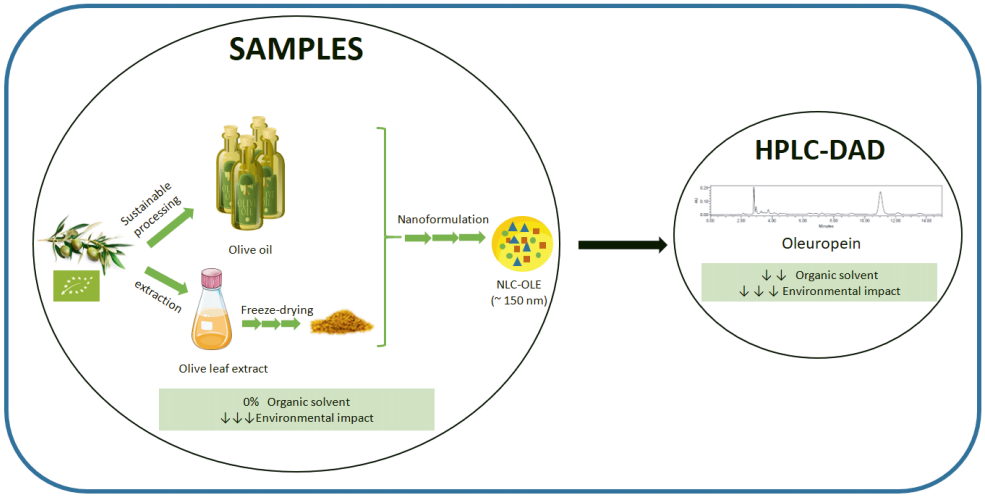

Development and validation of an eco-friendly HPLC-DAD method for the determination of oleuropein and its applicability to several matrices: olive oil, olive leaf extracts and nanostructured lipid carriers

Amaia Huguet-Casquero[a,b], Tania Belén López-Méndez[a], Eusebio Gainza[b], Jose Luis Pedraz[a,c]*

[a] NanoBioCel Group, Laboratory of Pharmaceutics, School of Pharmacy, University of the Basque Country (UPV/EHU), Spain.

[b] Biosasun S.A., Iturralde 10, Etxabarri-Ibiña, Zigoitia, 01006, Spain.

[c] Biomedical Research Networking Centre in Bioengineering, Biomaterials and Nanomedicine (CIBER-BBN), Spain.

* Corresponding author: Jose Luis Pedraz.

ABSTRACT

Oleuropein is a natural ingredient largely used in nutritional supplements. This study reports on the development, validation and application of an HPLC method based on UV-vis detection for determining oleuropein in olive oil, olive leaf extracts and nanoparticles. The principles of Green Chemistry were taken into account for both the samples manufacturing and HPLC method development. A Zorbax C18 column was used on which a mobile phase containing acetonitrile-water was applied in isocratic elution mode injecting 10 µl of sample at 1.2 ml/min constant flow-rate, 30ºC temperature and 15 minutes run time. Method linearity (r2>0.999) was assessed in the range of 50 to 420 µg/ml. Precision expressed by RSD% was always better than 2%. Accuracy was in all cases within 98-102% of the expected concentration value. The sensitivity of the method was at the level of 0.08 µg/ml as limit of detection and at 0.25 µg/ml as limit of quantification. The results witness that the method is suitable for the quantification of oleuropein in a variety of samples with reduced environmental impact.

1. Introduction

Olives and their juice are considered the cornerstone of the Mediterranean diet, which has been historically linked with the higher longevity and the reduced incidence of some chronic diseases in the Mediterranean population. These health benefits have been attributed by the scientific evidence to some of the 20 types of olive polyphenols found in olive trees[1]. Among these, oleuropein (OLE) (Figure 1), the major constituent of the sercoiridoid family, has gained special attention. Mainly due to its hydrophilic nature as well as other factors (i.e. olive harvesting time, processing method) it is normally found in high quantities in olive leaf (*Olea europaea* L.) but lower (sub-ppm) in olive oil.[2-4] Apart from being considered one of the main responsible for the organoleptic properties of food it is also used for chemical standardization of marketed olive-derived products (i.e. olive leaf extracts, supplements and olive oil). Beyond this, several pharmacological benefits have been attributed to this natural polyphenol during the last decades. Even the European Medicines Agency (EMA) and the European Food Safety Authority (EFSA) have emitted their own assessment reports about its health-promoting properties in human health.[5,6] In particular, OLE has been reported to exert antiinflamatory,[7] platelet anti-aggregant,[8] antimicrobial,[9] hypoglycemic,[10] anticancer,[11,12] antiviral,[13] hypolipidimic,[14] antioxidant and neuroprotective[15] effects among others. Literature offers a long list of other natural compounds that have also been proved to possess important pharmacological activities.[16] All these evidence, together with the recently increased environmental awareness, have promoted a trend towards the consumption of natural-origin products and thus, the use of bioactive compounds like olive polyphenols has gained the attention of the pharmaceutical, food and chemical industries. Most of these natural molecules are obtained from agro-industrial waste through extraction processes in which not only the high energy consumption but also the use of large amount of organic solvents contribute to its overall environmental impact. Therefore, both from a toxico-pharmacological and ecofriendly point of view, those harmful aspects should be minimized through the application of green chemistry.

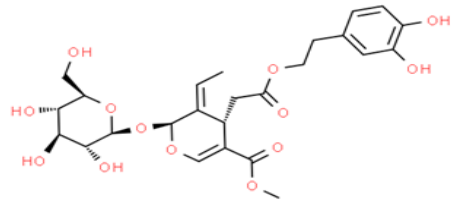

Figure 1. Oleuropein.

Another issue that must be addressed to achieve the required properties of olive polyphenol based by-products is their lability against both external and systemic factors. Specifically, OLE is rapidly degraded after light and oxygen exposure and once in the human organism its bioavailability is compromised

by enzymatic degradation and limited absorption in the target site.[17-19]

Taking into account the aforementioned facts, polymeric and lipid-based nanoparticles have been proposed as innovative drug delivery systems (DDS) that could protect and improve the efficacy of the encapsulated compounds until their release in the target site. Among these DDS, nanostructured lipid carriers (NLC) offer several advantages such as the avoidance of organic solvents during the manufacturing process, higher drug loading, long-term stability and scaling-up feasibility.[20,21] In order to determine the yield of the nanoformulation process, the amount of encapsulated drug should be quantified and thus, precise analytical methods are needed.

High performance liquid chromatography (HPLC) coupled with diode array detector (DAD) is one of the most common analytical methods in pharmaceutical and food industries for routine quantification analysis. More specifically, reverse phase (RP)-HPLC has emerged as a sensitive, rapid and accurate technique that allows the separation and determination of analytes in several nutraceutical and pharmaceutical forms including nanoparticles.

As a result, several HPLC methods have been reported for OLE quantification in olive leaf and olive leaf extracts,[22,23] olive oil,[24,25] olive stems and roots,[4] olive pomace and fruit.[26] However, they have some limitations such as the use of large amounts of organic solvents due to long analysis time, lack of validation results, more complex methods using gradients and mass detectors, tedious sample preparation techniques and lack of method applicability for the quantification of oleuropein in nanoparticle formulations.

Taking the aforementioned, the goal of the present work was to validate a rapid and versatile RP-HPLC-DAD method for the determination of OLE in olive oil, olive leaf extracts and nanoparticles obtained through eco-friendly processes.

2. Materials and Methods

2.1. Materials

An oleuropein reference standard (>98% purity) was purchased from Sigma-Aldrich (St Louis, MO). Oleuropein (>80% purity) for nanoencapsulation was kindly donated by Nonaherbs Bio (Tech) (China). Olive leaf, organic extra virgin olive oil (EVOO) and organic extra virgin olive oil rich in olive polyphenols

(EVOO-ph) were donated by Biosasun S.A. (Álava, Spain). HPLC-grade methanol (MeOH), acetonitrile (ACN) and ortophosphoric acid (85%) were purchased from Scharlab®. Water (H_2O) was purified in a Milli-Q Plus system (Millipore®) with a conductivity of 18.2 MÙ.cm at 25°C. Precirol® ATO 5 (Glycerol distearate) was a kind gift from Gattefosé (France). Polysorbate, Tween®80 was purchased from Panreac Química (Castellar del Vallès, Barcelona, Spain). Poloxamer 188 was kindly provided by Merck (Darmstadt, Germany). All other reagents and solvents used in this study were of analytical grade.

2.2. Instrumentation

A Waters 2795 Alliance HPLC system (Waters Corporation, Milford, MA, USA) equipped with a binary HPLC pump (Waters 2487), a diode array detector (Waters 2489), a column oven (Waters Column Heater Module), and an auto sampler (Waters 717 plus Autosampler) was used. Data acquisition, analysis and reporting were performed using Empower 2 chromatography software (Milford, MA, USA). Analysis was performed using a Zorbax® C18 column (Agilent, Wilmington, DE, USA) with 5 µm in particle size, 4.6 mm in internal diameter and 250 mm in length.

2.3. Chromatographic conditions

Separation of OLE was performed on isocratic mode with a mobile phase consisting of a mixture of ACN-H_2O (20:80, v/v). The pH of the mobile phase was adjusted to 3.0 using ortophosphoric acid. Mobile phase was degassed in an ultrasonic bath for 15 minutes before analysis. The analysis was carried out at 1.2 mL/min flow rate with a detection wavelength of 230 nm and the injection volume was arranged as 10 µL. Column temperature was set to 30ºC. Method run time was 15 min. All tested samples were filtered through a 0.45µm pore-size polyvinylidene fluoride (PVDF, Scharlau®) filter prior to analysis. Each working day injection was carried out after pre-conditioning of the column at the optimized temperature (30ºC) and flow rate for 15 min.

2.4. Preparation of standard solutions

Standards were prepared in deionized water and filtered through a 0.45µm pore size PVDF-filter before injection. All standards were protected from light. A stock standard solution of 1 mg/ml was prepared in Milli-Q water. Seven working standard solutions (50, 75, 100, 280, 350, 385 and 420 µg/ml) were prepared by diluting in Milli-Q water the corresponding aliquots of stock standard solution in 5ml amber volumetric flasks.

2.5. System Suitability

System suitability testing is essential for the assurance of the quality performance of the chromatographic system. For this purpose, six replicates of the OLE reference standard at a concentration of 280 µg/ml was analyzed. System performance and chromatographic parameters such as the number of theoretical plates (N), tailing factor (T), resolution (Rs) and capacity factor (k') were taken into consideration.

2.6. Method Validation

The analytical method for quantification of OLE was validated according to the International Conference on Harmonization (ICH) guidelines Q2 (R1)[27] in terms of specificity, selectivity, linearity, range, precision, accuracy, limit of detection (LOD) and limit of quantification (LOQ).

2.6.1. Linearity

Linearity was determined in seven different concentration levels (50, 75, 100, 280, 350, 385 and 420 µg/mL). Experiments were carried out in triplicate. Peak areas were plotted against the analyte concentration to obtain a regression line. Linear calibration function was fitted by least-squares methodology.

The range of the method was validated by checking that the interval between the upper and lower concentration (amounts) of analyte in the sample (including these concentrations) for which it has been demonstrated that the analytical procedure has a suitable level of precision, accuracy and linearity.

2.6.2. Specificity

In order to demonstrate that no interference occurred due to the other sample constituents, specificity test was carried out by comparing the chromatograms obtained from the EVOO hydroalcoholic extraction solution (MeOH-H_2O, 50:50, v/v), deionized water, mobile phase and supernatant of blank nanoparticles (without OLE) with the OLE reference standard solution and samples containing OLE.

2.6.3. LOD and LOQ

In this study a calibration curve was prepared at low concentrations (0.2 µg/mL, 0.4 µg/mL, 0.6 µg/mL, 1 µg/mL and 6 µg/mL). This method can be applied in all cases, and it is most applicable when the analysis method does not involve background noise. It uses a range of low values close to zero for calibration curve, and with a more homogeneous distribution will result in a more relevant assessment.

The LOD and LOQ were assessed by applying the following equations:

$$LOD = 3.3\sigma/S$$

$$LOD = 10\sigma/S$$

Where σ is the standard deviation of the response of ten blank samples and *S* is the slope of the calibration curve.

2.6.4. Precision

Precision is a measure of how close results are to one another. Precision of the method was determined by repeatability (intra-day precision) and intermediate precision (inter-day precision) studies. Intra-day precision was assessed by analyzing three replicates of the standard solutions: at three levels of low (50µg/mL), medium (280 µg/mL) and high (420 µg/mL) concentrations on the same day. Inter-day precision was evaluated through the analysis of three levels of the standard solutions at low (50 µg/mL), medium (280 µg/mL) and high (420 µg/mL) concentration levels in three different days. Results were expressed as relative standard deviation (RSD).

2.6.5. Accuracy

Accuracy is the closeness of the test results obtained by the analytical method to the true value. With this aim and following ICH Q2(R1)[27] recommendations, accuracy of the method was studied by the addition of known amounts of OLE to blank samples, working at the three concentration levels into the linear range previously established for the analyte (50, 280 and 420 µg/ml). From the obtained data the average recovery values of the lowest, intermediate and upper concentration levels were calculated.

2.7. Method Applicability and sample preparation

All samples were prepared by dilution in deionized water with the exception of EVOO and EVOO-ph for which an extraction process was carried out.

2.7.1. Organic extra virgin olive oil rich in polyphenols (EVOO-ph)

Organic *Olea europaea* fruit juice rich in olive polyphenols (EVOO-ph) was obtained from organic olives of Arroniz and Arbequina varieties following the protocols of Biosasun. Briefly, olives were harvested in

early November, when the fruit is yet in a low ripening index, and leaves were discarded. Immediately after, olives were grinded and centrifuged in a horizontal centrifuge (Baby 2-l, Pieralisi MAIP SPA, Zaragoza, Spain) at low temperature (<27ºC). The obtained product was kept in High Density Polyethylene (HDPE) containers for decantation for 2 months at low temperature (<27ºC) and finally, packaged in amber bottles. EVOO was also obtained through the same methodology but only Arroniz variety olives were employed.

With the aim to determine the OLE content in EVOO-ph through the validated HPLC method, it was processed through a simple and rapid method. Briefly, EVOO-ph was subjected to sonication in a water bath for 15 minutes in order to obtain a homogeneous sample. Then, 4 grams of the sample were diluted in 20 ml of a MeOH-H_2O (50:50, v/v) solution and left to mix under magnetic stirring for 4 hours. After that, the obtained solution was filtered through a 0.45µm pore-size PVDF-filter prior to its analysis by the validated HPLC method. As blank-control, pure EVOO was also processed as aforementioned and analysed.

2.7.2. Organic *Olea europaea* L. extracts

Organic olive leaves discarded during the olive oil manufacturing process were used for OLE extraction. Briefly, *Olea europaea* dried leaves (10kg) were ground and introduced into a brew bag. Solid-liquid extraction was conducted by immersing the brew bag into a pre-heated water bath (50L, 80ºC) for 4 hours. After extraction, the aqueous solution of olive polyphenols was stored at 4ºC, protected from light, until use. The *Olea europaea* L. extract was also subjected to a freeze-drying process for 42 hours (Telstar Lyobeta freeze-dryer, Terrasa, Spain). For this purpose, the following drying cycle was programmed: freezing for 3.0 h, primary drying for 12h, and secondary drying for 24 h. The pressure was set to 0.2 mBar during the primary drying. Table 1 summarizes the exact parameters of the process.

Table 1 Freeze-drying process steps for *Olea europaea* L. extracts.

Freeze-drying Step	Temperature (ºC)	Time (hh.mm)	Pressure (mBar)
Freezing	-50	3 h 00 min	-
Chamber vacuum			0.2
Primary Drying	-50	5h 00 min	0.2
	20	7 h 00 min	0.2
Secondary Drying	20	24h 00 min	-

Enumeration of moulds and yeast in the obtained *Olea europaea* L. aqueous and freeze-dried extracts was conducted following the ISO 21527-1:2008 and ISO 21527-2:2008 guidelines.

In order to quantify the OLE content in the obtained aqueous and freeze-dried extracts, they were diluted 1:20 and 1:1 in deionized water, respectively, and filtered through a 0.45µm pore-size PVDF-filter prior to its analysis by the validated HPLC method.

2.7.3. Oleuropein-loaded nanostructured lipid carriers (NLC-OLE)

For OLE nanoencapsulation, a commercial OLE powder (purity >80%, Nonaherbs®) from olive leaves was employed. OLE-loaded nanoparticles were obtained by the hot melt homogenization method as previously described by our group.[28] Briefly, EVOO (liquid at room temperature) and the solid lipid Precirol ATO® 5 (melting point: 56ºC) were mixed and melted 5ºC above the solid lipid melting point until a clear and homogeneous phase was obtained. The aqueous phase was prepared by dispersing Tween® 80 and Poloxamer 188 in purified water. OLE was also dissolved in purified water (0.66 mg/ml). When the lipid phase was melted and the aqueous phase was heated to the same temperature, OLE solution was added to the lipid phase and immediately after, the hot aqueous phase was added to the melted oily phase, and then sonicated at 50 W (Branson Sonifier 250, Danbury, CT, USA). The obtained nanoemulsion was mixed by magnetic stirring at room temperature and then stored for 2 h at 4 ºC to allow the re-crystallization of the lipids and NLC formation. Afterwards, particles were collected using a 100-kDa molecular weight cut-off centrifugal filter unit (Amicon, "Ultracel-100k", Millipore, Spain) by centrifugation at 2500 rpm and washed three times with MillliQ water. The obtained supernatants were collected to determine by HPLC the encapsulation efficiency. Blank-NLCs without OLE were also prepared and used as the control.

OLE content in nanoparticles was assessed by an indirect method. The supernatant obtained from the ultracentrifugation process was diluted 1:10 in water, filtered through a 0.45µm pore-size filter of PVDF-filter and the analyte concentration was determined by the validated HPLC method. Blank-NLCs without OLE were analysed as the control. Encapsulation efficiency (EE) was calculated following the equation:

$$EE\ (\%) = (\text{Total amount of OLE} - \text{Amount of free OLE}) / (\text{Total amount of OLE}) \times 100$$

2.8. Greenness evaluation of the HPLC method to olive-derived samples

With the aim to assess the impact of the proposed method on health and environment the Environment Assessment Tool (EAT) free software developed by Gaber et al. was employed.[29] This tool is based on the type and amount of organic solvents used in sample/standard pre-treatment and mobile phase preparation, as well as the elution program employed (isocratic or gradient). Other factors involved in the energy-consumption are not taken into account (i.e. temperature, type of detector). Therefore, to conduct this assessment the type and amount of solvents employed for each sample preparation were introduced in the tool, as well as, the chromatographic conditions (flow rate, mobile phase composition, analysis time) and the safety (*S*), health (*H*) and environment (*E*) impacts were obtained. The sum of *S*, *H* and *E* gave the total EAT value. For this metric, the higher the score the greener the method. Calculation is done according to the following equation:

$$\text{HPLC-EAT}=S1m1+H1m1+E1m1+S2m2+H2m2+E2m2+\ldots+Snmn+Hnmn+Enmn$$

Where *S*, *E* and *H* are safety, environmental and health factors, respectively, for *n* number of solvents and *m* is the mass of the solvent. Mobile phases comprised of either pure H_2O or H_2O containing buffer salts and/or analytical modifiers are considered to have zero *E*, *H* and *S*, values due to the outweighing effect of organic solvents. Detailed information is provided elsewhere.[29.] Furthermore, we employed the EAT tool to rank the greenness of the different HPLC methods for OLE quantification found in the literature and we compared them with our method.

2.9. Statistical analysis

The statistical analysis of the validation data was obtained using EMPOWER PRO 2 software (Milford, MA, USA). Environment Assessment Tool (EAT) was employed for the greenness evaluation of the HPLC method.

3. Results and Discussion

3.1. Method Development

The proposed RP-HPLC-DAD method was developed with the aim to provide a simple and versatile technique for OLE quantification in different samples derived from organic certified olive trees and obtained by green methods, with shortened time and cost analysis.

HPLC is a powerful analytical technique and one of the most widely employed in industry. Among these, the most popular is the RP-HPLC which usually uses mixtures of water and ACN. Despite the toxicity of ACN, replacing it with another non-toxic solvent such as alcohols is not an easy work due to the advantages that H_2O-ACN mixtures can offer in efficient RP-HPLC separation methods (i.e. better separation efficiencies, lower viscosity, higher transparency in UV region). Therefore, with the aim to reduce the volume of organic waste by shortening the retention time of OLE and reducing the amount of ACN employed in the mobile phase as well as effectively separating the OLE peak in compliance with ICH Q2(R1)[27] requirements, a new RP-HPLC-DAD method for OLE determination was developed, based on previous work of our group and from an eco-friendly perspective.

Previously, our group defined a gradient method for OLE determination (ultrapure water with ortophosphoric acid *pH=3 as eluent A and ACN as eluent B) (data not published). The gradient started at 5% of eluent B, increasing to 20% in 6 min, and remained constant until minute 10. At this time eluent B was increased to 100% and maintained for 3 minutes. At minute 13, eluent B was decreased to 5% and kept constant until minute 18. Injection volume was 20 µl, the flow rate 1 ml/min and the detector wavelength was set to 280 nm. Acetic acid was also assayed for pH adjustment in eluent A but since it gave a small signal in the baseline it was discarded. With this method, OLE eluted at minute 9.3 but no resolution was achieved in real samples and high noise was detected in the baseline. Since OLE eluted when the mobile phase composition was ACN-H_2O (20:80 v/v) we decided to try it in isocratic mode, keeping the other chromatographic parameters constant. Baseline noise was eliminated and OLE displayed the same retention time as before. The Zorbax extended C-18 column was employed for these tests and lack of reproducibility was shown, probably due to the fact that this column is more suitable for high pH values. Therefore, due to its long-term stability and suitability at low pH values, as well as its properties we decided to try a Zorbax SB-CN C18 column and better peak shape and reproducibility were achieved. Taking the aforementioned, ACN and H_2O were selected as mobile phase solvents and pH was always adjusted to 3.0 with ortophosphoric acid. Initially, several ACN-H_2O proportions were assayed with OLE reference standard, commercial OLE extract and olive leaf aqueous extract and results were studied to obtain acceptable retention times, good symmetry, shape and separation between peaks. Results are displayed in Table 2. Despite the fact that shortened retention time was obtained with ACN-H_2O (25:75, v/v, *pH 3.0), retention factor (k') and resolution values were lower or too close to the acceptance criteria (Rs> 1.5) in the studied samples. Therefore, the mobile phase composed of ACN -H_2O (20:80, v/v, *pH 3.0) was selected for the following optimisation steps.

Table 2 HPLC method development results

Mobile phase composition (ACN:H_2O)	Sample	Results			
		k′ (2> k<10)**	Resolution (>1.5) **	Symmetry (>1) **	R_T (min)
25:75	Oleuropein reference standard	1.53*	-	1.14	7.4
	Olea europaea L. extract	1.59*	1.54	1.14	7.5
	Oleuropein for nanoencapsulation	1.59*	1.56	1.19	7.4
20:80	Oleuropein reference standard	2.74	-	1.21	11.0
	Olea europaea L. extract	2.83	2.62	1.16	11.1
	Oleuropein for nanoencapsulation	2.79	2.84	1.17	11.0

*results that do not accomplish acceptance criteria. ** acceptance criteria. R_T (retention time)

The detector wavelength was set to 255 and 230 nm, and as 230 nm gave a significantly higher area value for the same OLE concentration it was selected as the best one. All the development process was carried out with the analyte dissolved in water. However, theory states that better results are obtained when a sample is dissolved in the mobile phase and based on bibliography, OLE seemed to have better results when dissolved in methanol and thus, both solvents were assayed as well as water. No significant differences were obtained in the peak quality parameters (data not shown) and since one of the objectives of this method was to keep the organic solvent use to a minimum, water was selected as the sample dissolution media. Finally, column temperature was adjusted to 30ºC in order to slightly improve the resolution and reduce the retention time from 12 to 11 minutes.

3.2. Method Validation

Method validation was carried out following ICH Q2 (R1) guidelines.[27]

3.2.1. System Suitability

Once the method was optimized with the best conditions, the system suitability parameters were investigated. Since ICH Q2 (R1) guidelines[27] do not indicate any acceptance criteria to evaluate the system suitability, US Food and Drug Administration (FDA) guidelines and European Pharmacopoeia (EP) established criteria for HPLC methods of pharmaceutical analysis were followed[30.] Therefore, the analyte capacity factor (k′), peak symmetry or tailing factor, number of theoretical plates (N) and resolution (Rs) were investigated. As it is shown in Table 3, the developed method accomplished the acceptance criteria for all the studied parameters in the OLE reference standard.

Table 3. Results from System Suitability Study

Parameter	Acceptance criteria	Results
Theoretical plates (N)	EP: ≥ 1000 FDA: > 2000	11474.47 11270.17
USP tailing (T) Symmetry factor EP	FDA: ≤ 2 EP: 0.8 to 1.5	1.21 ± 0.01
Capacity factor (k')	EP: ≥ 2 FDA: > 2	2.743
R_T %RSD	EP: ≤ 2 FDA: ≤ 2	0.04

3.2.2. Specificity

The specificity test allows to verify if the method is selective enough to quantify the analyte of interest in the presence of other substances that can interfere in the analysis of a complex sample. To assess this, the retention times of OLE standard and samples solutions' chromatograms were compared (Figure 2). Moreover, blank samples' chromatograms were studied. Similar retention times (~ 11 min) were observed in the chromatograms of the standard and sample solutions. Furthermore, no interfering peaks were observed in the blank chromatograms (Figure 2B, D and F). The chromatograms of the samples also showed other peaks of unknown compounds that absorb in the same wavelength as OLE.

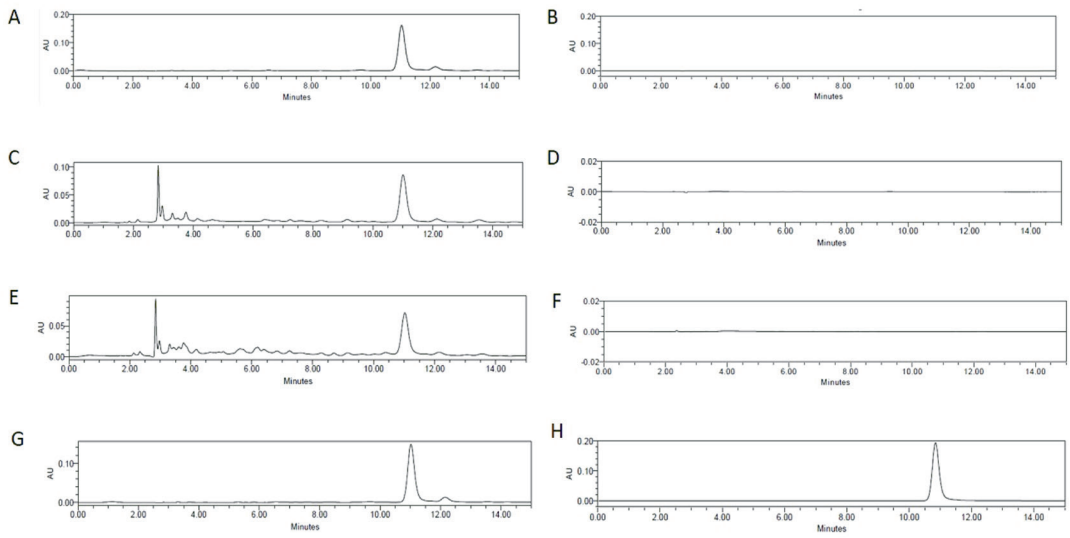

Figure 2. Chromatograms of NLC-OLE supernatant (**A**), Blank-NLC supernatant (**B**), *Olea europaea* L. aqueous extract (**C**), Water (**D**), EVOO-ph (**E**), EVOO (**F**), OLE for nanoencapsulation (purity> 80%, Nonaherbs®) (**G**), OLE reference standard (**H**).

Nevertheless, good resolution was shown for these peaks that did not co-elute with the OLE peak, so they did not interfere in the analysis (Figures 2A, C, E and G). Therefore, the proposed chromatographic method offered an adequate selectivity for OLE analysis in EVOO, olive leaf extracts and NLCs.

3.2.3. Linearity

Based on the analysis of seven concentrations from 50 to 420 µg/ml, in triplicate, the linearity of the developed analytical method was evaluated (Figure 3). The square of correlation coefficient (r^2) value was found to be over the acceptance criteria (> 0.999) indicating that the developed method is linear in the considered range. Therefore, a good linearity was stablished over the studied range (50-420 µg/ml) demonstrating the suitability of the proposed method.

Linearity parameter	Reference Standard Solution
Linearity range (µg/ml)	50-420
Slope	11.27
Intercept	-49.43
Determination coefficient (r^2)	0.9991
Correlation coefficient (r)	0.9995
SD of slope	0.07
SD of intercept	17.21

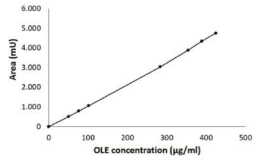

Figure 3. Regression data and curve of the calibration curve for quantitative determination of OLE by HPLC.

3.2.4. LOD and LOQ

The lowest concentration at which an analyte can be detected (LOD) or quantified (LOQ) with acceptable precision and accuracy was calculated from the standard deviation of the response and the slope obtained from the linear regression of a calibration curve with concentrations close to zero (Table 4). To assess these parameters, the following eight concentrations were prepared and analysed in triplicate: 0.2 µg/mL, 0.4 µg/mL, 0.6 µg/mL, 1 µg/mL, 6 µg/mL. According to the obtained results, the LOD was found to be 0.08 µg/mL, whereas the LOQ was found to be 0.25 µg/mL.

Table 4 Curve calibration parameters for LOD and LOQ determination

Linearity Parameter	Reference Standard Solution
Linearity range (µg/ml)	0.2-6.0
Slope	7.98
Intercept	0.44
Determination coefficient (r^2)	0.9994
Correlation coefficient (r)	0.9997
SD of slope	0.06
SD of intercept	0.20

3.2.5. Precision

For precision analysis, OLE standard solutions (50, 280 and 420 µg/ mL) were prepared in triplicate, and analyzed on the same day (repeatability) or in three different days (intermediate precision). As shown in Table 5 both repeatability and intermediate precision did not exceed the maximum established RSD value: ≤2. The highest RSD value was found to be 1.92%. Therefore, the good precision of the method was confirmed.

Table 5 Results from intra-day (repeatability) and inter-day (intermediate) precision studies

Level	Intra-day		Inter-day	
	% of recovery	RSD (%)	% of recovery	RSD (%)
Low	100.3	0.53	101.0; 99.2; 101.8	1.34
Medium	98.8	1.92	101.1;99.1;102.5	1.72
High	102.9	0.71	100.5; 99.5;102.9	1.72

3.2.6. Accuracy

In the present work, the accuracy of the method was studied using the average recovery values of the lowest, intermediate and upper concentration levels of the calibration curve (50, 280 and 420 µg/ml), covering the linear range of the analyte. The supernatant of empty nanoparticles, distilled water and EVOO extraction solution were spiked with OLE standard solutions and analysed after three repeated injections for each sample, in triplicate. Results were expressed as the percentage of recoveries with their respective RSD (Table 6). For all samples at the three concentration levels tested, recovery was within 100 ± 1.89%. Since RSD values were ≤2, accuracy of the method was confirmed.

Table 6 Results from accuracy study

OLE (µg/ml)	Distilled water		NLC-Supernatant		EVOO extraction solution	
	Recovery (%)	RSD (%)	Recovery (%)	RSD (%)	Recovery (%)	RSD (%)
50	100.3	0.53	99.0	1.43	102.5	1.08
280	98.8	1.89	97.3	1.62	99.0	0.79
420	102.9	0.73	98.0	0.95	97.8	1.80

3.3. Method applicability to real samples

The developed and validated method in this work was proposed to study the presence of OLE in different sample matrices obtained through environmentally friendly processes. More specifically, we looked

for an analytical method that with reduced organic solvent use could be able to quantify the OLE content in EVOO, *Olea europaea* L. extracts and EVOO based nanoparticles. Results are results are summarized in Table 7. The European Food Safety Authority has released a claim concerning the effectiveness of the ingestion of olive polyphenols on protecting low-density lipoprotein cholesterol (LDL) from oxidative stress (Commission Regulation (EU) 432/2012). On this basis, marketed olive oils should have a minimum content of 5 mg of oleuropein (or related polyphenols) per 20 grams of product in order to be acknowledged with the proposed health claim ("*Olive oil polyphenols contribute to the protection of blood lipids from oxidative stress*"). However, these polyphenols are rarely found in regular olive oils and thus, it is difficult to find these products in the market labelling the claim. In fact, we have only detected three of them in the market: Oleohealth®, Oliveheart® and Secret to live®. Nevertheless, the last one corresponds to a food supplement composed of olive oil with the addition of olive leaf extract. Evidence suggests that specific factors, such as the ripening state of the olive on harvest time, olive variety and olive oil processing method (temperature and pressure) have an important influence on that.[31-33] Other authors state that it is a consequence of the lack of adequate analytical methods to quantify OLE and related hydroxytyrosol and tyrosol in olive oils.[34] Routine analysis techniques for olive oils employ two-step extraction methods. Firstly, an extraction process with n-hexane is normally conducted to discard fat components followed by one or two hydroalcoholic extraction steps. In this work, the first step was avoided and extraction with MeOH-H_2O (50:50, v/v) seemed to be enough for OLE isolation.

Table 7 OLE quantification from different samples. Results are expressed as mean ± standard deviation.

Sample	Oleuropein content
EVOO-ph (mg/g)	0.52 ± 0.03
Olea europaea L. aqueous extract (mg/g)	5.18 ± 0.1
Olea europaea L. freeze-dried extract (mg/g)	115.01 ± 1.94
NLC-OLE supernatant (mg/ml)	30.62 ± 0.06

Other authors have proved that the defatting step led to a difference of 3% in the obtained results and thus, from an environmental point of view, in our case, it was not an essential step to carry out. Following our validated method, EVOO-ph showed a concentration of 0.52 mg per gram of oil (Table 7)

whereas EVOO did not exert any signal. Taking into account these results, the intake of at least 10 gr of EVOO-ph might be enough for protecting LDL from oxidation and thus, the product accomplishes the requirements for labelling the aforementioned claim. Beyond this health claim, the truth is that currently there is no recommended dose for OLE nor toxicity established for this compound and related phenols. Evidence in clinical trials suggests that OLE is safe in high doses up to 240 mg per person per day. Susalit et al. reported in a clinical study with hypertensive patients that the intake of 200 mg per person per day of OLE could effectively lower blood pressure in subjects with stage-1 hypertension and that the only side effects that might be related to this polyphenol may include headache and muscle discomfort.[35] In other clinical trial it was demonstrated that a daily intake of 51.1 mg of OLE combined with 9.7mg of hydroxytyrosol for 12 weeks significantly improved insulin sensitivity and pancreatic β-cell secretory capacity in men at risk of developing the metabolic syndrome.[36] In contrast, Castañer et al. also demonstrated the effectiveness of the intake of only 25 ml per day of high polyphenol content olive oil (around 8 mg of total polyphenols per person per day) to reduce systemic cardiovascular risk factors and the possibility to modulate genes involved in some chronic degenerative diseases.[37] Therefore, clinical data suggest that most of the pharmacological effects of these polyphenols need the intake of such an amount that could not be reached with the maximum recommended intake of olive oil per person per day. As a result, *Olea europaea* L. extracts emerge as an alternative source of olive polyphenols. In this work, *Olea europaea* L. aqueous extract was obtained through a green extraction method, using high temperatures and distilled water. The use of any organic solvent was avoided during the extraction process. Unknown peaks (probably other minor polyphenols) were found in the chromatograms of the studied extracts but the OLE peak showed good resolution (>1.5) and thus, no peak interfered in OLE quantification, indicating that the method was valid for OLE analysis in these samples.

Aqueous extracts offer several advantages such as better bioactivity and less toxicity than their organic equivalents. However, they are most likely to be contaminated with yeast and molds because of their high water content and, at the same time, low concentration of the bioactive compounds is normally found in these kind of extracts, especially when obtained through solvent-free extraction processes.[38] In industrial processes extraction is normally followed by a purification step, in which the main disadvantage is not only the high energy consumption but also the excessive use of organic solvents. Whilst several efforts have been conducted to minimize the use of hazardous solvents during extraction, this is not possible for the purification steps which are usually based on industrial-scale chromatography methods.

Aimed to address this issue, we proposed the application of freeze-drying as a greener alternative for the purification of OLE which offers less harmful residues and lower waste amounts than conventional large-scale chromatography. Freeze-drying is a common process in pharmaceutical, biotechnological and nutraceutical industries normally employed for improving the shelf life and storage capabilities of drugs and natural compounds. From a biological point of view, freeze-drying is also used for yeast preservation with the addition of cryoprotectants. However, some authors have also postulated the possibility to inactivate or even reduce those cells' viability by this drying technology. More specifically, the freezing step followed by sublimation is thought to influence yeast and moulds inactivation whereas if freezing slowly, large ice crystals might be formed damaging cell membranes.[39] Given this scenario, with the aim of both decreasing risks of microbial contamination as well as increasing OLE purity in the final product, *Olea europaea* L. extract was freeze-dried for 36 hours. As a result, OLE content was increased from 5.18 to 115.01 mg/g and the amount of yeast and molds was reduced from 18,000 to < 100 UFC/g after the lypophilization process (Table 7). Therefore, the proposed procedure in this work offers a greener alternative for OLE extraction and purification through the avoidance of organic solvent use in both steps which could be applied to other natural compounds and might be easily implemented in industrial-scale processes meeting current Good Manufacturing Process (cGMP) regulations.

Finally, with the aim to protect and improve the efficacy of OLE after oral administration, EVOO based NLCs were proposed in this work. The use of organic solvents was avoided during the nanoformulation process and a biodegradable matrix composed of glyceryl distearate (Precirol® ATO 5) and organic EVOO was employed. Given this, the HPLC method of the present work was also aimed to indirectly quantify the encapsulation efficiency of the nanoencapsulation process. Formulation components from the NLCs supernatants (residual lipids and surfactants) did not interfere in OLE determination, as shown in the specificity assay. Therefore, the developed RP-HPLC-DAD method could be applied for OLE quantification in nanoparticles. OLE content in NLC-OLE supernatant was found to be 30.62 ± 0.06 mg/ml and thus, the encapsulation efficiency was 94.09 ± 0.01 %. In light of these results, it could be assumed that the analyte was successfully encapsulated in the EVOO-based NLCs, through the hot-melt emulsification method and therefore, it was validated as an adequate system for OLE encapsulation. We have only found one research article where an HPLC-DAD method was used for OLE determination in nanoemulsions, but the retention time was high (30 min) and no data about linearity nor system suitability was reported.[40] Therefore, to the best of our knowledge this is the first RP-HPLC-DAD method that has been validated for the quantification of OLE in NLCs and which is also applicable to *Olea europaea* L. extracts and olive oil.

3.4. Greenness assessment of the validated RP-HPLC-DAD method

Apart from validating an HPLC method for OLE quantification in the reported samples, offering the conventional standard parameters of good accuracy, precision and selectivity, greenness of the method was also taken into account. With this aim and from an eco-friendly perspective the well-known and established principles of the green chemistry were taken into account to optimize the developed HPLC method.[41] Green chemistry can be summarized by three words: Reduce, Replace and Recycle but when applying it to HPLC techniques only reduce and replace are viable options and thus, in this work, the amount of organic solvent employed for OLE quantification was reduced by shortening the analysis time and increasing the water proportion in the mobile phase composition and sample preparation process. The EAT[29] was used for greenness assessment of the validated HPLC method with regard to its potential health, safety and environmental impact. For this purpose, EAT was applied to our method and those found in the literature for OLE quantification. The obtained results were used for comparison of our method with those from the literature (Table 8). As shown in Table 8, the total EAT value was strongly influenced by the use of organic solvents for sample pre-treatment and for instance, method D exhibited an EAT value of 69 for samples prepared in water and a value of 97 for those prepared with MeOH. The same occurred for our method (*G*) in which samples prepared in water (olive leaf extracts and nanoparticles) showed an EAT value of 12.87 whereas for samples of EVOO in which an hydroalcoholic extraction step was conducted, EAT value was increased to 34.02. Nevertheless, it is worth metioning that our method displayed the lowest EAT values for samples pre-treated with or without organic solvents. From the studied analysis, *F* was found to be the most similar to our method. The total EAT value for *F* was found to be 114 because they employed 100 ml of MeOH-H_2O (50:50, v/v) for chromatographic sample preparation. However, EAT could be reduced to ~19 by only decreasing the amount of solvent to 10ml.

Table 8 Summary of HPLC methods from the literature used for HPLC-EAT ranking

Method	No. of analytes	Type of sample	OLE R_T (min)	Analysis time (min)	Mobile phase	Elution method		Flow rate (ml min^{-1})	Validation	Sample preparation for HPLC	Total EAT
						Isocratic (v/v)	Gradient (steps)				
A[26]	2	EVOO and Olive fruit	10.6	~25	H_2O–ACN	70 : 30	—	0.5	No	*n*-Hexane, EtOH	67.20
B[23]	12	Olive leaf	18.0	62	H_2O–ACN/MeOH (50 : 50)	—	5	1.0	No	MetOH 80%	77.35
C[24]	7	Olive leaf	24.9	70	H_2O–ACN	—	5	1.0	No	MetOH 50%	135.56
D[22]	1	Olive leaf	27.0	60	H_2O–ACN	—	8	1.0	No	H_2O	69.62
										Or MetOH	97.79
E[4]	3	Stems and roots	50.0	100	H_2O–MeOH	—	12	1.0	No	MetOH	157.90
F[42]	2	Dietary supplement	11.0	15	H_2O–ACN	—	6	0.8	Yes	MetOH 50%	114.2
G[a]	1	EVOO, Olive leaf, and NLC	11.0	15	H_2O–ACN	80 : 20	—	1.2	Yes	H_2O	12.87
										Or MeOH 50%	34.02

[a] G is our validated method.

Focusing on our method the overall EAT values were decreased to 12.87 for *Olea europaea* L. extracts and nanoparticles analysis whereas the total EAT value for EVOO samples was found to be 34.02. As aforementioned EVOO samples' EAT impact was higher due to the use of MeOH during the sample pre-treatment process.

Nevertheless, it has to be taken into account that other published methods usually employ another extraction step with n-hexane and even double-extraction step with ethanol which led to a higher EAT value. Therefore, our method was demonstrated to have the lowest impact on health, safety and environment for OLE quantification.

Beyond olive polyphenols, several other natural compounds have recently gained special attention due to its pleiotropic pharmacological activities and low toxicity. There is a clear trend towards the study of isolated natural polyphenols such as curcumin, resveratrol or quercetin among others. A number of preclinical data states their potential therapeutic effects as well as their unfortunately, typical limiting factors (i.e. low bioavailability, poor stability). As a result, many researchers are developing novel formulations to improve the stability and bioavailability of these promising compounds in which analytical techniques are mandatory. RP-HPLC is one of the main preferred techniques for that purpose and researchers take advantage of the amount of published methods for the determination of this kind of molecules. However, most of these methods were developed for the simultaneous determination of a number of molecules in a complex extract with long analysis time and thus, special attention should be paid to precisely adapt the analytical method to the determination of the isolated molecule of interest, with the aim to optimize time and avoid unnecessary waste of organic solvents. We have validated an RP-HPLC-DAD method for the determination of OLE in NLCs' supernatant, aqueous extracts and EVOO samples with a low environmental impact which could be also applied for the determination of other phenolic compounds in a variety of formulations.

4. Conclusions

The RP-HPLC-DAD method developed and validated in this work represents an alternative approach for the quantification of OLE in several matrices such as olive oil, *Olea europaea* leaf extracts and lipid nanoparticles with a minimized environmental impact. The validation procedure was carried out according to ICH Q2(R1) guidelines and from an environmental perspective evaluating specificity, linearity, accuracy, precision and greenness. The method proved to be reliable and simple, complying with the requirements

of these parameters in the range of 50–420 µg/mL. The LOD was found to be 0.08 µg/mL and the LOQ 0.25 µg/mL. RSD obtained in the assays indicate that this method is adequate to quantify OLE in polyphenol rich-olive oil and aqueous and lyophilized extract of olives leaves as well as nanoparticulated systems obtained through solvent-free methods. Besides, the method was proved to reduce the toxic impact in regard to the environment, health and safety compared to other HPLC methods. The proposed method could be applied to the determination of other phenolic compounds in a variety of samples.

5. Abbreviations

ACN	Acetonitrile
DAD	Diode array detector
DDS	Drug delivery systems
EAT	Environmental Assessment Tool
EVOO	Extra virgin olive oil
EVOO-ph	Extra virgin olive oil rich in polyphenols
HDPE	High Density Polyethylene
H_2O	Water
HPLC	High performance liquid chromatography
k'	Capacity factor
LOD	Limit of detection
LOQ	Limit of quantification
MeOH	Methanol
N	Number of theoretical plates
NLC	Nanostructured lipid carrier
NLC-OLE	Oleuropein loaded nanostructured lipid carrier
OLE	Oleuropein
PVDF	Polyvinylidene fluoride
Rs	Resolution
R_T	Retention time
RP-HPLC-DAD	Reverse phase high performance liquid chromatography coupled with diode array detector
RSD	Relative standard deviation
T	Tailing factor

6. Conflicts of interest

The authors declare no competing conflicts of interest.

7. Acknowledgements

A. Huguet-Casquero thanks the Spanish Ministry of Economy and Competitiveness for the Industrial Doctorate fellowship grant (DI-15-07513). This work was done under the R&D projects of BIOSASUN. Authors wish to thank the ICTS "NANBIOSIS" and the Drug Formulation Unit (U10) of the CIBER-BBN. Furthermore, they thank the support from the University of the Basque Country (UPV/EHU), the Basque Country Government (Grupos Consolidados, No ref: IT907-16to JL. P). Finally, the authors acknowledge the Laboratorios Innoagral (Grupo Hesperides) for the microbiological assays.

8. References

1 H.E. Billingsley and S. Carbone, Nutr. Diabetes, 2018, 8, 13, DOI: 10.1038/s41387-018-0025-1.

2 G. Sindona, in Olives and Olive Oil in Health and Disease Prevention, ed. V. R. Preedy and R. R. Watson, Academic Press, San Diego, 2010, pp. 95–100.

3 M. I. Alarcón Flores, R. Romero-González, A. Garrido Frenich and J. L. Martínez Vidal, Food Chem., 2012, 134, 2465–2472, DOI: 10.1016/j.foodchem.2012.04.058.

4 F. Ortega-García and J. Peragón, J. Sci. Food Agric., 2010, 90, 2295–2300, DOI: 10.1002/jsfa.4085.

5 European Commission Regulation, EC No. 432/2012 establishing a list of permitted health claims made on foods, other than those referring to the reduction of disease risk and to children's development and health, 2012.

6 EMA monograph, Assessment report on Olea europaea L., folium-, 2017.

7 M. L. Castejón, M. Sánchez-Hidalgo, M. Aparicio-Soto, A. González-Benjumea, J. G. Fernández-Bolaños and C. Alarcón-de-la-Lastra, J. Funct. Foods, 2019, 58, 95–104, DOI: 10.1016/j.jff.2019.04.033.

8 H. Zbidi, S. Salido, J. Altarejos, M. Perez-Bonilla, A. Bartegi, J. A. Rosado and G. M. Salido, Blood Cells, Mol., Dis., 2009, 42, 279–285, DOI: 10.1016/j.bcmd.2009.01.001.

9 G. Bisignano, A. Tomaino, R. L. Cascio, G. Crisafi, N. Uccella and A. Saija, J. Pharm. Pharmacol., 1999, 51, 971–974.

10 H. F. Al-Azzawie and M.-S. Alhamdani, Life Sci., 2006, 78, 151371–1377, DOI: 10.1016/j.lfs.2005.07.029.

11 H. Shamshoum, F. Vlavcheski and E. Tsiani, Biofactors, 2017, 43, 517–528, DOI: 10.1002/biof.1366.

12 P. Przychodzen, R. Wyszkowska, M. Gorzynik-Debicka, T. Kostrzewa, A. Kuban-Jankowska and M. Gorska-Ponikowska, Anticancer Res., 2019, 39, 1243–1251, DOI:10.21873/anticanres.13234.

13 Z. He, X. Deng, P. P. But, V. E. Ooi, H. Xu, S. H. Lee and S. Lee, Chem. Pharm. Bull., 2001, 49, 1471–1473.

14 H. Ahmadvand, A. Noori, M. G. Dehnoo, S. Bagheri and R. A. Cheraghi, Asian Pac. J. Trop. Dis., 2014, 4, S421–S425, DOI: 10.1016/S2222-1808(14)60481-3.

15 C. Angeloni, M. Malaguti, M. C. Barbalace and S. Hrelia, Int. J. Mol. Sci., 2017, 18(11), 2230, DOI: 10.3390/ijms18112230.

16 A. Harvey, R. Edrada-Ebe and R. Quinn, Nat. Rev. Drug Discovery, 2015, 14, 111–129, DOI: 10.1038/nrd4510.

17 S. C. Edgecombe, G. L. Stretch and P. J. Hayball, J. Nutr., 2000, 130, 2996–3002.

18 P. Lin, W. Qian, X. Wang, L. Cao, S. Li and T. Qian, Biomed. Chromatogr., 2013, 27, 1162–1167, DOI: 10.1002/bmc.2922.

19 E. González, A. M. Gómez-Caravaca, B. Giménez, R. Cebrián, M. Maqueda, A. Martínez-Férez, A. Segura- Carretero and P. Robert, Food Chem., 2019, 279, 40–48, DOI: 10.1016/j.foodchem.2018.11.127.

20 G. Calixto, J. Bernegossi, B. Fonseca-Santos and M. Chorilli, Int. J. Nanomed., 2014, 9, 3719–3735, DOI: 10.2147/IJN.S61670.

21 M. Moreno-Sastre, M. Pastor, C. J. Salomon, A. Esquisabel and J. L. Pedraz, J. Antimicrob. Chemother., 2015, 70, 11-2945–2955, DOI: 10.1093/jac/dkv192.

22 S. AlShaal, F. Karabet and M. Daghestani, Determination of the Antioxidant Properties of the Syrian Olive Leaves Extracts and Isolation Oleuropein by HPLC Techniques, 2019, vol. 6, pp. 97–110.

23 O. Ghomari, F. Sounni, Y. Massaoudi, J. Ghanam, L. B. Drissi Kaitouni, M. Merzouki and M. Benlemlih, Biotechnol. Rep., 2019, 23, DOI: 10.1016/j.btre.2019.e00347.

24 S. Ghasemi, D. E. Koohi, M. S. B. Emmamzadehhashemi, S. S. Khamas, M. Moazen, A. K. Hashemi, G. Amin, F. Golfakhrabadi, Z. Yousefi and F. Yousefbeyk, J. Food Sci. Technol., 2018, 55, 4600–4607, DOI: 10.1007/s13197-018- 3398-1.

25 M. Ricciutelli, S. Marconi, M. C. Boarelli, G. Caprioli, G. Sagratini, R. Ballini and D. Fiorini, J. Chromatogr. A, 2017, 1481, 53–63, DOI: 10.1016/j.chroma.2016.12.020.

26 G. Tamasi, M. C. Baratto, C. Bonechi, A. Byelyakova, A. Pardini, A. Donati, G. Leone, M. Consumi, S. Lamponi, A. Magnani and C. Rossi, Food Sci. Nutr., 2019, 7, 2907–2920, DOI: 10.1002/fsn3.1142.

27 International Conference on Harmonisation of Technical Requirements for Registration of Pharmaceuticals for Human Use ICH, Q2 (R1), Validation of Analytical Procedures: Text and Methodology.

28 M. Pastor, M. Moreno-Sastre, A. Esquisabel, E. Sans, M. Viñas, D. Bachiller, V. J. Asensio, Á. Del Pozo, E. Gainza and J. L. Pedraz, Int. J. Pharm., 2014, 477, 485–494.

29 Y. Yasser Gaber, U. Törnvall, M. A. Kumar, M. Amine and R. Hatti-Kaula, Green Chem., 2011, 13, 2021–2025, DOI: 10.1039/c0gc00667j.

30 G. Shabir, J. Chromatogr. A, 2003, 987, 57–66.

31 D. Ryan, P. D. Prenzler, S. Lavee and K. Robards, J. Agric. Food Chem., 2003, 51(9), 2532–2538, DOI: 10.1021/jf0261351.

32 B. Jimenez, A. Sánchez-Ortiz, M. L. Lorenzo and A. Rivas, Eur. J. Lipid Sci. Technol., 2014, 116, 1634–1646, DOI: 10.1002/ejlt.201400010.

33 C. Romero, M. Brenes, K. Yousfi, P. García, A. García and A. Garrido, J. Agric. Food Chem., 2004, 52, 479–484, DOI: 10.1021/jf0305251.

34 M. Bellumori, L. Cecchi, M. Innocenti, M. Clodoveo, F. Corbo and N. Mulinacci, Molecules, 2019, 24, 2179, DOI: 10.3390/molecules24112179.

35 E. Susalit, N. Agus, I. Effendi, R. R. Tjandrawinata, D. Nofiarny, T. Perrinjaquet-Moccetti and M. Verbruggen, Phytomedicine, 2011, 18, 251–258, DOI:10.1016/j.

36 phymed.2010.08.016.

37 M. de Bock, J. Derraik, C. Brennan, J. Biggs, P. Morgan, S. Hodgkinson, P. Hofman and W. Cutfield, PLoS One, 2013, 8, 3, DOI: 10.1371/journal.pone.0057622.

38 O. Castañer, M. Covas, O. Khymenets, K. Nyyssonen, V. Konstantinidou, H. Zunft, R. de la Torre, D. Muñoz-Aguayo, J. Vila and M. Fitó, Am. J. Clin. Nutr., 2012, 95(5), 1238–44, DOI: 10.3945/ajcn.111.029207.

39 L. Oberoi, T. Akiyama, K. Lee and S. J. Liu, Phytomedicine, 2011, 18, 259–265, DOI: 10.1016/j.phymed.2010.07.006.

40 S. Bourdoux, D. Li, A. Rajkovic, F. Devlieghere and M. Uyttendaele, Compr. Rev. Food Sci. Food Saf., 2016, 15, 1056–1066, DOI: 10.1111/1541-4337.12224.

41 P. Gharehbeglou, S.M. Jafari, A. Homayouni, H. Hamishekar and H. Mirzaei, Food Hydrocolloids, 2019, 89, 44–55, DOI: 10.1016/j.foodhyd.2018.10.020.

42 P. T. Anastas and J. C. Warner, Chem. Soc. Rev., 2010, 39, 301–312, DOI: 10.1039/B918763B.

43 T. Bertolini, L. Vicentini, S. Boschetti, P. Andreatta and R. Gatti, J. Pharm. Biomed. Anal., 2016, 129, 198–202, DOI: 10.1016/j.jpba.2016.07.001.

Chapter 2

Encapsulation of oleuropein in nanostructured lipid carriers: biocompatibility and antioxidant efficacy in lung epithelial cells

Pharmaceutics, 2020, 12(5), 429;

DOI: https://doi.org/10.3390/pharmaceutics12050429

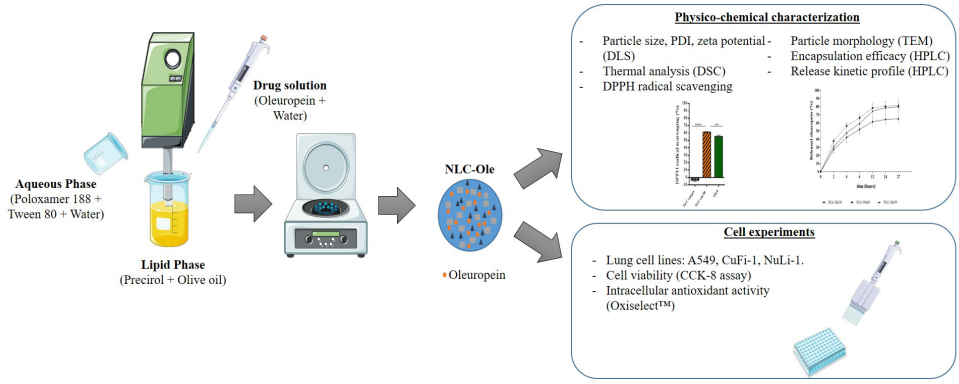

Encapsulation of oleuropein in nanostructured lipid carriers: biocompatibility and antioxidant efficacy in lung epithelial cells

Amaia Huguet-Casquero[a,b], María Moreno-Sastre[a], Tania-Belén López-Méndez[a], Eusebio Gainza[b], Jose Luis Pedraz[a,c*]

[a] NanoBioCel Group, Laboratory of Pharmaceutics, School of Pharmacy, University of the Basque Country (UPV/EHU), Spain.
[b] Biosasun S.A., Iturralde 10, Etxabarri-Ibiña, Zigoitia, 01006, Spain.
[c] Biomedical Research Networking Centre in Bioengineering, Biomaterials and Nanomedicine (CIBER-BBN), Spain.

* Corresponding author: Jose Luis Pedraz.

ABSTRACT

Oxidative damage has been linked to a number of diseases. Oleuropein (OLE), a natural occurring polyphenol from olive leaves (*Olea europaea* L.), is known to be a potent antioxidant compound with inherent instability and compromised bioavailability. Therefore, in this work, nanostructured lipid carriers (NLCs) were proposed for OLE encapsulation to protect and improve its antioxidant efficacy. The lipid matrix, composed of olive oil and Precirol, was optimized prior to OLE encapsulation. The characterization of the optimized oleuropein-loaded NLCs (NLC-OLE) showed a mean size of 150 nm, a zeta potential of −21 mV, an encapsulation efficiency of 99.12%, sustained release profile, and improved radical scavenging activity. The cellular *in vitro* assays demonstrated the biocompatibility of the NLCs, which were found to improve and maintain OLE antioxidant efficacy in the A549 and CuFi-1 lung epithelial cell lines, respectively. Overall, these findings suggest a promising potential of NLC-OLE to further design a pulmonary formulation for OLE delivery in lung epithelia.

Keywords: oleuropein; polyphenols; nanoparticle; natural antioxidant; nanotechnology; olive oil

1. Introduction

Reactive oxygen species (ROS) have an essential role in normal cell function and signalling. However, their overproduction leads to an oxidative stress status that ultimately contributes to the development of several pathological events such as inflammation, fibrosis, genotoxicity and carcinogenesis. As a result, oxidative stress has been linked to more than 50 diseases involving several human organs [1-4]. Among them, the respiratory tract is one of the main sites for the presence of prooxidant molecules. Moreover, clinical evidence suggests that many lung diseases are associated with a reduced antioxidant defence together with an increased accumulation of ROS [5]. Although current strategies towards oxidative damage have been focused on the use of small ROS scavenger drugs (i.e. Edaravone, N-acetylcysteine, Cerovive®) their toxicity, together with their low clinical efficacy, has been discouraging [5, 6] . Given this, natural antioxidants have emerged as alternative or even complementary candidates with minimized toxicity.

Extracted from olive leaves, oleuropein (OLE), is widely known for its potent antioxidant efficacy which, interestingly, seems to be the basis for its pleiotropic pharmacological activities: hypoglycemic [7], antiviral [8], antimicrobial [9], platelet anti-aggregant [10], anticancer [11, 12], hypolipidimic [13] and anti-inflamatory [14, 15] among others. Even the European Medicines Agency (EMA) as well as the European Food Safety Agency (EFSA) have emitted their own assessment reports about the health-promoting properties of this natural compound in human health [16, 17]. Despite its promising properties, the therapeutic use of OLE is limited by its poor stability against environmental (light, oxygen, temperature) and human biological conditions (pH, enzymes) [18], resulting in compromised bioactivity, bioaccessibility and bioavailability [19]. Along with these limitations, the lack of target specificity hampers the therapeutic application of OLE.

In this context, micro and nanoencapsulation technologies have been proposed as promising strategies[20]. Currently, some encapsulation methods for *Olea europaea* leaf extracts have been described, such as W/O nanoemulsions and W/O/W double emulsions [21-23], spray-drying [24, 25], formation of inclusion complexes with cyclodextrin[26], electrostatic extrusion [27], biopolymer complexes/double emulsions [21] and liposomes [28]. However, they have some limitations such as the use of organic solvents, tedious and time consuming manufacturing processes, high particle sizes, and low yield (for spray drying). Furthermore, low amount of OLE is normally encapsulated in the final formulation (~ 1-2 % w/w) and there is a lack of tests ensuring the preservation of OLE antioxidant activity in biological systems. Given this scenario, lipid nanoencapsulation and particularly, nanostructured lipid carriers

(NLCs) offer special advantages: scale-up feasibility, long-term stability, high drug loading, sustained release, good biocompatibility, biodegradable properties, and most importantly, the increased local deposition of the drug [29-32]. Moreover, the lipid excipients used for NLC formulation have documented biological anti-inflammatory effects in several disease models which might result in a synergistic effect with the encapsulated compound [33, 34]. NLCs are made up by up of a lipid core formed by a mixture of solid and liquid lipids, stabilized by surfactants and offer the possibility of incorproating both lipophilic and hydrophilic drugs [35]. The selection of the encapsulating material is critical in the design of the nanoparticles [36]. In this work, Precirol and olive oil were chosen to form the lipid core due to its efficacy in sustained release formulations and its ability to reduce the possible cytotoxicity effect of residual surfactants that might be present in the final nanoformulation, respectively [37].

Hence, the goal of this work was to elaborate OLE-loaded NLCs to modulate the antioxidant activity of the encapsulated compound in lung epithelial cells. With the aim to obtain a nanoformulation with suitable physico-chemical properties, a preformulation study was conducted varying the amount of liquid and solid lipids of the nanoparticle matrix. The most promising nanoformulation was chosen for the evaluation of OLE encapsulation, *in vitro* release profile, thermal behaviour, and chemical antioxidant activity. Finally, the biocompatibility of OLE-loaded NLCs as well as their cellular antioxidant efficacy were investigated in three lung epithelial cell models.

2. Materials and Methods

2.1. Materials

2.1.1. Chemicals

Precirol® ATO 5 (glycerol distearate) was a kind gift from Gattefosé (France). Polysorbate, Tween® 80 was purchased from Panreac Química (Castellar del Vallès, Barcelona, Spain). Organic extra virgin olive oil was donated by Biosasun S.A. (Álava, Spain). Poloxamer 188 and 2, 2-diphenyl-1- picrylhydrazyl (DPPH) were kindly provided by Merck (Darmstadt, Germany). D-trehalose anhydrous was purchased from ACROS Organics™ (Geel, Belgium). OLE (>80%) was donated by Nonaherbs Bio(Tech) (China). Ascorbic acid was purchased from Sigma-Aldrich Chemicals (St. Louis, MO, USA). The ultrapure water was from a Milli-Q Water System. Other chemicals were all analytical grade.

2.1.2. Cell culture reagents

A549 (ATCC® CCL-185™), CuFi-1 (ATCC® CRL-4013™) and NuLi-1 (ATCC® CRL-4011™) cells were bought from the American Type Culture Collection (ATCC; Manassas, VA, USA). Roswell Park Memorial Institute (RPMI) 1640 medium without phenol red, N-2-hydroxyethylpiperazine-N-2-ethane sulfonic acid (HEPES), penicillin-streptomycin (PEST), inactivated fetal bovine serum (FBS), Dulbecco's Phosphate Buffered Saline (DPBS), and trypsin-EDTA (0.5%) without phenol red were purchased from Gibco™ (Life Technologies, Spain). Serum-free Bronchial Epithelial Growth Medium (BEGM Bullet Kit; CC-3170) made of BEBM basal medium and SingleQuot additives; Airway Epithelial Cell Basal Medium and Bronchial Epithelial Cell Growth Kit additives were purchased from Lonza (Clonetics, Lonza, Walkersville Inc., Walkersville, MD, USA). Dimethyl sulphoxide (DMSO) was purchased form Scharlau (Spain), Human Placental Collagen Type IV (Sigma Cat. No. C-7521) and Cell Counting Kit-8 (CCK-8) were bought form Sigma-Aldrich (Saint Louise, MO, USA). OxiSelect™ Cellular Antioxidant Cell Kit was bought from Quimigen (Madrid, Spain) to Cell Biolabs, Inc. (San Diego, CA, USA).

2.2. Preparation of Nanostructured Lipid Carriers (NLC)

2.2.1. Blank-NLCs

Nanostructured lipid carriers, NLCs, were elaborated by the hot melt emulsification method as previously described by our research group [38] with few modifications. Briefly, Precirol® ATO 5 (solid lipid; melting point: 56ºC) and olive oil (liquid at room temperature (RT)) were chosen to form the lipid core. Several solid-liquid lipid proportions ranging from 10:90 to 90:10 were employed for each batch manufacturing to study their effect in formulation parameters. This lipid phase was melted 5ºC above the solid lipid (Precirol® ATO 5) melting point until a clear and homogeneous phase was obtained. The aqueous phase was prepared by dispersing 1.3% (w/v) of Tween® 80 and 0.66% (w/v) of Poloxamer 188 in Milli-Q water and heating to the same temperature as the lipid phase. Straightaway, the hot aqueous phase was added to the melted oily phase, and then sonicated for 30s at 50 W (Branson Sonifier 250, Danbury, CT, USA). The formed nanoemulsion was maintained under magnetic stirring during 10 minutes at RT and stored for 2 h at 4 ºC to allow the re-crystallization of the lipids and NLC formation. Then, particles were collected using a 100-kDa molecular weight cut-off centrifugal filter unit (Amicon, "Ultracel-100k", Millipore, Spain) at 2500 rpm for 10 min and washed three times with MillliQ water. All the nanoparticles prepared were freeze-dried for 36 h (Telstar Lyobeta freeze-dryer, Terrasa, Spain). Prior to the lypophilization process of the resulting NLC suspension, a solution of a cryoprotectant (trehalose (15% w/w)) was

added to the collected nanoparticles.

2.2.2. Oleuropein-loaded NLCs (NLC-OLE)

From the developed formulations, the lipid matrix which accomplished with the best physico-chemical characteristics was selected for OLE encapsulation studies. OLE-loaded NLCs were prepared as described above, but adding the corresponding volume of a saturated solution of OLE in purified water (0.66 mg/ml). As OLE is hydrophilic and slightly thermosensitive, it was blended in the molten lipid phase just prior to the addition of the aqueous phase and the following sonication process. The targeted loading of OLE in NLCs were 30% (NLC-OLE30), 40% (NLC-OLE40) and 50% (NLC-OLE50) (w/w).

2.3. Characterization of lipid nanoparticles

2.3.1. Size and zeta potential

The mean particle size (Z-average diameter) was measured by Dynamic Light Scattering (DLS) and zeta potential was determined through Laser Doppler micro-electrophoresis (Malvern® Zetasizer Nano ZS, Model Zen 3600; Malvern instruments Ltd., UK). Prior to the measurements, nanoparticles were dispersed in Milli-Q water (pH 5.6) at optimal intensity. For zeta potential, the measured electrophoretic mobility was converted into zeta potential through Smoluchowski approximation. Each assay was performed in triplicate before and after nanoparticles' lyophilisation and data are presented as mean ± standard deviation (SD).

2.3.2. Thermogravimetric analysis

To assess the moisture content of freeze-dried nanoparticles, a thermogravimetric analysis was performed (NETZSCH, STA 449 F1 Jupiter®, Netzsch). Samples (NLC-empty, NLC-OLE30, NLC-OLE40 and NLC-OLE50) were heated from 25 to 200 °C at a heating rate of 5 °C/min under nitrogen atmosphere. Results are expressed as water content (%).

2.3.3. High Performance Liquid Chromatogragy (HPLC) method

Chromatographic analysis was performed using Alliance 2795 Waters equipment coupled to an UV/vis detector. Chromatographic separation was performed in a Zorbax Eclipse Plus® C18 column (250 mm x

4.6 mm I.D.; 5.0 µm; Agilent Technologies, UK) column. The mobile phase consisted of acetonitrile: water (25:75 (v/v)) and pH was adjusted with ortophosphoric acid to 3. The system was operated isocratically at a flow rate of 1.0 ml/min, and the detection was performed at 230nm. The retention time of OLE was 7.6 min at room temperature and total run time of HPLC analysis was 10 min. Prior to injection (10 µl) samples were diluted in water and filtered (0.45 µm). The method was validated in terms of linearity, accuracy and specificity, over the range of expected concentrations. A linear correlation was observed in the concentration range of 6.20-420 µg/mL, with a coefficient of determination r^2 = 0.999 and RSD<2%. The limit of detection and limit of quantification were 0.2 µg/ml and 1.0 µg/ml, respectively. The method was specific for OLE and no interfering peaks were observed near its retention time.

2.3.4. Encapsulation efficiency

Encapsulation efficiency (EE) of OLE into NLCs was determined indirectly by measuring the amount of free OLE (non-encapsulated OLE) in the supernatant obtained after the filtration/centrifugation process. OLE concentration was quantified by the explained HPLC method. Considering the initial amount of OLE added to each formulation, the EE was calculated as:

$$EE\ (\%) = ((\text{Total amount of OLE} - \text{Amount of free OLE}) / (\text{Total amount of OLE})) \times 100$$

2.3.5. Microscopy analysis

NLC surface characteristics and morphology were examined under transmission electron microscopy (TEM, JEOL JEM-1400 Plus a 120 kV, Peabody, MA, USA). For this purpose, lyophilized samples were suspended in Milli-Q water at an optimal concentration of 4 mg/ml and sonicated in a water bath for one minute. Then, samples were placed on a carbon grid and treated with negative staining uranyl acetate (2%) for particles visualization. Images were captured with a digital camera sCMOS (Hamamatsu, Hawthorne, CA, UK).

2.3.6. *In vitro* drug release studies

In order to obtain qualitative and quantitative information on OLE release from NLCs, *in vitro* drug release studies were conducted using Quix-Sep Micro Dialyzers (Membrane Filtration Products Inc., Seguin, TX, USA) at 37ºC under magnetic stirring in phosphate buffer saline (PBS, pH 7.4). A dialysis regenerated cellulose tubular membrane having a molecular weight cut-off (MWCO) between 12,000 and 14,000 Da

was used. First, cellulose membranes were soaked in the dissolution medium (PBS) for 12 hours prior to its use to ensure thorough wetting of the membrane before placing it in a Quix-Sep cell. To carry out this study, the NLC-OLE30, NLC-OLE40 and NLC-OLE50 suspensions (25 mg/mL) were placed in the cell system which was immersed in 30 mL of PBS preheated solution (pH 7.4) as the dissolution medium. At fixed time intervals up to 27 h, dissolution mediums were removed from the incubation and replaced with new preheated PBS medium. Samples were kept at 4ºC until they were analysed by HPLC (see section 2.3.3). The release study was carried out under proper sink conditions. Results were expressed as percentage of OLE released compared to the total compound encapsulated in the nanoformulation. Experiments were run in triplicate for each point of release kinetics. To further study OLE release kinetics and mechanism, the obtained cumulative release data was computed with the DDsolver program and fitted to several kinetic models: zero order, first order, Higuchi, Baker-Londslade, Hixson-Crowell, Hopfenger, and Korsmeyer-Peppas [39]. Regression coefficient (r^2) was calculated to determine the best-fit model.

2.3.7. Differential Scanning Calorimetry (DSC)

The thermal behaviour of the freeze dried NLCs, was studied by differential scanning calorimetry (DSC-50, Shimadzu, Japan). One to two milligrams of each sample was weighed and placed on an aluminium pan and crimped. The samples were heated from 25 ºC to 350 ºC at the rate of 10ºC/min. Pure solid lipid powder (Precirol® ATO5), OLE powder, pure solid surfactant (Poloxamer 188) and cryoprotectant (trehalose anhydrous) were also subjected to DSC analysis to gather additional information. The crystallinity index (CI) of NLCs was calculated from the enthalpy of fusion using the following equation:

$$CI\ (\%) = (\text{Enthalpy NLC [J/g]}) / (\text{Enthalpy solid lipid[J/g]}) \times 100$$

2.3.8. Radical scavenging activity assessment by the 2,2-diphenyl-1-picrylhydrazyl (DPPH) method

Radical scavenging activity of the nanoparticles was investigated spectrophotometrically, analysing their ability to scavenge DPPH radical [40]. Briefly, a solution of DPPH was prepared with a concentration of 0.1 mM in absolute ethanol. Freeze-dried NLC-OLE50 was diluted in PBS to obtain a final concentration of 1.25 mg/ml and was left to release the drug for 24h in the same conditions as described in section 2.3.6. Equivalent concentrations of OLE (0.2 mg/ml) and NLC-empty (1.25 mg/ml) were also prepared in PBS and assayed in the same conditions. Ascorbic acid (0.2mg/ml) was used as the method control. A total of 500 µL of each sample was added to 3300 µL of DPPH-ethanol solution. The reaction mixture was incubated for 60 min protected from light on a shaker at 37ºC. After that, the absorbance of the reaction

solutions was recorded at 517 nm by UV–Vis spectrophotometry (6705 UV/Vis Spectrophotometer JENWAY). DPPH radical scavenging activity was calculated according to the following equation:

$$\text{DPPH scavenging activity (\%)} = ((Abs_{control} - Abs_{sample})/(Abs_{control})) \times 100$$

Where Abs_{sample} is the absorbance of DPPH solution after reacting with the sample, and $Abs_{control}$ is the absorbance of blank 0.1 mM DPPH solution. Ethanol was used as the blank. All measurements were carried out in triplicate and results are expressed as mean ± SD.

2.4. Cell experiments

2.4.1. Cell culture

Human lung adenocarcinoma epithelial cells (A549) were grown and maintained in RPMI 1640 medium (pH 7.4) supplemented with 10% (v/v) inactivated FBS, 1% PEST, and 1% HEPES, without phenol red and incubated at 90% humidity, 5% (v/v) CO_2 atmosphere at 37 ºC. Cells were allowed to grow until 90% of confluence, then they were trypsinized (Trypsin-EDTA) and seeded in plates for each experiment. Cystic fibrosis (CuFi-1) cell line, derived from a CF human bronchial epithelium homozygous for the CFTR ΔF508 mutation, was grown and maintained in serum-free BEGM medium. Cells were incubated at 37 °C, 90% humidity and 5% CO_2. All culture-flasks were pre-coated with 60 µg/mL solution of Human Placental Collagen Type IV at least 18 hours in advance, then air-dried and rinsed 2-3 times with DPBS. Cells were allowed to grow until 80% of confluence, trypsinized (Trypsin-EDTA) and seeded in plates for each experiment. Plates were also pre-treated with collagen as explained before. Human normal bronchial epithelial (NuLi-1) cells were grown and maintained under the same conditions as CuFi-1 cell line but in serum-free Airway Epithelial Cell Basal medium supplemented with Bronchial Epithelial Cell Growth Kit additives.

2.4.2. Cell viability studies

Biocompatibility of empty nanoparticles (NLC-empty) and OLE-loaded nanoparticles (NLC-OLE50) was evaluated in the A549, CuFi-1 and NuLi-1 cell lines. Each cell line was plated in 96-well microtiter plates at a density of 10,000 cells/well (A549) and 15,000 cells/well (NuLi-1, CuFi-1) in a final volume of 100 µL of the corresponding cell medium. Cells were treated with NLC-OLE50 suspended in cell medium at concentrations ranging from 14.45 to 462.5 µM (in terms of encapsulated OLE) and the equivalent amounts of NLC-empty, for 24 h at 37 ± 2 ºC, 90% humidity and 5% CO_2. Controls were set with dimethyl

sulfoxide (DMSO) as the negative or death control, and medium without formulation as the positive control. Free OLE was assayed for comparison. After 24h of incubation, cell viability was determined with the CCK-8. Cells were washed with sterile DPBS and then 10% of CCK-8 in medium was added to each well and incubated in a wet chamber for 4 h at 37º ± 2ºC and 5% CO_2. The resulting colored solution was quantified using a microplate reader (Infinite1 200 PRO, Tecan, Männedorf, Switzerland). The spectrophotometric absorbance was measured at 450/650 nm wavelength. Results were calculated in relation to the untreated cells (~100% viability) and are expressed as the percent of cell viability ± S.D. of the values collected from the three separate experiments performed in triplicate for each sample and each cell line.

2.4.3. Cellular antioxidant activity (CAA) assay

Cellular ROS scavenging activity of NLC-OLE50 was measured using OxiSelect™ Cellular Antioxidant Activity Assay Kit in the A549, CuFi-1 and NuLi-1 cell lines. 2',7'-dichlorodihydrofluorescin diacetate (DCFH-DA) was used as the fluorogenic probe. Cells were seeded as previously explained in clear bottom black polystyrene 96-well plates for 24 hrs. After that, all media was removed and washed gently with DPBS w/o calcium and magnesium three times. Cells were then treated with OLE, both free and nanoencapsulated, at the following concentrations: 115µM, 231.2µM, and 462.5µM. After 24 h of samples incubation at 37ºC, 90% humidity, and 5% CO_2, the CAA assay was carried out. Briefly, wells were washed with sterile DPBS and then 50 µl of DCFH-DA solution was added. Plates were incubated for 60 min at 37ºC, 90% of humidity and 5% CO_2 in order to allow the cell-permeable fluorogenic probe dye (DCFH-DA) diffuse into the cells. After incubation, all solutions were removed and wells were washed three times with DPBS. After addition of 100 µl of 2,2'-azobis (2-amidinopropane) dihydrochloride (ABAP) solution, as the free radical initiator, fluorescence was read at 37 ºC for 60 min with 5 min intervals with excitation wavelength 480 nm and emission wavelength 530 nm.

Each plate included cell control wells (cells without any treatment), negative control wells (cells pretreated only with DPBS and DCFH-DA), and positive control wells (cells pretreated with ABAP and DCFH-DA). Quercetin was used as a standard in each experiment and was added following provider instructions, just prior to the addition of DCFH-DA with the aim to validate the assay in the selected cell models. Absence of green fluorescence in the studied samples was confirmed before the assay. Each assay was carried out in triplicate for each cell line.

2.5. Statistical analysis

All results are expressed as the mean ± standard deviation (SD) unless otherwise stated. All statistical analyses were calculated using GraphPad Prism 6 Statistics software (San Diego, CA, USA) and $p < 0.05$ was considered as significant. A multiple-sample and two-sample *t* test with unequal standard deviations was used to verify the significant difference between data in cellular antioxidant and DPPH assays, respectively. For cell viability results, a two-way ANOVA was run.

3. Results and discussion

3.1. Optimization and physico-chemical characterization of nanoparticles: particle size, morphology and zeta potential

In the first step of this work, NLCs were prepared through the hot melt emulsification method followed by ultrasonication (HME-Us) as previously described by our group [38]. The rationale for using this technique relies on its versatility and easy scale-up. HME-Us has gained a lot of importance after the Food and Drug Administration encouraged the use of continuous processes among the pharmaceutical industry [41] and overcomes most of the limitations offered by the conventional micro- and nanoemulsification techniques. Avoidance of organic solvents, shorter and fewer steps of the process as well as the increased homogeneous spreading of the particles are some of the advantages of this method [42, 43]. Altogether, this makes HME-Us an industrially and environmentally friendly technique which has largely been applied in the preparation of NLCs for multiple applications [44, 45].

Unlike other lipid nanoparticles, the lipid core of NLCs is composed by the blend of a liquid lipid and a solid lipid. The presence of this liquid lipid leads to a more amorphous matrix and a less crystalline state of the carrier, which results in the accommodation of a higher amount of drug molecules compared to other lipid nanoformulations [45]. In this work, Precirol® ATO 5 as the solid lipid and olive oil as a natural liquid lipid were chosen for the lipid core formulation. Precirol® ATO 5 has largely been used as a component of lipid matrix for sustained release formulations and has proven to be effective in the formulation of NLCs for pulmonary delivery [30, 38, 46]. As for liquid lipids, the medium chain triglycerides, known under the brand name Miglyol® 812, are the most commonly employed. However, we selected olive oil as it is thought to reduce the possible cytotoxicity effect of residual surfactants that might be present in the final nanoformulation [37]. Accordingly, we employed an aqueous phase composed by the minimum amount of Tween® 80 (1.3 %, w/v) and Poloxamer 188 (0.66%, w/v), which lead to a nanoformulation

with good physico-chemical stability as previously demonstrated by our group [47, 48]. Particle size and superficial charge are important parameters in NLCs development. Whilst particles sizes below 500 nm are generally thought to escape from phagocytosis by macrophages [49], negative superficial charge of around -20mV is generally correlated with good physical stability of the nanoparticle dispersion [50] as well as their attraction to the positively charged proteins from damaged tissues [45, 51]. Finally, aimed to improve NLC stability, 15% (w/w) of trehalose was chosen as a cryoprotectant since it was found to be the most suitable one for the lyophilization process [38].

Therefore, the aim of this work was to obtain, through the HME-Us method, a NLC formulation with the highest amount of olive oil as the liquid lipid and adequate physico-chemical characteristics. To attain this purpose, various solid-liquid lipid ratios from 10:90 (formulation 1) to 90:10 (formulation 9) were tested. Aqueous phase composition was always the same for all the formulations. As summarized in Table 1, it seemed that the higher the olive oil content, the smaller the particle size, which was then confirmed by TEM micrographs (see Supplementary Materials). These results were in line with other authors, who also reported a decrease in particle size of NLCs when the liquid lipid amount was increased [52-54]. Nevertheless, all formulations displayed adequate sizes between 100 and 200 nm. Due to the dissociation of protons from the carboxylic groups of Precirol after dilution in deionized water (pH 5.6), NLCs exerted a negative superficial charge, which was found to be around -20 mV for all nanoformulations and thus all of them might have good physical stability [55, 56]. In contrast, olive oil content significantly affected the freeze-drying process of the NLCs. Particularly, we found that the amount of olive oil in the lipid core should be ≤50% (w/w) to successfully achieve a lyophilized product (Supplementary Materials, Section S1).

Considering all the aforementioned, formulation 6 with an adequate particle size (~140nm) and superficial charge (~ -22 mV) as well as the highest amount of olive oil in the lipid core (40%, w/w) that allowed a successful lypophilization process, was selected for the forthcoming loading studies.

3.2. Physico-chemical characterization of OLE-loaded nanoparticles

3.2.1. Particle size, z-potential, encapsulation efficiency, morphology and moisture.

As shown in Figure 1A, OLE-loaded NLCs exhibited sizes of around 140 nm (NLC-OLE30), 120 nm (NLC-OLE40) and 150 nm (NLC-OLE50). For the zeta potential, no significant differences were found after OLE

Table 1. Physico-chemical characterization of the developed nanoformulations with different solid lipid (Precirol ATO 5): liquid lipid (olive oil) ratio in the lipid core.

Formulation code	Lipid Core (Precirol:Olive oil, % w/w)	Size (nm)	Z potential (mV)
1	10:90	134.30 ± 5.23	-17.08 ± 1.20
2	20:80	129.62 ± 3.65	-17.03 ± 5.89
3	30:70	123.88 ± 2.43	-18.03 ± 4.01
4	40:60	121.73 ± 1.86	-17.66 ± 4.59
5	50:50	130.27 ± 4.55	-19.82 ± 2.84
6	60:40	141.69 ± 11.43	-21.64 ± 3.72
7	70:30	152.76 ± 27.17	-25.34 ± 4.52
8	80:20	148.50 ± 0.03	-26.16 ± 4.93
9	90:10	158.44 ± 7.57	-19.16 ± 2.52

incorporation into the lipid matrix, indicating that physical stability of the nanoparticles was not disturbed by OLE loading. With regard to the water content, similar low moisture values ranging from 0.4% (NLC-OLE30) to 1.33% (NLC-OLE40) were found. As depicted by the TEM micrographs (Figure 1B), OLE-loaded nanoparticles displayed a uniform and rounded shape. According to the 100nm scale-bars in the images, the mean diameter was found to be less than 200 nm in all cases, validating the results obtained with DLS techniques (Figure 1A). Finally, the entrapment efficiency of OLE (Figure 1A) was above 95% in all cases, and thus, the developed NLCs were validated as an adequate delivery system for future applications.

3.2.2. *In vitro* drug release

Results from the performed *in vitro* release studies, at physiological pH and temperature (pH 7.4 and 37 ºC, respectively), are reported in Figure 1C as the percentage of OLE released over time. A sustained release of the olive polyphenol was detected in all cases up to 27h, which might suggest that OLE was protected inside the core of the lipid carries. For the NLC-OLE40 and NLC-OLE50 formulations, a total OLE-release of ~80% was found by the end of the study (27h). However, NLC-OLE30 showed a significantly lower percentage of released OLE (65% after 27h). It is known that the release profile of OLE could have a significant effect on its antioxidant and bioactive properties. Therefore, aimed to ensure that the obtained release patterns of NLCs were sustained as well as to describe the release mechanism of OLE from the developed NLC matrices, mathematical kinetic models were applied to the experimental data obtained in the release assay (Table 2) [57, 58].

A

Formulation	Size (nm)	Z potential (mV)	Encapsulation eficiency (%)	Release at 27 h	Moisture (%)
NLC-empty	141.69 ± 11.43	-21.64 ± 3.72	-	-	1.16
NLC-OLE30	139.45 ± 5.80	-23.26 ± 1.74	96.57 ± 0.0	65.00 ± 5.04%	0.40
NLC-OLE40	120.70 ± 2.14	-25.13 ± 1.79	95.01 ± 6.6	81.18 ± 6.36%	1.33
NLC-OLE50	156.36 ± 3.77	-21.90 ±0.82	99.12 ± 0.7	79.71 ± 7.64%	0.93

B

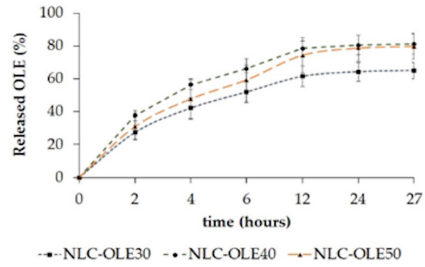

C

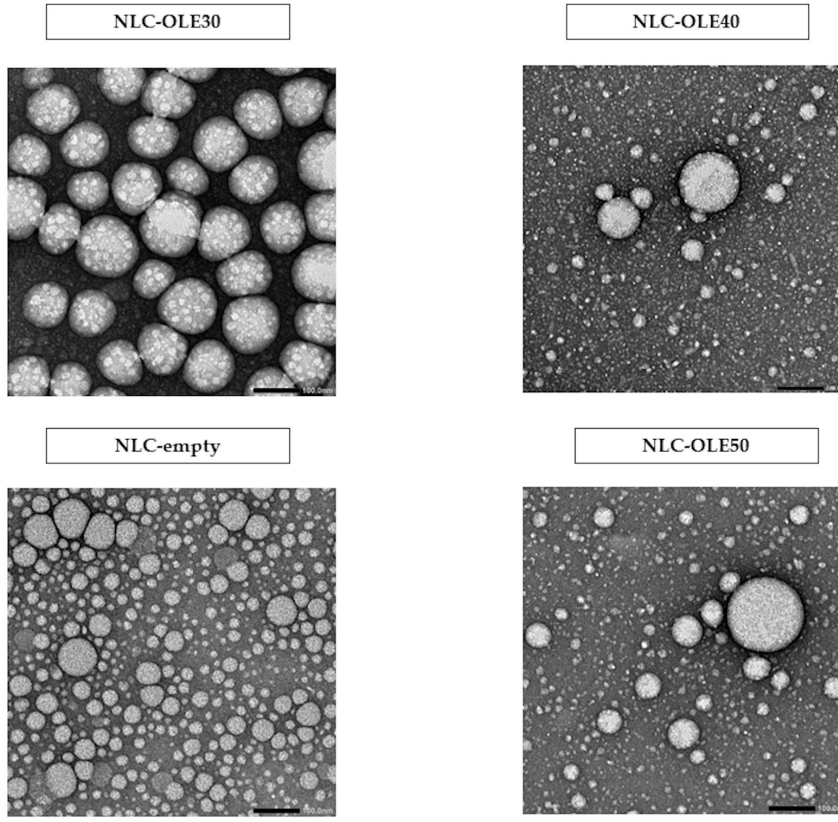

Figure 1. Physico-chemical characterization of freeze-dried nanostuctured lipid carriers: empty (NLC-empty) and oleuropein (OLE) loaded, with a targeted loading of 30% (NLC-OLE30%), 40% (NLC-OLE40%), and 50% (NLC-OLE50) (w/w). (**A**) Particle size, Z potential, encapsulation efficiency, total released OLE and moisture content of NLCs. (**B**) *In vitro* release of OLE from the developed NLCs. (**C**) TEM micrographs of OLE-loaded and empty nanoparticles (NLC-empty). The scale bar indicates 100 nm.

The regression coefficient value (r^2) was used to choose the model that best fitted the data. In this work, Korsmeyer-Peppas showed the highest r^2 for all nanoparticle formulations with r^2 = 0.977 (NLC-OLE30), r^2 = 0.998 (NLC- OLE40) and r^2 = 0.999 (NLC- OLE50), respectively. This type of release has been reported before for some nanostructured lipid carriers [59-61]. In addition, the diffusional exponent '*n*' of the Korsmeyer-Peppas model also described the OLE release mechanism, which in this case was in the range 0.46 to 0.59, indicating that OLE was released by an anomalous transport mechanism [58]. These results imply that probably a combination between erosion and diffusion contributes to the release of the olive polyphenol from the lipid matrix of the nanoparticle.

All in all, we demonstrated the sustained release of OLE via a nanocarrier delivery system that could provide the opportunity to maintain prolonged targeted lung exposures to OLE and thus, longer residence time in lung tissue.

3.2.3. DSC

Crystallization and thermal behavior of nanoparticles are important properties that determine their utility as drug delivery systems [62, 63]. Given this context, DSC thermograms and endothermic events of the bulk solid lipid, bulk OLE, and NLCs (NLC-empty, NLC-OLE30, NLC-OLE40 and NLC-OLE50) were analyzed. Results of the conducted thermal analysis are shown in Figure 2 and Table 3.

Table 2. Oleuropein release parameters of different kinetic models.

SAMPLE	KINETIC MODELS															
	Zero order		**First order**		**Higuchi**		**Baker-Iondslade**		**Hixson-Crowel**		**Hopfenger**		**Korsmeyer-Peppas**			
	r^2	k	r^2	k	r^2	k	r^2	k	r^2	k	r^2	k	r^2	kp	n	
NLC-OLE30	-0.100	3.035	0.551	0.072	0.776	14.87	0.844	0.005	0.871	0.02	0.776	0	**0.977**	21.29	0.46	
NLC-OLE40	-0.157	0	0.741	0.113	0.723	0.019	0.847	0.009	0.585	0.02	0.596	0.020	**0.998**	26.59	0.52	
NLC-OLE50	0.150	3.680	0.836	0.108	0.840	17.89	0.947	0.009	0.708	0.02	0.733	0.022	**0.999**	20.61	0.59	

r^2, determination coefficient; K, release kinetic constant; kp, Korsmeyer-Peppas constant; n, diffusion release exponent.

Solid lipid Precirol® ATO 5 is known to have a melting range from 50ºC to 60ºC. As shown in Figure 2, bulk Precirol® ATO 5 exhibits a sharp and single endothermic peak at 56.00ºC related to its melting point. Since the diester fraction of the glyceride is apparently the only fraction present in the bulk material, the main modification in which Precirol crystallizes should be the stable β-form, as occurs with most solid lipids. The DSC curve of bulk OLE (Figure 2) exerted a small but broad endothermic event, ascribed to its melting point, at 64.70ºC, which ended up at around 103ºC, followed by its decomposition. This result emphasizes the chemical stability of OLE under the nanoparticles´ manufacturing conditions. Poloxamer 188 showed a sharp melting endothermic peak at 56.69ºC and trehalose anhydrous displayed its melting endotherm at 211.82ºC. For the thermograms of OLE-loaded and unloaded NLCs, they showed two broadening endothermic peaks. The highest temperature endotherms (around 56ºC) can be seen as a shoulder and are similar to the peak of Poloxamer 188. The other endothermic event, around 50ºC, was at lower temperatures than that of the solid lipid. It can be seen that these peaks were broader for NLC-empty. Therefore, there was a clear melting point depression in all NLCs' thermograms. This phenomenon is generally ascribed to the transformation of the bulk solid lipid into its nanoparticle form as a result of their higher specific surface area or the possible chemical interactions between solid lipid and liquid lipid/or surfactants/ or drugs that could take place during the nanoparticle production process and affect crystallization and result in a lower melting enthalpy. Furthermore, the melting peak of OLE (64.7ºC) seemed to be absent in NLC-OLE formulations, suggesting that the encapsulated olive polyphenol was in an amorphous state. As a result, we assumed that NLCs might offer a greater bioavailability of OLE, as the melting point, an indicator of intermolecular attractive forces, is usually lower for non-crystalline substances.

As expected, the addition of olive oil into the nanoparticle matrix clearly decreased the energy required to melt the lipid (Table 3). On the other hand, Table 3 shows the enthalpy values for bulk Precirol (-150.56 J/g), NLC-empty (-90.21 J/g), NLC-OLE30 (-56.22 J/g), NLC-OLE40 (57.15 J/g), and NLC-OLE50 (63.09 J/g). Furthermore, all nanoformulations showed a lower crystallinity index (CI) than bulk solid lipid. Interestingly, OLE-loaded NLCs displayed a greater decrease in both enthalpy and CI values compared to NLC-empty. This energy reduction could be ascribed to the transformation of the solid lipid (Precirol) into a less-ordered metastable β'-form, which leads to a disruption of the crystalline structure and diminish the CI, whicht could allow enough space to accommodate OLE molecules.

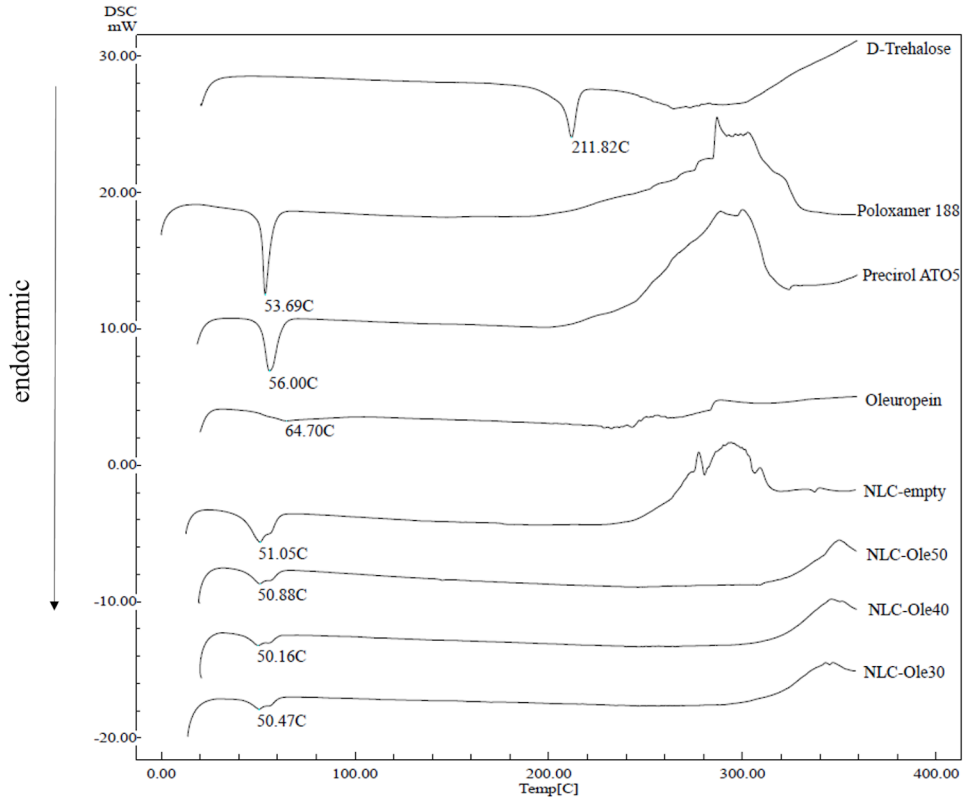

Figure 2. Differential scanning calorimetry (DSC) graphs of pure excipients (D-trehalose, Poloxamer 188, Precirol ATO 5, oleuropein (OLE), developed nanoparticles with OLE (NLC-OLE30, NLC-OLE40, NLC-OLE50), and without OLE (NLC-empty).

Table 3. Thermal properties of Precirol and nanoparticles (NLC-empty, NLC-OLE30, NLC-OLE40, NLC-OLE50).

Sample	Melting point (ºC)	Onset (ºC)	Endset (ºC)	Enthalpy (-J/g)	CI (%)
Precirol® ATO5	56.00	50.12	62.97	-150.56	100.00
NLC-empty	51.05	40.18	61.28	-90.21	59.92
NLC-OLE30	50.47	41.71	61.34	-56.22	37.34
NLC-OLE40	50.16	43.27	61.38	-57.15	37.96
NLC-OLE50	50.88	40.86	62.67	-63.09	41.90

CI (%): Crystallinity index.

Thus, the developed NLCs seemed to be a potential carrier for OLE, and NLC-OLE50 was selected to continue with the rest of the assays, since this formulation exhibited good physico-chemical characteristics together with the highest OLE amount.

3.2.4. Radical scavenging activity by DPPH assay

The main bioactivity of OLE is related to its ability to eliminate free radicals and to prevent lipid peroxidation, which, in the end, contributes to alleviate the injuries caused by oxidative stress as described elsewhere. Given this, the next step of this work was to verify that the antioxidant activity of OLE was not disturbed by the nanoformulation process, and thus the radical scavenging activity of NLC-OLE50 was assayed. As shown in Figure 3, free OLE had an antioxidant power of 55.33 ± 1.94%, which was significantly enhanced by its incorporation in NLCs (61.22 ± 0.38%). These results could be ascribed to the higher specific area of the nanoparticles for chemical quenching as well as the protection of the polyphenol against external agents into the lipid matrix. Similarly, the encapsulation of other natural compounds such as β-carotene or quercetin into protein-based and polyvinyl alcohol–based nanoparticles, respectively, as well as the co-loading of tocopherol and ascorbic acid in nutriosomes have been shown to significantly improve their DPPH radical scavenging activity [64-66]. It is worth noting that unloaded-NLCs did not exhibit any radical scavenging activity (-3.84 ± 1.79 %) and thus, the lipid excipients of the carrier had no influence on the antioxidant power of NLC-OLE50. Hence, we demonstrated that the nanoencapsulation process through the hot-melt homogenization technique did not decreased OLE activity but improved it.

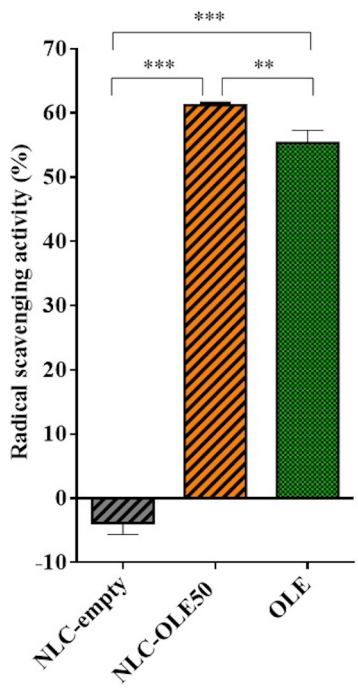

Figure 3. 2,2-diphenyl-1-picylhydrazyl (DPPH) radical scavenging assay of NLC-OLE50 and equivalent amounts of free OLE and NLC-empty. Results are expressed as mean % of DPPH radical scavenging activity compared to the control ± SD; n=3; *p<0.05, *** p<0.001.

3.3. Cell experiments

In light of the characterization results, NLC-OLE50 seemed to be a promising carrier for OLE with enhanced antioxidant activity and thus we continued to study its efficacy in lung epithelial cell models. Several authors have reported micro and nanoencapsulation methods for olive leaf extracts but to the best of

our knowledge, there is a lack of studies regarding the impact that the formulation process could have on the bioactivity of this polyphenol in a biological system [22, 23, 52].

3.3.1. Cell viability studies

Nanotoxicology has gained special attention during the last decades. The main disadvantage of nanoscale drug delivery systems is their potential cytotoxicity [44]. Generally, nanoparticle toxicity is correlated with the type of excipients and organic solvents employed during the manufacturing process that remain in the final formulation. In this work, we proposed NLCs made up with generally recognized as safe (GRAS) excipients and the use of organic solvents was avoided during their preparation. Moreover, the encapsulated natural compound is known to have low toxicity. Altogether, they lead us to hypothesize that NLC-OLE50 will result in a highly biocompatible formulation with minimum toxicity to the lung epithelium. Therefore, with the aim to prove our hypothesis and thereafter, select the appropriate NLCs concentration for cellular oxidative stress studies, the biocompatibility of the formulations was assayed by the CCK-8 test in A549, CuFi-1 and NuLi-1 cell lines as models of pathological and healthy pulmonary epithelia (Figure 4).

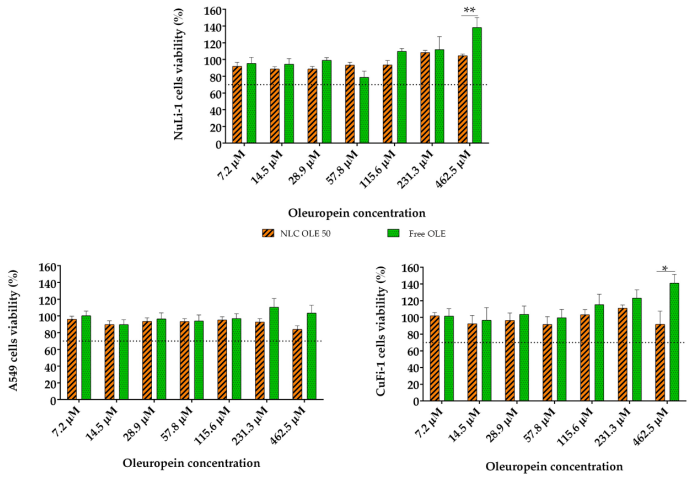

Figure 4. Effect of nanoencapsulated (NLC-OLE50) and free oleuropein (OLE) at different concentrations on the viability of A549, NuLi-1 and CuFi-1 cell lines within 24h. The results are given as the mean % of living cells compared to the control ± SD, n = 3. * $p < 0.05$, ** $p<0.01$.

Different concentrations of OLE ranging from 7.2 to 462.5 μM and its equivalent amount in NLCs were tested after 24 h of incubation. Equivalent concentrations of empty NLCs were also assayed as the control. Cell viability values >70% are considered as "no toxicity" [67] and thus, we assumed that NLCs as well as OLE were biocompatible with the tested lung epithelial cell lines. It is worth noting that NLC-empty did not shown any toxic effect, confirming the biocompatibility of the excipients of the NLCs (Supplementary Materials, Section S2). This finding is in accordance with other reports that demonstrated the good tolerability of lipid nanoparticles in lung epithelial cell lines [30, 68, 69]. Considering these results, OLE concentrations from 115.6 to 462 μM and their equivalent amount in NLC-OLE50 were chosen for the following antioxidant activity studies.

3.3.2. Antioxidant activity of NLCs in lung epithelial cells: CAA assay

The oxidative stress pathway has gained special attention as a novel target for the treatment of a number of diseases. Particularly within the lungs, oxidative stress has been correlated with cystic fibrosis progression as well as cancerogenesis mechanisms among others, in which natural antioxidants have been proposed as promising candidates[1, 3-6]. Our optimized NLC-OLE50 had been demonstrated, by chemical analysis, to improve the radical scavenging power of OLE. Moreover, the size of our NLCs fell within the favorable range (100–200 nm) for an efficient cellular uptake, most likely to be taken up through the cell membranes by endocytosis mechanisms [70, 71]. Beyond this, we had demonstrated a sustained release of the olive polyphenol from the lipid matrix within 24h and thus, we assumed that OLE, which is protected inside the lipid core, might be progressively released to the cell, avoiding its rapid degradation and metabolism to other polyphenols (i.e. hydroxytyrosol, tyrosol, oleuropein aglycone), thus preserving or even improving its efficacy against oxidative stress. Altogether, this lead us to hypothesize that NLC-OLE50 could be a promising carrier for OLE towards oxidative stress related injuries in lung epithelia. However, the lack of *in vivo* data about OLE efficacy in the lungs encouraged as to conduct a preliminary cell-based study to further confirm its effectiveness in lung cells.

Given this scenario, the radical scavenging activity of NLC-OLE50 and OLE was measured in ABAP-stressed A549, CuFi-1, and NuLi-1, as human-lung epithelial cell models, after 24 h of exposure to the mentioned treatments. The morphology of the cells was always checked to ensure that the induced oxidative damage did not cause cell death. Obtained results are displayed in Figure 5 as the percentage of intracellular ROS levels compared to the positive control (~100% of ROS levels).

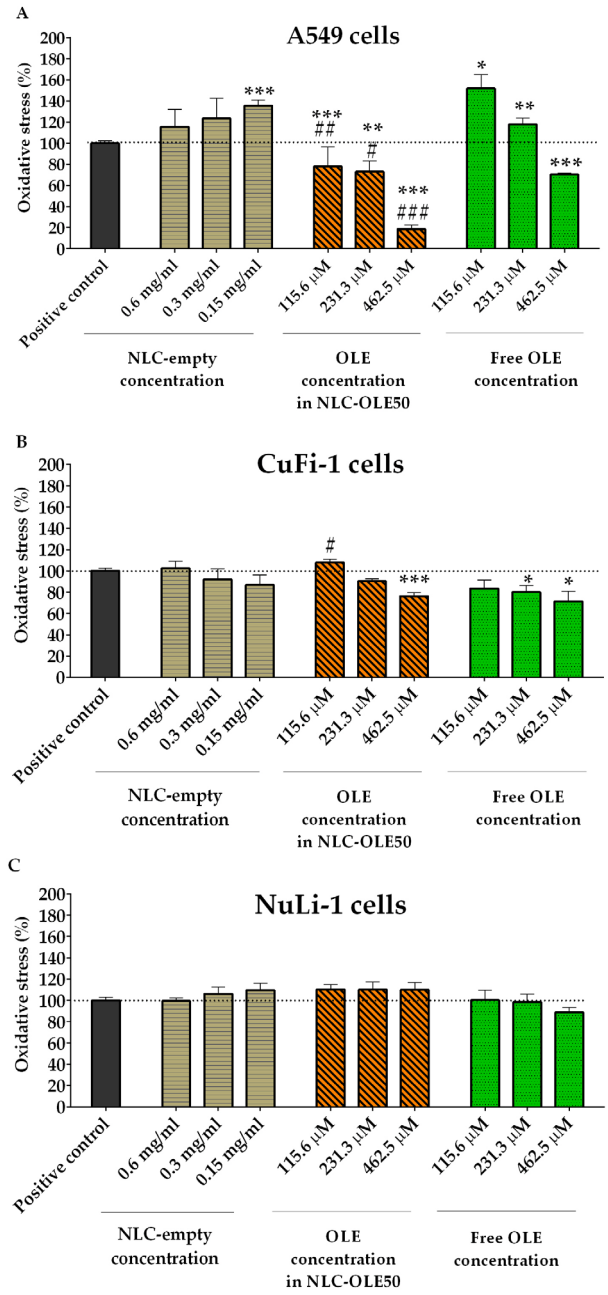

Figure 5. Antioxidant activity of free oleuropein (OLE), encapsulated OLE (NLC-OLE50) and empty nanoparticles (NLC-empty) in ABAP-stressed A549 (A), CuFi-1 (B) and NuLi-1 (C) cells. The mean percentages of DCF fluorescence, as a measure of oxidative stress, are shown in relation to the positive control (set to 100%). Depicted results are the means ± standard error of the mean of at least three independent experiments. * $p < 0.05$, ** $p<0.01$, ***$p<0.001$ vs positive control; # $p<0.05$, ## $p<0.01$, ### $p<0.001$ vs free OLE.

Following our hypothesis, NLC-OLE50 clearly alleviated the oxidative stress status of A549 cells, which was found to be dose-dependent (Figure 5A). It should be noted that non-encapsulated OLE was only able to reduce ROS at the highest concentration tested (462.5 μM, $p<0.001$) and, most importantly, it exerted prooxidant effects at 115μM ($p<0.05$) and 231μM ($p<0.01$).

This result is in line with other authors who have demonstrated the prooxidant activity of OLE in some specific cancer cell lines of human breast cancer [72, 73] and hepatocarcinoma [74]. However, there is still a lack of studies to further justify these findings. Therefore, we assumed that NLC-OLE50 significantly enhanced the antioxidant power of OLE in A549 cell line, and this finding might be ascribed to a better permeability across cell membranes of the NLCs as well as their well-known higher uptake by the cellular model [65, 75, 76]. For the CuFi-1 human cells, NLC-OLE50 was demonstrated to preserve the moderate antioxidant power of OLE. Similarly, Hatahet et al. showed that the encapsulation of quercetin into NLCs did not improve its antioxidant activity, but preserved it in acute monocytic leukaemia cells [77]. Evidence suggests that the misfolded CFTR protein can be modulated through antioxidant and prooxidant effects in cell environment and thus, we assumed that NLC-OLE50 and OLE might have interacted with the misfolded CFTR protein in CuFi-1 cells [1, 78, 79]. Unexpectedly, with regard to healthy epithelial cells (NuLi-1), neither free nor encapsulated OLE exerted any effect against ABAP produced peroxyl radical reaction, which could be ascribed to the inherent capacity of normal airways to cope with oxidative stress by themselves [79].

Given the aforementioned, the cellular antioxidant effects of NLC-OLE50 clearly depend on the studied cell line, which could be correlated with their different cellular uptake mechanisms. Nanoparticles are generally thought to be internalized through endocytosis mechanisms (i.e. phagocytosis, pinocytosis, clathrin-mediated and caveolae/raft-mediated transports). Previous studies from our group demonstrated that the composition of the nanoparticles together with the type of cell can determine the predominant endocytosis mechanisms for their uptake and intracellular distribution, which ultimately affect the delivery of the active compound and the efficacy of the formulation [80-82]. These findings are in line with other authors who have demonstrated that the uptake of nanospheres by A549 cells could occur by clathrin-mediated endocytosis (PLGA and chitosan-PLGA nanospheres, 100 nm) as well as by the caveolae/raft-dependent transport (wheat germ agglutinin-conjugated PLGA nanospheres, 200 nm) [83]. On the other hand, evidence also suggests that depending on the size, shape and surface charge of the nanoparticles, a particular cellular internalization route may be preferred over others. From the scarce

data available about nanoparticles efficacy in cystic fibrosis cells, we found that authors have given special attention to the surface chemistry of the NLCs as an important influence factor for their cellular uptake and thus, one possibility to enhance our NLC activity in CuFi-1 cells could be the modification of their superficial charge. However, whilst some authors have suggested that decreasing the surface charge of nanoparticles up to -50mV could enhance their cellular uptake (CuFi-1 cells) [84], others have postulated that positive superficial charge is required to promote their internalization (CFBE41o- cells)[85] and thus it is highlighted again that special attention should be given not only to particle superficial charge but also to the cell line and its predominant endocytosis mechanisms of transport. Similarly, the A549 cells were also shown to be more sensitive to OLE activity compared to the CuFi-1 and NuLi-1 cells. Since passive diffusion through cellular membranes is almost similar for al cells, scientific evidence suggests that differences in the active membrane transports are likely responsible for the differences observed in the CAA results between cell lines. Accordingly, the glucose moiety of OLE is known to interact with the membrane glucose transporter proteins (GLUT), allowing its diffusion into the cells. It is known that GUT are overexpressed in A549 cell membranes and thus we assumed that a higher uptake of OLE could have occurred in these cells, which ultimately might have led to a more pronounced intracellular antioxidant effect compared to the other cell lines [86]. A similar phenomenon has been found for the natural flavonoids quercetin, catechin and epicatechin which had superior antioxidant activities in Caco-2 compared to the HepG2 cell lines, probably due to a higher accumulation in Caco-2 cells [87, 88]. However, little data is available about the role of transporters in cellular accumulation and evidence for individual phenolic compounds remains at a basic level. Finally, it should be noted that NLC-empty did not show any effect in the tested cell lines with the exception of A549 cells, in which the highest tested concentration seemed to increase ROS generation but without toxic effects.

All in all, the preserved antioxidant activity of OLE in NLCs holds great promise for transporting this natural polyphenol to the lung epithelia but further studies should be conducted to elucidate their internalization mechanism and intracellular trafficking processes in the proposed cells, which can be modulated by optimizing the formulations toward more efficient nanocarriers.

4. Conclusions

Whilst a number of preclinical data have revealed the therapeutic properties of olive polyphenols as plant extracts or pure synthetic molecules, scarce studies are available concerning isolated OLE and

more specifically, naturally obtained OLE. In this work, OLE, a natural antioxidant with poor stability and compromised bioavailability, was successfully formulated in highly biocompatible NLCs. Optimized nanoparticles exhibited a mean size of 150 nm and demonstrated to be effective in loading up to 50% (w/w) of OLE with an encapsulation efficiency of 99.12%. Additionally, NLCs showed a sustained release kinetic of OLE from the lipid core and an enhanced antioxidant power was proven in the DPPH assay. Moreover, the rapid and simple proposed formulation process avoided the use of organic solvents and OLE loading was significantly higher compared to the other reported methods [25, 27, 28, 89]. NLCs were found to be biocompatible in three lung epithelial cell lines, indicating their safety for lung administration. Interestingly, NLCs were shown to enhance and maintain the OLE protection effect against oxidative stress in lung cancer and cystic fibrosis cells, respectively, and thus, they could hold great promise for transporting this natural polyphenol to the lung epithelial cells. Nonetheless, further formulation studies should be conducted to obtain an adequate final formulation for pulmonary administration of NLC-OLE50 (i.e. dry powder for inhalation) [90-92].

Supplementary Materials: The following are available online at https://www.mdpi.com/1999-4923/12/5/429/s1, Section S1: Nanoparticle morphology and success in freeze-drying process of blank nanoparticles. Section S2: Cell viability assay of NLC-empty.

Author Contributions: A.H-C. for design and performance of experiments, data analysis and writing. M. M-S collaborated in the performance and analysis of in vitro release and cell experiments. TB.L-M. revision of the manuscript. E.G. revision of the manuscript. JL.P. conceptualization, advised all research, design of experiments, evaluation and discussion of results, revision of manuscript and provided research funding. All authors have read and agreed to the published version of the manuscript.

Funding: A.H-C. thanks the Spanish Ministry of Economy and Competitiveness for the Industrial Doctorate fellowship grant (DI-15-07513). This work was done under the R&D projects of BIOSASUN and supported by the University of the Basque Country (UPV/EHU) and the Basque Country Government (Grupos Consolidados, No ref: IT907-16 to JL. P).

Acknowledgments: Authors wish to thank the ICTS "NANBIOSIS" and the Drug Formulation Unit (U10) of the CIBER in Bioengineering, Biomaterials and Nanomedicine (CIBER-BBN) at the University of Basque Country (UPV/EHU). Finally, the authors acknowledge SGIker (UPV/EHU) for their technical and

human support on TEM images in this study.

Conflicts of Interest: The authors declare no conflict of interest.

References

1 Galli, F.; Battistoni, A.; Gambari, R.; Pompella, A.; Bragonzi, A.; Pilolli, F.; Iuliano, L.; Piroddi, M.; Dechecchi, M.C.; Cabrini, G. Oxidative stress and antioxidant therapy in cystic fibrosis. Biochim. Biophys. Acta **2012**, 1822, 690–713. [Google Scholar] [CrossRef]

2 Ziady, A.G.; Hansen, J. Redox balance in cystic fibrosis. Int. J. Biochem. Cell Biol. **2014**, 52, 113–123. [Google Scholar] [CrossRef] [PubMed]

3 Van der Vliet, A.; Janssen-Heininger, Y.M.W.; Anathy, V. Oxidative stress in chronic lung disease: From mitochondrial dysfunction to dysregulated redox signaling. Mol. Asp. Med. **2018**, 63, 59–69. [Google Scholar] [CrossRef] [PubMed]

4 Reuter, S.; Gupta, S.C.; Chaturvedi, M.M.; Aggarwal, B.B. Oxidative stress, inflammation, and cancer: How are they linked? Free Radic. Biol. Med. **2010**, 49, 1603–1616. [Google Scholar] [CrossRef] [PubMed]

5 Ciofu, O.; Smith, S.; Lykkesfeldt, J. Antioxidant supplementation for lung disease in cystic fibrosis. Cochrane Database Syst. Rev. **2019**, 2019. [Google Scholar] [CrossRef]

6 Nash, K.M.; Ahmed, S. Nanomedicine in the ROS-mediated pathophysiology: Applications and clinical advances. Nanomed. Nanotechnol. Biol. Med. **2015**, 11, 2033–2040. [Google Scholar] [CrossRef]

7 Al-Azzawie, H.F.; Alhamdani, M.-S. Hypoglycemic and antioxidant effect of oleuropein in alloxan-diabetic rabbits. Life Sci. **2006**, 78, 1371–1377. [Google Scholar] [CrossRef]

8 He, Z.; Deng, X.; But, P.P.; Ooi, V.E.; Xu, H.; Lee, S.H.; Lee, S. In Vitro Evaluation of Secoiridoid Glucosides from the Fruits of Ligustrum Lucidum as Antiviral Agents. Chem. Pharm. Bull. **2001**, 49, 1471–1473. [Google Scholar] [CrossRef]

9 Bisignano, G.; Tomaino, A.; Cascio, R.L.; Crisafi, G.; Uccella, N.; Saija, A. On the in-vitro antimicrobial activity of oleuropein and hydroxytyrosol. J. Pharm. Pharmacol. **1999**, 51, 971–974. [Google Scholar] [CrossRef]

10 Zbidi, H.; Salido, S.; Altarejos, J.; Perez-Bonilla, M.; Bartegi, A.; Rosado, J.A.; Salido, G.M. Olive tree wood phenolic compounds with human platelet antiaggregant properties. Blood Cells Mol. Dis. **2009**, 42, 279–285. [Google Scholar] [CrossRef]

11 Shamshoum, H.; Vlavcheski, F.; Tsiani, E. Anticancer effects of oleuropein. Biofactors **2017**, 43, 517–528. [Google Scholar] [CrossRef] [PubMed]

12 Przychodzen, P.; Wyszkowska, R.; Gorzynik-Debicka, M.; Kostrzewa, T.; Kuban-Jankowska, A.; Gorska-Ponikowska, M. Anticancer potential of oleuropein, the polyphenol of olive oil, with 2-methoxyestradiol, separately or in combination, in human osteosarcoma cells. Anticancer Res. **2019**, 39, 1243–1251. [Google Scholar] [CrossRef] [PubMed]

13 Ahmadvand, H.; Noori, A.; Dehnoo, M.G.; Bagheri, S.; Cheraghi, R.A. Hypoglycemic, hypolipidemic and antiatherogenic effects of oleuropein in alloxan-induced Type 1 diabetic rats. Asian Pac. J. Trop. Dis. **2014**, 4, S421–S425. [Google Scholar] [CrossRef]

14 Castejon, M.L.; Sánchez-Hidalgo, M.; Aparicio-Soto, M.; González-Benjumea, A.; Fernández-Bolaños, J.G.; Alarcón-de-la-Lastra, C. Olive secoiridoid oleuropein and its semisynthetic acetyl-derivatives reduce LPS-induced inflammatory response in murine peritoneal macrophages via JAK-STAT and MAPKs signaling pathways. J. Funct. Foods **2019**, 58, 95–104. [Google Scholar] [CrossRef]

15 Crascì, L.; Lauro, M.R.; Puglisi, G.; Panico, A. Natural antioxidant polyphenols on inflammation management: Anti-glycation activity vs metalloproteinases inhibition. Crit. Rev. Food Sci. Nutr. **2018**, 58, 893–904. [Google Scholar] [CrossRef]

16 European Medicines Agency. Assessment Report on Olea europaea L., folium; EMA: London, UK, 2017.

17 European Commission. Regulation EC No. 432/2012 establishing a list of permitted health claims made on foods, other than those referring to the reduction of disease risk and to children's development and health. Off. J. Eur. Union **2012**, L136, 1–40. [Google Scholar]

18 De Vos, P.; Faas, M.M.; Spasojevic, M.; Sikkema, J. Encapsulation for preservation of functionality and targeted delivery of bioactive food components. Int. Dairy J. **2010**, 20, 292–302. [Google Scholar] [CrossRef]

19 Carrera-González, M.; Ramírez-Expósito, M.; Mayas, M.; Martínez-Martos, J. Protective role of oleuropein and its metabolite hydroxytyrosol on cancer. Trends Food Sci. Technol. **2013**, 31, 92–99. [Google Scholar] [CrossRef]

20 Puglia, C.; Lauro, M.R.; Tirendi, G.G.; Fassari, G.E.; Carbone, C.; Bonina, F.; Puglisi, G. Modern drug delivery strategies applied to natural active

compounds. Expert Opin. Drug Deliv. **2017**, 14, 755–768. [Google Scholar] [CrossRef]

21 Mohammadi, A.; Jafari, S.M.; Esfanjani, A.F.; Akhavan, S. Application of nano-encapsulated olive leaf extract in controlling the oxidative stability of soybean oil. Food Chem. **2016**, 190, 513–519. [Google Scholar] [CrossRef]

22 Gharehbeglou, P.; Jafari, S.M.; Homayouni, A.; Hamishekar, H.; Mirzaei, H. Fabrication of double W1/O/W2 nanoemulsions loaded with oleuropein in the internal phase (W1) and evaluation of their release rate. Food Hydrocoll. **2019**, 89, 44–55. [Google Scholar] [CrossRef]

23 Reddy, K.B. In Vitro-In Vivo Characterization of Oleuropein loaded Nanostructured Lipid Carriers in the Treatment of Streptococcus pneumoniae induced Meningitis. Asian J. Pharm. **2019**, 13. [Google Scholar] [CrossRef]

24 Kosaraju, S.L.; D'ath, L.; Lawrence, A. Preparation and characterisation of chitosan microspheres for antioxidant delivery. Carbohydr. Polym. **2006**, 64, 163–167. [Google Scholar] [CrossRef]

25 González, E.; Gómez-Caravaca, A.M.; Giménez, B.; Cebrián, R.; Maqueda, M.; Martínez-Férez, A.; Segura-Carretero, A.; Robert, P. Evolution of the phenolic compounds profile of olive leaf extract encapsulated by spray-drying during in vitro gastrointestinal digestion. Food Chem. **2019**, 279, 40–48. [Google Scholar] [CrossRef] [PubMed]

26 Mourtzinos, I.; Salta, F.; Yannakopoulou, K.; Chiou, A.; Karathanos, V.T. Encapsulation of olive leaf extract in β-cyclodextrin. J. Agric. Food Chem. **2007**, 55, 8088–8094. [Google Scholar] [CrossRef] [PubMed]

27 Belščak-Cvitanović, A.; Stojanović, R.; Manojlović, V.; Komes, D.; Cindrić, I.J.; Nedović, V.; Bugarski, B. Encapsulation of polyphenolic antioxidants from medicinal plant extracts in alginate–chitosan system enhanced with ascorbic acid by electrostatic extrusion. Food Res. Int. **2011**, 44, 1094–1101. [Google Scholar] [CrossRef]

28 Tavakoli, H.; Hosseini, O.; Jafari, S.M.; Katouzian, I. Evaluation of physicochemical and antioxidant properties of yogurt enriched by olive leaf phenolics within nanoliposomes. J. Agric. Food Chem. **2018**, 66, 9231–9240. [Google Scholar] [CrossRef]

29 Weber, S.; Zimmer, A.; Pardeike, J. Solid lipid nanoparticles (SLN) and nanostructured lipid carriers (NLC) for pulmonary application: A review of the state of the art. Eur. J. Pharm. Biopharm. **2014**, 86, 7–22. [Google Scholar] [CrossRef]

30 Moreno-Sastre, M.; Pastor, M.; Esquisabel, A.; Sans, E.; Viñas, M.; Fleischer, A.; Palomino, E.; Bachiller, D.; Pedraz, J.L. Pulmonary delivery of tobramycin-loaded nanostructured lipid carriers for Pseudomonas aeruginosa infections associated with cystic fibrosis. Int. J. Pharm. **2016**, 498, 263–273. [Google Scholar] [CrossRef]

31 Müller, R.H.; Shegokar, R.; Keck, C.M. 20 years of lipid nanoparticles (SLN & NLC): Present state of development & industrial applications. Curr. Drug Discov. Technol. **2011**, 8, 207–227. [Google Scholar] [CrossRef]

32 Puglia, C.; Pignatello, R.; Fuochi, V.; Furneri, P.M.; Lauro, M.R.; Santonocito, D.; Cortesi, R.; Esposito, E. Lipid nanoparticles and active natural compounds: A perfect combination for pharmaceutical applications. Curr. Med. Chem. **2019**, 26, 4681–4696. [Google Scholar] [CrossRef] [PubMed]

33 Schneider, H.; Braun, A.; Füllekrug, J.; Stremmel, W.; Ehehalt, R. Lipid based therapy for ulcerative colitis-modulation of intestinal mucus membrane phospholipids as a tool to influence inflammation. Int. J. Mol. Sci. **2010**, 11, 4149–4164. [Google Scholar] [CrossRef] [PubMed]

34 Beloqui, A.; Memvanga, P.B.; Coco, R.; Reimondez-Troitiño, S.; Alhouayek, M.; Muccioli, G.G.; Alonso, M.J.; Csaba, N.; de la Fuente, M.; Préat, V. A comparative study of curcumin-loaded lipid-based nanocarriers in the treatment of inflammatory bowel disease. Colloids Surf. B Biointerfaces **2016**, 143, 327–335. [Google Scholar] [CrossRef] [PubMed]

35 Müller, R.H.; Radtke, M.; Wissing, S.A. Nanostructured lipid matrices for improved microencapsulation of drugs. Int. J. Pharm. **2002**, 242, 121–128. [Google Scholar] [CrossRef]

36 Pyo, S.M.; Müller, R.H.; Keck, C.M. Encapsulation by nanostructured lipid carriers. In Nanoencapsulation Technologies for the Food and Nutraceutical Industries; Academic Press: Cambridge, MA, USA, 2017; pp. 114–137. [Google Scholar]

37 Talegaonkar, S.; Bhattacharyya, A. Potential of lipid nanoparticles (SLNs and NLCs) in enhancing oral bioavailability of drugs with poor intestinal permeability. AAPS PharmSciTech **2019**, 20, 121. [Google Scholar] [CrossRef]

38 Pastor, M.; Moreno-Sastre, M.; Esquisabel, A.; Sans, E.; Viñas, M.; Bachiller, D.; Asensio, V.J.; Del Pozo, Á.; Gainza, E.; Pedraz, J.L. Sodium colistimethate loaded lipid nanocarriers for the treatment of Pseudomonas aeruginosa infections associated with cystic fibrosis. Int. J. Pharm. **2014**, 477, 485–494. [Google Scholar] [CrossRef]

39 Zuo, J.; Gao, Y.; Bou-Chacra, N.; Löbenberg, R. Evaluation of the DDSolver software applications. BioMed Res. Int. **2014**, 2014. [Google Scholar] [CrossRef]

40 Li, F.; Jin, H.; Xiao, J.; Yin, X.; Liu, X.; Li, D.; Huang, Q. The simultaneous loading of catechin and quercetin on chitosan-based nanoparticles as effective antioxidant and antibacterial agent. Food Res. Int. **2018**, 111, 351–360. [Google Scholar] [CrossRef]

41 The Food and Drug Administration, Center for Drug Evaluation and Research (CDER). Quality Considerations for Continuous Manufacturing: Guidance for Industry; FDA: White Oak, MD, USA, 2019; p. 27.

42 Bhagurkar, A.M.; Repka, M.A.; Murthy, S.N. A Novel Approach for the Development of a Nanostructured Lipid Carrier Formulation by Hot-Melt Extrusion Technology. J. Pharm. Sci. **2017**, 106, 1085–1091. [Google Scholar] [CrossRef]

43 Singh, Y.; Meher, J.G.; Raval, K.; Khan, F.A.; Chaurasia, M.; Jain, N.K.; Chourasia, M.K. Nanoemulsion: Concepts, development and applications in drug delivery. J. Control. Release **2017**, 252, 28–49. [Google Scholar] [CrossRef]

44 Moreno-Sastre, M.; Pastor, M.; Salomon, C.J.; Esquisabel, A.; Pedraz, J.L. Pulmonary drug delivery: A review on nanocarriers for antibacterial chemotherapy. J. Antimicrob. Chemother. **2015**, 70, 2945–2955. [Google Scholar] [CrossRef] [PubMed]

45 Beloqui, A.; Solinís, M.Á.; Rodríguez-Gascón, A.; Almeida, A.J.; Préat, V. Nanostructured lipid carriers: Promising drug delivery systems for future clinics. Nanomed. Nanotechnol. Biol. Med. **2016**, 12, 143–161. [Google Scholar] [CrossRef] [PubMed]

46 Pastor, M.; Basas, J.; Vairo, C.; Gainza, G.; Moreno-Sastre, M.; Gomis, X.; Fleischer, A.; Palomino, E.; Bachiller, D.; Gutiérrez, F.B.; et al. Safety and effectiveness of sodium colistimethate-loaded nanostructured lipid carriers (SCM-NLC) against P. aeruginosa: In vitro and in vivo studies following pulmonary and intramuscular administration. Nanomed. Nanotechnol. Biol. Med. **2019**, 18, 101–111. [Google Scholar] [CrossRef] [PubMed]

47 Moreno-Sastre, M.; Pastor, M.; Esquisabel, A.; Sans, E.; Viñas, M.; Bachiller, D.; Pedraz, J.L. Stability study of sodium colistimethate-loaded lipid nanoparticles. J. Microencapsul. **2016**, 33, 636–645. [Google Scholar] [CrossRef] [PubMed]

48 Gartziandia, O.; Herran, E.; Pedraz, J.L.; Carro, E.; Igartua, M.; Hernandez, R.M. Chitosan coated nanostructured lipid carriers for brain delivery of proteins by intranasal administration. Nanomed. Nanotechnol. Biol. Med. **2015**, 134, 304–313. [Google Scholar] [CrossRef]

49 Mansour, H.M.; Rhee, Y.S.; Wu, X. Nanomedicine in pulmonary delivery. Int. J. Nanomed. **2009**, 4, 299–319. [Google Scholar] [CrossRef]

50 Das, S.; Ng, W.K.; Tan, R.B.H. Are nanostructured lipid carriers (NLCs) better than solid lipid nanoparticles (SLNs): Development, characterizations and comparative evaluations of clotrimazole-loaded SLNs and NLCs? Eur. J. Pharm. Sci. **2012**, 47, 139–151. [Google Scholar] [CrossRef]

51 Lamprecht, A.; Schäfer, U.; Lehr, C. Size-dependent bioadhesion of micro- and nanoparticulate carriers to the inflamed colonic mucosa. Pharm. Res. **2001**, 18, 788–793. [Google Scholar] [CrossRef]

52 Soleimanifard, M.; Sadeghi Mahoonak, A.; Ghorbani, M.; Heidari, R.; Sepahvand, A. The formulation optimization and properties of novel oleuropein-loaded nanocarriers. J. Food Sci. Technol. **2019**. [Google Scholar] [CrossRef]

53 Ma, Q.H.; Wang, Y.W.; Lin, X.F.; Luo, D.; Gu, N. Preparation, Characterization and Photoprotection of Tocopherol Loaded Nanostructured Lipid Carriers. In Proceedings of the 2007 IEEE/ICME International Conference on Complex Medical Engineering, Beijing, China, 23–27 May 2007; pp. 203–208. [Google Scholar]

54 Gokce, E.H.; Korkmaz, E.; Dellera, E.; Sandri, G.; Cristina Bonferoni, M.; Ozer, O. Resveratrol-loaded solid lipid nanoparticles versus nanostructured lipid carriers: Evaluation of antioxidant potential for dermal applications. Int. J. Nanomed. **2012**, 7, 1841–1850. [Google Scholar] [CrossRef]

55 Obeidat, W.M.; Schwabe, K.; Müller, R.H.; Keck, C.M. Preservation of nanostructured lipid carriers (NLC). Eur. J. Pharm. Biopharm. **2010**, 76, 56–67. [Google Scholar] [CrossRef]

56 Chen, Y.; Zhou, L.; Yuan, L.; Zhang, Z.; Liu, X.; Wu, Q. Formulation, characterization, and evaluation of in vitro skin permeation and in vivo pharmacodynamics of surface-charged tripterine-loaded nanostructured lipid carriers. Int. J. Nanomed. **2012**, 7, 3023–3033. [Google Scholar] [CrossRef]

57 Siepmann, J.; Siepmann, F. Mathematical modeling of drug release from lipid dosage forms. Int. J. Pharm. **2011**, 418, 42–53. [Google Scholar] [CrossRef] [PubMed]

58 Dash, S.; Murthy, P.N.; Nath, L.; Chowdhury, P. Kinetic modeling on drug release from controlled drug delivery systems. Acta Pol. Pharm. Drug Res. **2010**, 67, 217–223. [Google Scholar]

59 Kalam, M.A.; Sultana, Y.; Ali, A.; Aqil, M.; Mishra, A.K.; Aljuffali, I.A.; Alshamsan, A. Part I: Development and optimization of solid-lipid nanoparticles using Box-Behnken statistical design for ocular delivery of gatifloxacin. J. Biomed. Mater. Res. Part A **2013**, 101, 1813–1827. [Google Scholar] [CrossRef] [PubMed]

60 Ferreira, M.; Chaves, L.L.; Lima, S.A.C.; Reis, S. Optimization of nanostructured lipid carriers loaded with methotrexate: A tool for inflammatory

and cancer therapy. Int. J. Pharm. **2015**, 492, 65–72. [Google Scholar] [CrossRef]

61 Nagaich, U.; Gulati, N. Nanostructured lipid carriers (NLC) based controlled release topical gel of clobetasol propionate: Design and in vivo characterization. Drug Deliv. Transl. Res. **2016**, 6, 289. [Google Scholar] [CrossRef]

62 Liu, C.; Li, B.; Mi, C. Fast transient thermal analysis of gold nanoparticles in tissue-like medium. IEEE Trans. Nanobiosci. **2009**, 8, 271–280. [Google Scholar] [CrossRef]

63 Freitas, C.; Müller, R.H. Correlation between long-term stability of solid lipid nanoparticles (SLN™) and crystallinity of the lipid phase. Eur. J. Pharm. Biopharm. **1999**, 47, 125–132. [Google Scholar] [CrossRef]

64 Wu, T.; Yen, F.; Lin, L.; Tsai, T.; Lin, C.; Cham, T. Preparation, physicochemical characterization, and antioxidant effects of quercetin nanoparticles. Int. J. Pharm. **2008**, 346, 160–168. [Google Scholar] [CrossRef]

65 Yi, J.; Lam, T.I.; Yokoyama, W.; Cheng, L.W.; Zhong, F. Beta-carotene encapsulated in food protein nanoparticles reduces peroxyl radical oxidation in Caco-2 cells. Food Hydrocoll. **2015**, 43, 31–40. [Google Scholar] [CrossRef]

66 Rezvani, M.; Manca, M.L.; Caddeo, C.; Escribano-Ferrer, E.; Carbone, C.; Peris, J.E.; Usach, I.; Diez-Sales, O.; Fadda, A.M.; Manconi, M. Co-loading of ascorbic acid and tocopherol in eudragit-nutriosomes to counteract intestinal oxidative stress. Pharmaceutics **2019**, 11, 13. [Google Scholar] [CrossRef] [PubMed]

67 Doktorovova, S.; Souto, E.B.; Silva, A.M. Nanotoxicology applied to solid lipid nanoparticles and nanostructured lipid carriers—A systematic review of in vitro data. Eur. J. Pharm. Biopharm. **2014**, 87, 1–18. [Google Scholar] [CrossRef] [PubMed]

68 Hu, L.; Jia, Y.; Ding, W. Preparation and characterization of solid lipid nanoparticles loaded with epirubicin for pulmonary delivery. Pharmazie **2010**, 65, 585–587. [Google Scholar] [CrossRef] [PubMed]

69 Patlolla, R.R.; Chougule, M.; Patel, A.R.; Jackson, T.; Tata, P.N.V.; Singh, M. Formulation, characterization and pulmonary deposition of nebulized celecoxib encapsulated nanostructured lipid carriers. J. Control. Release **2010**, 144, 233–241. [Google Scholar] [CrossRef] [PubMed]

70 Yuan, H.; Miao, J.; Du, Y.; You, J.; Hu, F.; Zeng, S. Cellular uptake of solid lipid nanoparticles and cytotoxicity of encapsulated paclitaxel in A549 cancer cells. Int. J. Pharm. **2008**, 348, 137–145. [Google Scholar] [CrossRef]

71 Sahay, G.; Alakhova, D.Y.; Kabanov, A.V. Endocytosis of nanomedicines. J. Control. Release **2010**, 145, 182–195. [Google Scholar] [CrossRef]

72 Reboredo-Rodríguez, P.; González-Barreiro, C.; Cancho-Grande, B.; Forbes-Hernández, T.Y.; Gasparrini, M.; Afrin, S.; Cianciosi, D.; Carrasco-Pancorbo, A.; Simal-Gándara, J.; Giampieri, F.; et al. Characterization of phenolic extracts from Brava extra virgin olive oils and their cytotoxic effects on MCF-7 breast cancer cells. Food Chem. Toxicol. **2018**, 119, 73–85. [Google Scholar] [CrossRef]

73 Liu, L.; Ahn, K.S.; Shanmugam, M.K.; Wang, H.; Shen, H.; Arfuso, F.; Chinnathambi, A.; Alharbi, S.A.; Chang, Y.; Sethi, G.; et al. Oleuropein induces apoptosis via abrogating NF-κB activation cascade in estrogen receptor–negative breast cancer cells. J. Cell. Biochem. **2019**, 120, 4504–4513. [Google Scholar] [CrossRef]

74 Katsoulieris, E.N. The olive leaf extract oleuropein exerts protective effects against oxidant-induced cell death, concurrently displaying pro-oxidant activity in human hepatocarcinoma cells. Redox Rep. **2016**, 21, 90–97. [Google Scholar] [CrossRef]

75 Du, Y.; Bao, C.; Huang, J.; Jiang, P.; Jiao, L.; Ren, F.; Li, Y. Improved stability, epithelial permeability and cellular antioxidant activity of ß-carotene via encapsulation by self-assembled a-lactalbumin micelles. Food Chem. **2019**, 271, 707–714. [Google Scholar] [CrossRef] [PubMed]

76 Carbone, C.; Arena, E.; Pepe, V.; Prezzavento, O.; Cacciatore, I.; Turkez, H.; Marrazzo, A.; Di Stefano, A.; Puglisi, G. Nanoencapsulation strategies for the delivery of novel bifunctional antioxidant/σ1 selective ligands. Colloids Surf. B Biointerfaces **2017**, 155, 238–247. [Google Scholar] [CrossRef]

77 Hatahet, T.; Morille, M.; Shamseddin, A.; Aubert-Pouëssel, A.; Devoisselle, J.M.; Bégu, S. Dermal quercetin lipid nanocapsules: Influence of the formulation on antioxidant activity and cellular protection against hydrogen peroxide. Int. J. Pharm. **2017**, 518, 167–176. [Google Scholar] [CrossRef] [PubMed]

78 Ong, V.; Mei, V.; Cao, L.; Lee, K.; Chung, E.J. Nanomedicine for Cystic Fibrosis. SLAS Tech. **2019**, 24, 169–180. [Google Scholar] [CrossRef] [PubMed]

79 Cantin, A.M.; White, T.B.; Cross, C.E.; Forman, H.J.; Sokol, R.J.; Borowitz, D. Antioxidants in cystic fibrosis: Conclusions from the CF Antioxidant Workshop, Bethesda, Maryland, November 11-12, 2003. Free Radic. Biol. Med. **2007**, 42, 15–31. [Google Scholar] [CrossRef]

80 Delgado, D.; del Pozo-Rodríguez, A.; Solinís, M.Á.; Rodríguez-Gascón, A. Understanding the mechanism of protamine in solid lipid nanoparticle-based lipofection: The importance of the entry pathway. Eur. J. Pharm. Biopharm. **2011**, 79, 495–502. [Google Scholar] [CrossRef] [PubMed]

81 Del Pozo-Rodríguez, A.; Pujals, S.; Delgado, D.; Solinís, M.A.; Gascón, A.R.; Giralt, E.; Pedraz, J.L. A proline-rich peptide improves cell transfection of solid lipid nanoparticle-based non-viral vectors. J. Control. Release **2009**, 133, 52–59. [Google Scholar] [CrossRef] [PubMed]

82 Del Pozo-Rodríguez, A.; Delgado, D.; Solinís, M.A.; Gascón, A.R.; Pedraz, J.L. Solid lipid nanoparticles for retinal gene therapy: Transfection and intracellular trafficking in RPE cells. Int. J. Pharm. **2008**, 360, 177–183. [Google Scholar] [CrossRef]

83 Tahara, K.; Sakai, T.; Yamamoto, H.; Takeuchi, H.; Hirashima, N.; Kawashima, Y. Improved cellular uptake of chitosan-modified PLGA nanospheres by A549 cells. Int. J. Pharm. **2009**, 382, 198–204. [Google Scholar] [CrossRef]

84 Leal, J.; Liu, X.; Peng, X.; Mohanty, R.; Arasappan, D.; Wylie, D.C.; Schwartz, S.H.; Fullmer, J.J.; McWilliams, B.C.; Smyth, H.D. A combinatorial biomolecular strategy to identify peptides for improved transport across the sputum of cystic fibrosis patients and the underlying epithelia. bioRxiv **2019**, 659540. [Google Scholar] [CrossRef]

85 Fernández, E.; Santos-Carballal, B.; Weber, W.; Goycoolea, F.M. Chitosan as a non-viral co-transfection system in a cystic fibrosis cell line. Int. J. Pharm. **2016**, 502, 1–9. [Google Scholar] [CrossRef] [PubMed]

86 Hamdi, H.K.; Castellon, R. Oleuropein, a non-toxic olive iridoid, is an anti-tumor agent and cytoskeleton disruptor. Biochem. Biophys. Res. Commun. **2005**, 334, 769–778. [Google Scholar] [CrossRef] [PubMed]

87 Kellett, M.E.; Greenspan, P.; Pegg, R.B. Modification of the cellular antioxidant activity (CAA) assay to study phenolic antioxidants in a Caco-2 cell line. Food Chem. **2018**, 244, 359–363. [Google Scholar] [CrossRef] [PubMed]

88 Rodriguez-Mateos, A.; Toro-Funes, N.; Cifuentes-Gomez, T.; Cortese-Krott, M.; Heiss, C.; Spencer, J.P.E. Uptake and metabolism of (-)-epicatechin in endothelial cells. Arch. Biochem. Biophys. **2014**, 559, 17–23. [Google Scholar] [CrossRef]

89 Mohammadi, A.; Jafari, S.M.; Assadpour, E.; Faridi Esfanjani, A. Nano-encapsulation of olive leaf phenolic compounds through WPC–pectin complexes and evaluating their release rate. Int. J. Biol. Macromol. **2016**, 82, 816–822. [Google Scholar] [CrossRef]

90 Al-Qadi, S.; Grenha, A.; Carrión-Recio, D.; Seijo, B.; Remuñán-López, C. Microencapsulated chitosan nanoparticles for pulmonary protein delivery: In vivo evaluation of insulin-loaded formulations. J. Control. Release **2012**, 157, 383–390. [Google Scholar] [CrossRef]

91 Pontes, J.F.; Grenha, A. Multifunctional nanocarriers for lung drug delivery. Nanomaterials **2020**, 10, 183. [Google Scholar] [CrossRef]

92 Wan, K.Y.; Weng, J.; Wong, S.N.; Kwok, P.C.L.; Chow, S.F.; Chow, A.H.L. Converting nanosuspension into inhalable and redispersible nanoparticles by combined in-situ thermal gelation and spray drying. Eur. J. Pharm. Biopharm. **2020**, 149, 238–247. [Google Scholar] [CrossRef]

Supplementary Materials

S1. Nanoparticle morphology and success in freeze-drying process of blank nanoparticles

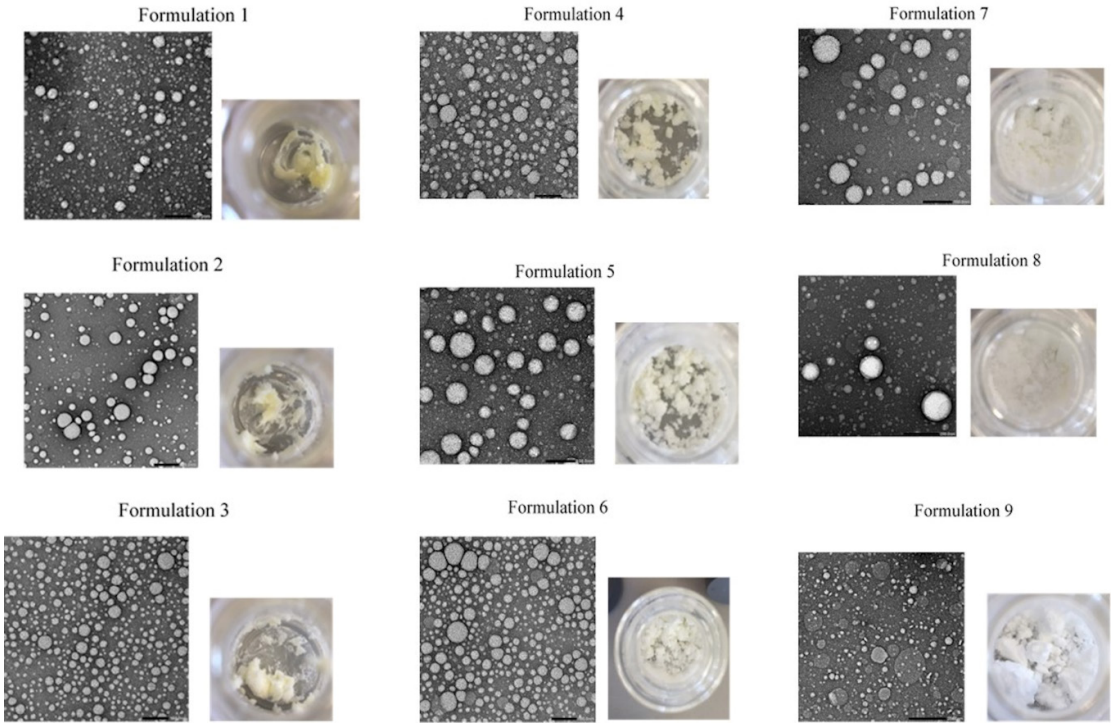

Figure S1. TEM micrographs and photographs of freeze-dried nanoformulations with different solid-liquid lipid ratios. The scale bar of TEM micrographs (bottom right) indicates 100 nm.

S2. Cell viability assay of NLC-empty

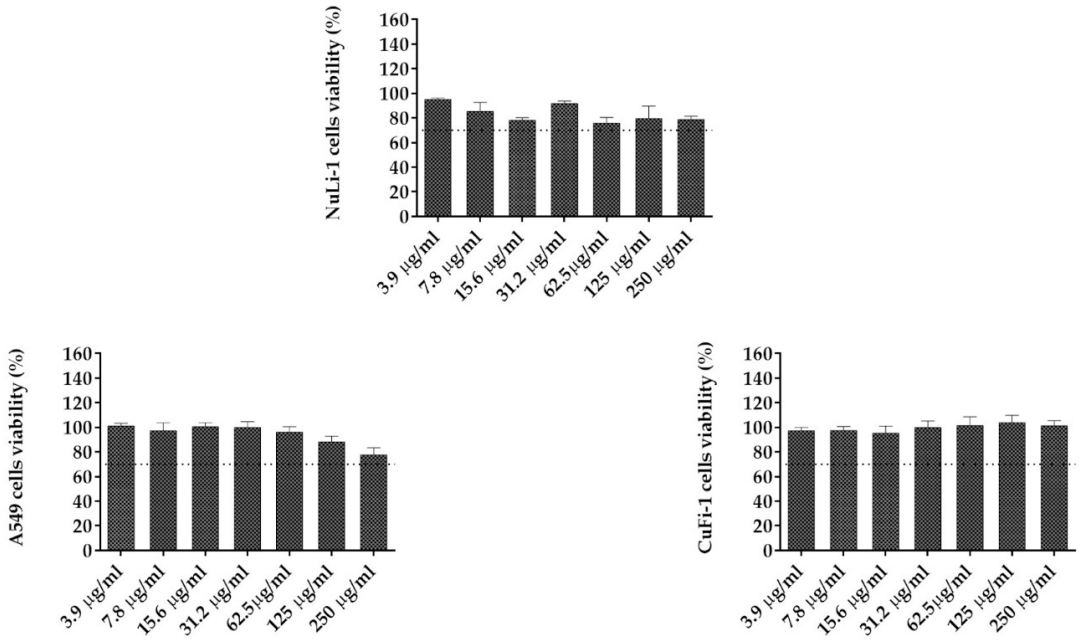

Figure S2. Effect of NLC-empty at different concentrations on the viability of NuLi (upper), A549 (bottom-left) and CuFi-1 (bottom-right) cells. Results are given as the mean % of living cells compared to the control ± SD, n = 3.

Chapter 3

Oral delivery of oleuropein-loaded lipid nanocarriers alleviates inflammation and oxidative stress in acute colitis

Huguet-Casquero et al. Int.J. Pharm. 2020 Jun 13;586:119515

https://doi.org/10.1016/j.ijpharm.2020.119515

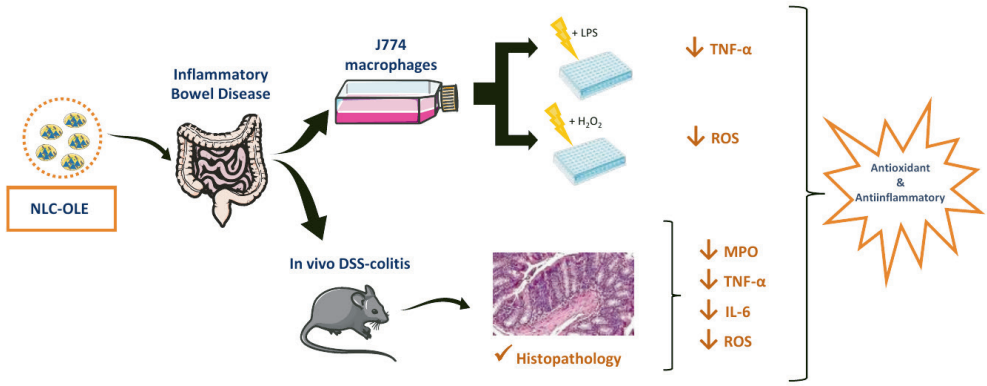

Oral delivery of oleuropein-loaded lipid nanocarriers alleviates inflammation and oxidative stress in acute colitis

Amaia Huguet-Casquero[a,b], Yining Xu, Eusebio Gainza[b], Jose Luis Pedraz [a,c*] Ana Beloqui [a,c*]

[a] NanoBioCel Group, Laboratory of Pharmaceutics, School of Pharmacy, University of the Basque Country (UPV/EHU), Spain.

[b] Biosasun S.A., Iturralde 10, Etxabarri-Ibiña, Zigoitia, 01006, Spain.

[c] Biomedical Research Networking Centre in Bioengineering, Biomaterials and Nanomedicine (CIBER-BBN), Spain.

[d] UCLouvain, Université catholique de Louvain, Louvain Drug Research Institute, Advanced Drug Delivery and Biomaterials, 1200 Brussels, Belgium

* Corresponding authors: Ana Beloqui, Jose Luis Pedraz.

ABSTRACT

Inflammation and oxidative stress pathways have emerged as novel targets in the management of inflammatory bowel diseases (IBD). Targeting the drug to the inflamed colon remains a challenge. Nanostructured lipid carriers (NLCs) have been reported to accumulate in inflamed colonic mucosa. The antioxidant/antiinflamatory polyphenol oleuropein (OLE) was loaded in NLCs (NLC-OLE). NLC-OLE showed to be more effective in decreasing the TNF-α secretion and intracellular reactive oxygen species (ROS) by activated macrophages (J774) compared to the conventional form of OLE. OLE efficacy was preserved within NLC-OLE ameliorating inflammation in a murine model of acute colitis: reduced levels of TNF-α and IL-6, decreased neutrophil infiltration and improved histopathology of the colon were reported. In addition, NLC-OLE enhanced the ROS scavenging activity of OLE in the colon after oral administration. These data suggest that the proposed NLC-OLE could be a promising drug delivery system for OLE in IBD treatment.

Keywords: oleuropein, polyphenols, nanostructured lipid carrier, inflammatory bowel disease, oxidative stress, olive oil

1. Introduction

Inflammatory bowel diseases (IBD) are multifactorial immune mediated gastrointestinal disorders. Clinically, they are characterized by chronic but relapsing diarrhoea and rectal bleeding which are usually accompanied by weight loss and abdominal pain. The main idiopathic forms involved in IBD are ulcerative colitis (UC) and Crohn's disease (CD). Whilst inflamed lesions in CD could be widespread to any part of the gastrointestinal tract (GIT), UC is limited to the colon.[1]

Current treatment for IBD aims to block the inflammatory pathway with the administration of corticosteroids, sulfasalazine, immunosuppressants and biological drugs (i.e. anti-TNFα or monoclonal antibodies). However, their unspecific targeting along with their undesirable side effects and the high daily doses needed, makes the search for new alternatives an urgent necessity.[2-4]

How are IBD originated still remains unclear but recently, redox impairment has gained special attention as one of the potential etiological factors for IBD development. The GIT is one of the main sites in the organism for the presence of prooxidant molecules. Clinical studies have shown that IBD patients have reduced antioxidant capacity even in the remission phase of the disease. Furthermore, inflammation is known to be caused, in part, by free radicals and thus, their increased amount in IBD together with the pro-inflammatory cytokines (i.e. TNF-α) have strong repercussion on the establishment/pathogenesis and progression of these diseases.[5] Given this scenario, it has been recently proposed that treating with antioxidants with additional anti-inflammatory effect might be a promising strategy for designing new therapies. A growing evidence support the use of polyphenolic compounds (i.e. curcumin, oleuropein, ellagic acid) as natural preventive treatments of IBD to relief intestinal inflammation.[6-10]

Oleuropein (OLE) is one of the most bountiful phenolic acids in olive leaves (*Olea europaea* L). Recently, the European Medicines Agency (EMA) has emitted its own assessment report about the health-promoting properties of this molecule in human health.[11] It is widely known for its potent antioxidant and anti-inflammatory activities which seem to be the cornerstone for its multiple pharmacological activities: antiviral, anticancer, antimicrobial, neuroprotective and gastroprotective, among others.[12,13]

Whilst a number of encouraging preclinical data have revealed the influence of polyphenols on intestinal inflammation as plant extracts or pure compounds, scarce studies are available concerning isolated

oleuropein. As for IBD, particularly OLE has shown to be effective in acute, chronic and colon-cancer associated colitis.[14-16] Nevertheless, OLE is limited by its poor stability not only against external factors (light, oxygen) but also across the human organism (pH, enzymes). Several studies suggest that OLE suffers a complex biotransformation process during gastric digestion.[17-19] Because of this, the efficacy results retrieved from the oral administration of OLE might be lower than those expected and high doses have been used to date for in vivo studies.

In this context, nanotechnology has emerged as a promising approach towards IBD treatment and/or prevention. Nanoscale drug delivery systems (DDS) can be specifically designed to accumulate in the inflamed areas of the bowel. The disrupted intestinal barrier along with the overproduction of mucus and the higher amount of immune-related cells can result in a greater accumulation of the nanoparticles in the inflamed colonic tissues as against the healthy ones.[7,20-23] Among the existing nano-sized DDS, nanostructured lipid carriers (NLCs) offer special advantages: sustained release, good biocompatibility and biodegradable properties. Moreover, the lipid excipients used for NLC formulation have documented biological anti-inflammatory effects in IBD.[7,20]

All in all, an optimal and colon-targeted NLC could enhance OLE efficacy at ameliorating inflammatory and oxidative stress symptoms in IBD by protecting the molecule inside the lipid core until its release on the specific site, as well as synergistically improving its anti-inflammatory activity thanks to the lipid excipients.

On this basis, this work aimed to analyze the behavior and efficacy of the anti-inflammatory and antioxidant compound oleuropein (OLE) encapsulated in olive oil-based NLCs, in terms of their potential efficacy for transport OLE to the specific site and preserve its efficacy in IBD. With this purpose OLE-loaded NLCs were evaluated (i) in accordance with their physicochemical characteristics; (ii) in vitro by assessing their ability to reduce TNF-α production and intracellular ROS levels from, respectively, LPS-activated and H_2O_2-stimulated J774 macrophages; and lastly (iii) in vivo, by evaluating the neutrophil infiltration, cytokines concentration (TNF-α, IL-6), ROS concentration as well as by histologically and macroscopically assessing the severity of inflammation in dextran sodium sulfate (DSS)-induced acute colitis mice model.

2. Materials and Methods

Sources for materials and some methods are shown in the Supplementary material.

2.1. Preparation of the formulations

2.1.1. Nanostructured lipid carriers

NLC-OLE were elaborated through the hot melt emulsification method followed by ultrasonication.[24] Briefly, Precirol® ATO 5 (0.66g) and olive oil (0.44g) were melted at 75ºC to obtain a clear and homogeneous oil phase. Oleuropein (OLE) was uniformly dispersed in deionized water. For aqueous surfactant phase preparation, Poloxamer 188 (0.66%) (w/v) and Tween® 80 (1.3%) (w/v) were dispersed in deionized water (15 ml). Prior to the emulsification step, OLE solution and the aqueous phase were heated to the same temperature (75ºC) as the lipid phase. Next, OLE solution was added to the lipid phase and immediately after the aqueous phase was added too. The mixture was sonicated for 30 s at 50 W (Branson Sonifier 250, Danbury, CT, USA) and gently shaken by magnetic stirring for 10 min at room temperature. Then, the obtained nanoemulsion was stored for 2 h at 4 ºC to give rise to the lipid re-crystallization and the resulting NLC formation. Afterwards, nanoparticles were centrifuged (2,500 rpm, 10 min) and washed three times in deionized water using 100-kDa cut-off centrifugal filter units (Amicon, "Ultracel-100k", Merck, Millipore, Spain). Blank nanoparticles were prepared as aforementioned without OLE (NLC-Blank).

Finally, a cryoprotectant aqueous solution (trehalose (15% w/w)) was added to the resulting NLCs and they were subjected to lypophilization for 36 h (Telstar Lyobeta freeze-dryer, Terrassa, Spain).

2.1.2. OLE suspension

An OLE suspension (OLEsus) was prepared as a control for in vitro and in vivo experiments. For this purpose, OLE was dispersed in deionized water to a concentration of 67 mg/ml.

2.2. *In vitro* cell experiments

2.2.1. Cell culture

J774 murine macrophages were maintained in RPMI 1640 media supplemented with 1% (v/v) PEST and 10% (v/v) FBS at 37ºC in a 5% CO_2 / 95% (v/v) air atmosphere. 75cm^2 flasks (Corning, Lowell, MA, USA) were used for cell grown.

2.2.2. Cell viability studies

CCK-8 method was used for assessing the cytotoxicity of the formulations in murine macrophages. Briefly, cells were seeded in 96-well microtiter plates (Nunc, Roskilde, DK) and their density was set to 20,000 cells/well. After an incubation period of 24 h (37 ºC, 5% CO_2) cells were treated for 4 h with OLEsus, NLC-OLE and the equivalent unloaded formulation (NLC-Blank) which were diluted in 100 µl of cell culture medium, at increasing concentrations (from 7.8 to 500 µg/ml of OLE concentration). Dimethyl sulfoxide (DMSO) was used as negative control (dead cells) and fresh medium as positive control (cells alive). The CCK-8 assay was then conducted as previously described by our group.[25] The spectrophotometric absorbance was measured at 450nm/630nm wavelength (MultiSkan Ex plate reader, Thermo Fisher Scientific, Waltham, MA, USA) and the IC_{50} values were calculated. All CCK-8 tests were conducted in triplicate.

2.2.3. Study of cellular anti-inflamatory effects

J774 cells were seeded in 24-well plates (200,000 cells/well) and left to adhere for 24 h. Murine macrophages were then treated for 4 h with the studied formulations. Based on the results from the cell viability studies, the following concentrations for each formulation were prepared in 1 ml of culture medium: (i) OLEsus (0.15 mg/ml) (ii) NLC-OLE (0.15 mg/ml of OLE) and the equivalent amount of unloaded nanoformulation. The cell-free supernatants were then collected and macrophages were stimulated with fresh medium containing 0.1 µg/ml of LPS for 24 h.[26,27] Supernatants were subsequently gathered and stored at -20 ºC until later assessment. TNF-α levels were quantified using a Mouse TNF-α uncoated ELISA Kit (Thermofischer, Invitrogen Corporation; Paisley, UK) following the manufacturer's instructions.

2.2.4. Study of cellular antioxidant effects

Intracellular levels of reactive oxygen species (ROS) were measured using the 2,7-dichlorofluorescein diacetate (DCFH-DA) reagent.[28] J774 cells were seeded at 25,000 cells/well in dark, clear-bottom 96-well microtiter plates and left to adhere for 24h. Cells were then loaded with 200 µl of 1 mM solution of DCFH-DA for 40 min at 37 ºC. Then, cells were washed once with DPBS and exposed for 4 h to 100 µl of OLEsus, NLC-OLE and NLC-Blank formulations dispersed in culture medium. The same non-cytotoxic concentrations used in section 2.2.3. were selected for this study. Afterwards, cells were washed once and 100 µl of a 0.03% hydrogen peroxide solution (H_2O_2, pro-oxidant agent) in DPBS was added to each well. The microplate was incubated for 30 min at 37 ºC.

Fluorescence intensity was measured with an excitation wavelength of 485 nm and an emission wavelength of 535 nm (Spectrophotometer SpectraMax M2e & program SoftMax Pro, Molecular Devices, LLC, USA). Data was reported as the intracellular percentage of ROS compared with oxidized control cells (H_2O_2-activated untreated cells). All assays were performed in triplicate, each comprising six replicates of each sample tested.

2.3. *In vivo* efficacy study against acute ulcerative colitis

Animal care and experimental protocols were in accordance with the *Université catholique de Louvain* animal committee (2018/UCL/MD/45). 8-week old male C57BL/6 mice (Janvier Laboratories, FR) weighing 21-26 g were housed under standard conditions, fed with standard laboratory food and supplied with tap water *ad libitum*. Acute colitis was established by the addition of DSS (3% (w/v)) in mice drinking water for the first 5 consecutive days of the study, and colonic symptoms were evaluated 7 days after the beginning of DSS treatment.[29] Animals were randomly separated into six groups (8 mice per group), namely: untreated control group (healthy mice), control DSS group, OLEsus-treated DSS group (0.5 g of OLE/kg), NLC-OLE-treated DSS group (1.7 g of NLC-OLE/kg) and NLC-Blank-treated DSS group (1.2 g of NLC-Blank/kg). NLC-OLE group received the same amount of OLE as the OLEsus group. NLC-Blank group received the same amount of NLC excipients as NLC-OLE group. Formulations were administered by oral gavage during the first five days of DSS-colitis induction. Control groups received deionized autoclaved water given by oral gavage instead of the formulations. Mice were fasted 12 h prior to the administration of the treatments. All animals were sacrificed on day 7 by cervical dislocation. Colons were excised and properly stored for later evaluation.

2.3.1. Clinical disease activity scoring

Severity of colitis was assessed by evaluating weight loss, stool consistency and rectal bleeding as previously described.[7,30] Recorded results were scored on a 0-3 scale as shown in Table 1.

Table 1. Assessment of inflammation by means of clinical and macroscopic score.

Score	Weight loss score	Consistency score	Blooding score
0	None	Normal pellets	None
1	1-5%	Slightly loose faeces	Slightly bloody
2	6-10%	Loose faeces	Bloody
3	11-18%	Watery diarrhoea	Blood in the whole colon

Score reflects degree of weight loss, diarrhea and fecal blooding score on the day of necropsy and is characterized on a scale of 0-3.

2.3.2. Colon weight/colon length ratio

After 7 days of colitis induction, mice were sacrificed and the luminal contents of the collected colons were rinsed with PBS. Then, colons were weighted and measured to further calculate the weight/length ratio which is considered a sensitive and reliable marker of the extent and severity grade of the colitis-associated inflammatory status.[31]

2.3.3. Histological appearance study

Small pieces of the colons (distal regions) from each study group were fixed in 4% buffered paraformaldehyde overnight, washed with ethanol (70% v/v) and embedded in paraffin. For each mouse, two sets of 3 serial sections with a thickness of 10 μm were cut 100 μm apart, and stained with hematoxylin-eosin for detailed histological study of colonic inflammation.

2.3.4. Myeloperoxidase (MPO) assay in colon tissue

MPO is commonly used as an indicator for neutrophil infiltration which, at the same time, is correlated with the severity of colonic inflammation in UC.[32] Briefly, at the time of necropsy, proximal portions of the colons (~25 mg) were placed on Eppendorf safe-lock tubes, snap frozen in liquid N_2 and stored at -80 ºC. For MPO activity investigation, tissue samples were gently homogenized on ice with HTAB buffer (0.5% HTAB in 50 mM potassium phosphate buffer, pH 6). Then, resulting samples were ultracentrifuged at 5,000 rpm for 20 min at 4 ºC (Eppendorf Centrifuge 5804R) to yield a supernatant fraction of around 300μl. An aliquot of the obtained supernatants (7μl) was placed on 96-well plates (Nunc, Roskilde, DK) along with 200 μl of a 50 mM potassium buffer solution supplemented with 0.167 mg/ml of O-dianisidine hydrochloride and 1% (v/v) of H_2O_2. Samples were analyzed in duplicate. Absorbance was measured spectrophotometrically at 460nm for 30 min (Spectrophotometer SpectraMax M2e & program SoftMax Pro, Molecular Devices, LLC, USA). Resulting data were expressed as MPO units per gram of total protein of sample. The bicinchoninic acid assay (BCA) method was used for protein quantitation in each supernatant sample (Thermofischer, Pierce™ Biotechnology; Illinois, USA). One unit of MPO activity was defined as the amount needed the degradation of 1 mmol/min of H_2O_2 at 25ºC.[31]

2.3.5. Determination of inflammatory cytokine levels in colon tissue

The colonic concentration of cytokines (TNF-α and IL-6) was quantified by the sandwich-type ELISA tech-

nique following the manufacturer's instructions for the Mouse TNF-α uncoated and IL-6 mouse ELISA kits (Thermofischer, Invitrogen Corporation; Paisley, UK). Frozen colonic tissue portions of each mice group were vigorously homogenized in 500 µl of extraction buffer (DPBS with 1% SDS and 1 tablet of complete protease inhibitor cocktail (Roche Diagnostics, Vilvoorde, BE) per 10 ml of solution) by means of an Ultra-Turrax (IKA T18 Basic, Staufen, Germany) and ultracentrifuged for 20 min at 5,000 rpm at 4ºC. Obtained supernatants were stored at -80 ºC until cytokine analysis. Data were normalized with the total protein concentration (BCA method) of each sample.

2.3.6. Determination of ROS levels in colon tissue

The tissue-associated ROS were analyzed to assess the degree of oxidative stress which correlates with the severity of colitis.[5,33] Briefly, at the time of necropsy, colon specimens from the central region were snap frozen in liquid N_2 and stored (-80ºC) until further assessment. For ROS quantitation, colon samples were placed in 1,000 µl TRIS-HCl buffer (50 mM, pH 7.4) on ice and gently homogenized with an UltraTurrax. The homogenate was ultracentrifuged at 5,000 rpm for 15 min at 4 ºC. A supernatant aliquot (50µl) was added to 96- well black plates (Fluotrac™, Greiner, GE) along with 50 µl of a prepared DCFH-DA (10µM) solution and left to react for 30 min at 37 ºC, under shaking and dark conditions. The autofluorescence of each tissue homogenate was also assayed and subtracted from the results. Excitation and emission wavelengths were set to 485 nm and 535 nm, respectively, for measuring the fluorescence intensity with a plate reader (Spectrophotometer SpectraMax M2e & program SoftMax Pro, Molecular Devices, LLC, USA). Data from triplicate assays were expressed as fluorescent intensity units (FU) per mg of total protein for each sample. Protein concentration in homogenates was quantified by the BCA method.

2.4. Statistical analysis

The results are expressed as the mean ± standard error of the mean (SEM) unless otherwise stated. GraphPad Prism 6.0 program (GraphPad Software Inc., San Diego, CA, USA) was employed for statistical analyses. Differences were considered statistically significant when $*p < 0.05$. The Shapiro-Wilk normality test was applied for normal distribution assessment. For those studies in which normality and homogeneity were confirmed, a one-way ANOVA test of multiple comparisons followed by Bonferroni's post-hoc test was performed. All other analyses were conducted using Student's t-test or a Mann–Whitney non-parametric test.

3. Results

3.1. Physicochemical properties of NLCs

The physicochemical behavior of NLC-OLE and NLC-Blank is summarized in Figure 1C. The size was found to be about 150 nm and both formulations presented a negative zeta potential. OLE was almost fully encapsulated in the NLCs. A round-shape of the nanoparticles was confirmed by TEM micrographs (Figure 1A and B). Previous *in vitro* release studies conducted at pH 7.4 and 37 ºC, demonstrated that about 80% of OLE was released in a sustained manner within 27h.[24]

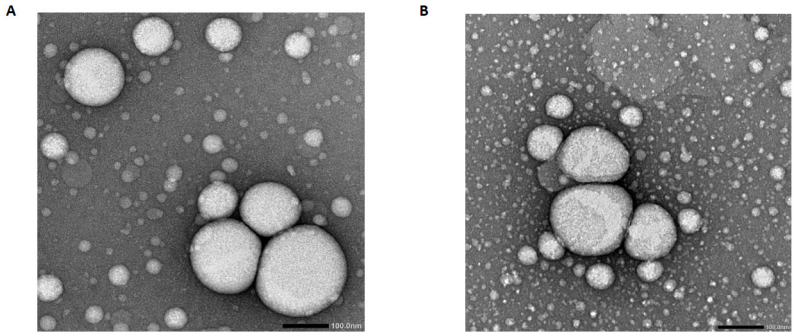

C

Formulation	Size (nm)	ζ (mV)	PDI	EE(%)
NLC-Blank	141.7±11.43	-21.64±3.72	0.2	-
NLC-OLE	141.2±12.3	-25.30±2.7	0.2	99.95%

Figure 1. Summary of NLCs characterization: (**A**) TEM micropgraphs of NLC-Blank, (**B**) TEM micrographs of NLC-OLE, and (**C**) particle size, zeta potential (ζ), polydispersity index (PDI) and encapsulation efficiency (EE) of NLC (n=3; data are expressed as the mean ± SD). The scale bar in TEM micrographs indicates 100 nm.

3.2. *In vitro* cell experiments in murine J774 macrophages

3.2.1. Cytotoxicity evaluation

The CCK-8 test (Figure 2A) was carried out to study the possible toxicity of the formulations and thereafter, select the appropriate concentration for antiinflamatory and oxidative stress studies in J774 macrophages. The IC_{50} of OLEsus was 200 µg/ml whereas NLC-OLE showed an IC_{50} of 680 µg/ml. NLC-Blank did not show any cytotoxic effect in the concentration ranges studied (up to 1200 µg/ml), demonstrating the safety of the nanocarrier matrix. Therefore, 150 µg/ml of OLEsus and its equivalent amount in NLC-OLE were selected for the forthcoming studies.

3.2.2. *In vitro* anti-inflamatory activity evaluation

The ability of the formulations to suppress TNF-α production from J774 cells was assessed by comparing NLC-OLE with OLEsus and NLC-Blank (Figure 2B). OLEsus did not exert any inhibitory effect in comparison with the control-(+) (LPS-stimulated non-treated cells). By contrast, NLC-OLE and NLC-Blank significantly reduced the secretion of TNF-α from the cells under the same studied conditions (*p<0.05). Moreover, both nanoformulations exerted a significantly higher effect when compared to OLEsus ($^{\#\#}$p<0.01) under the same conditions, but no difference was shown between the nanocarriers.

3.2.3. *In vitro* antioxidant activity evaluation

The inhibition of intracellular ROS production by H_2O_2-stressed murine macrophages was studied by comparing NLC-OLE with NLC-Blank and OLEsus (Figure 2C). Only NLC-OLE was able to significantly scavenge the generated ROS compared to the control (**p<0.01), enhancing the activity of OLE when encapsulated within NLCs compared to OLEsus ($^{\#\#}$p<0.01).

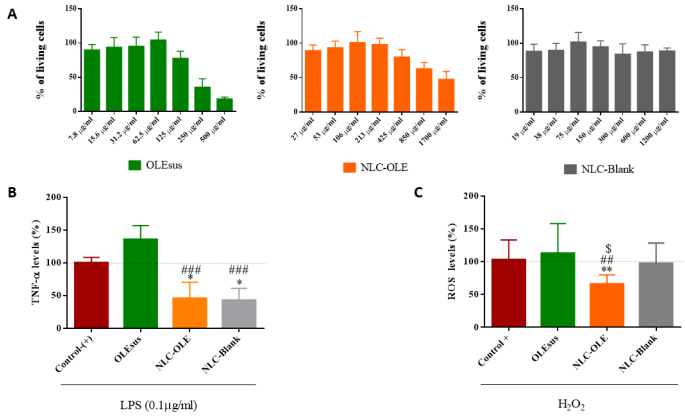

Figure 2. Summary of the *in vitro* studies in J774 cells. (**A**) Cytotoxicity results, (**B**) TNF-α quantitation in LPS-activated macrophages and (**C**) Intracellular ROS quantitation in H_2O_2-stressed macrophages of OLEsus, NLC-OLE and NLC-Blank. Data are expressed as the mean ± SD (* p<0.05 vs Control+. # p<0.05 vs OLEsus. $ p<0.05 vs NLC-Blank).

3.3. *In vivo* efficacy studies against acute colitis

3.3.1. Histological appearance evaluation and clinical activity determination

The clinical activity score (Figure 3) and the histological assessment results (Figure 4) proved the expected effects from the chemical induction of acute colitis in the DSS-groups compared to the untreated control

mice (healthy). No significant differences were found between DSS colitis induced groups. The same result was observed regarding the colon weight/length ratio (data not shown). Regarding histopathology, as shown in Figure 4A, disrupted mucosa architecture, high leukocyte infiltration as well as submucosal edema were observed in the control-DSS group. For OLEsus and NLC-OLE treated DSS groups (Figure 4B and D respectively) the colon structure was found to be similar to the healthy untreated control group (Figure 4C). Compared to the other treatments, NLC-Blank treated DSS group showed a higher infiltration of immune cells (Figure 4E) but the architecture of the crypts was well preserved in comparison with the control DSS group.

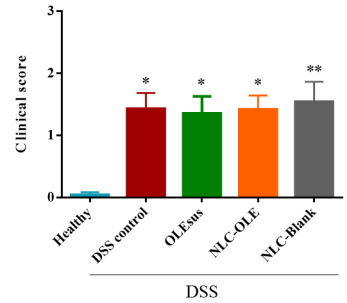

Figure 3. Clinical activity score after in vivo assessment. (n=8 mice per group).

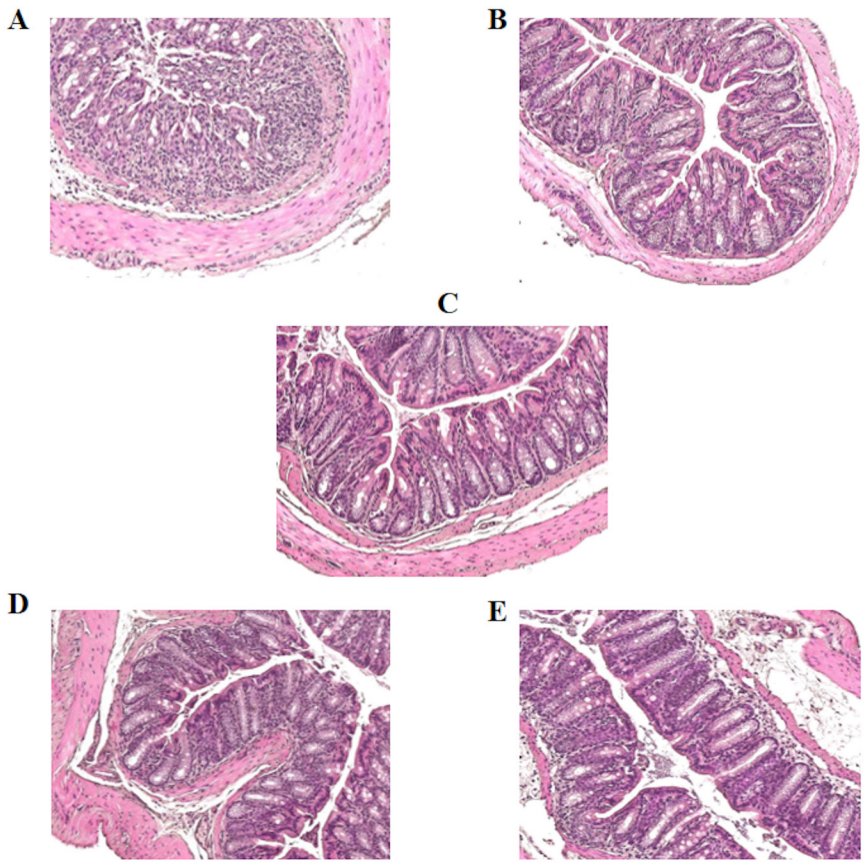

Figure 4. Representative figures of histopathology of the colon tissue after hematoxylin-eosin staining from: control DSS group (**A**), OLEsus-treated DSS group (**B**), non-treated healthy group (**C**), NLC-Ole treated DSS group (**D**) and NLC-Blank treated DSS group (**E**). Images are shown at the same magnification (100x).

3.3.2. Inflammatory and oxidative stress assessment in colon samples

MPO activity, the concentration of the pro-inflammatory cytokine TNF-α, the pleiotropic cytokine IL-6 and total ROS content in the colon are summarized in Figure 5. In all cases, control-DSS group showed a significant increase in the measured parameters compared to the healthy group (data not shown), thus confirming the colitis-induction. It is worth to note that MPO activity, TNF-α and IL-6 concentration for the OLEsus and NLC-OLE-treated DSS groups were decreased when compared with DSS group. However, no significant differences were found between OLEsus and NLC-OLE-treated DSS groups. No significant differences were observed in NLC-Blank treated DSS group. Interestingly, only NLC-OLE treatment was able to attenuate oxidative stress by significantly decreasing total ROS generation (*p<0.05) compared to DSS control, whereas OLEsus and NLC-Blank did not show any significant effect.

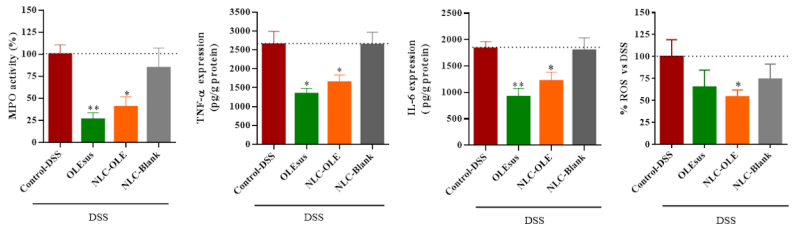

Figure 5. Effect of formulations in colitis associated inflammation and oxidative stress. From left to right, MPO activity, absolute levels of TNF-α and IL-6 and relative ROS presence in the colon. **p< 0.01, *p<0.05 vs DSS group. (n=7-8).

4. Discussion

ROS mediated oxidative stress together with inflammatory pathways have gained special interest as targets for new drug studies in UC.[5,34] OLE, the major polyphenol in olive leaves, is known to inhibit the inflammatory response through several pathways, such as suppressing the secretion of an array of cytokines (i.e. IL-1β, IL-17, TNF-α) probably, in part, due to its interaction with the nuclear factor (NF)-κB which, indeed, plays an important role in IBD. Additionally, this bioactive compound has shown ROS scavenging ability, although its precise mechanism of action still remains unclear[12,13]. Altogether, OLE is a good candidate for IBD management and some authors have revealed its effectiveness in both acute and chronic UC[14-16]. However, in these studies high doses of OLE were needed to be administered within the food for OLE to be effective. The reason for this could be that OLE, as well as the majority of the anti-inflammatory and antioxidant agents, presents several limiting factors. Particularly, it presents low absorption rates, poor stability after light and oxygen exposure, as well as rapid biotransformation upon gastric digestion

and thus, its bioactivity, bioaccessibility and bioavailability seem to be compromised.[17-19,35] Therefore, targeting the inflamed colonic mucosa with OLE is still a challenge. In this sense, lipid-based nanotechnology seems a promising strategy to overcome these limitations. Among all nanoscale drug delivery systems, NLCs can offer a greater drug loading capacity, an increased retention in the inflamed target site and biological anti-inflammatory properties.[6,7,20,23,36,37] Hence, we hypothesized that merging those properties with OLE could lead to a synergistic anti-inflammatory action of the lipid nanoparticles in IBD and a greater targeting to the colon resulting in an improved efficacy of OLE treatment. In this work, nanostructured lipid carriers loaded with oleuropein (NLC-OLE) were assessed both in vitro and in vivo, with the aim to evaluate its impact on IBD therapy.

NLCs were obtained through the hot-melt emulsification method and showed a mean particle size ~150 nm together with a moderately narrow size distribution (PDI~0.2). OLEsus was successfully incorporated into the nanocarrier (~ 100%). Moreover, due to the nature of the lipid core, NLCs exhibited a negatively charged surface (~ -25 mV) which is known to promote their accumulation in ulcerated tissues via interaction with the positively charged proteins.[21,38] Therefore, both the nanometer size and surface negative charge together turn NLC-OLE into promising candidates for IBD treatment.

Particularly, Precirol® ATO 5 and olive oil were chosen for the lipid core formulation. Precirol® ATO 5 has been approved by the FDA for the oral route administration and has been largely used as a component of the lipid matrix for sustained release formulations. As for liquid lipids, the medium chain triglycerides, known under the brand name Miglyol® 812, are the most commonly employed. However, in this work, we selected olive oil since it provided our NLCs with a suitable physico-chemical stability. Olive oil is also expected to help enhance OLE availability in the intestine and reduce the possible cytotoxicity effect of residual surfactants that might be present in the final nanoformulation.[39,40]

Innate immunity has an important role in IBD pathogenesis.[1] During active inflammation, particles in the nano-scale range are more easily internalized by a greater number of immune-related cells. Given this, the anti-inflammatory and antioxidant potential of NLC-OLE was evaluated *in vitro*. Firstly, TNF-α production by LPS-stimulated murine J774 macrophages was studied. Surprisingly, we found that OLE itself did not exert any inhibitory effect *in vitro* whereas NLC-OLE significantly inhibited TNF-α secretion ($^*p<0.05$). The negligible efficacy of OLEsus to suppress TNF-α production in LPS-stimulated macrophages has been also observed by others.[16,41] Interestingly, NLC-Blank was also able to attenuate TNF-α secretion in our

study. These results are consistent with those published by Beloqui et al.[7,36] who found that after 4 h of pre-treatment with budesonide and curcumin loaded NLCs and blank NLCs in LPS-activated J774 cells TNF-α levels were significantly reduced, whereas the active compound alone was not able to exert any effect. Serpe et al.[42] also observed the ability of solid lipid nanoparticles to significantly decrease the secretion of IL-1β and TNF-α in an *in vitro* model of human IBD whole-blood. Therefore, in light of these results, the nature of the NLCs might boost their ability to inhibit TNF-α secretion from LPS-stimulated J774 cells. Later, we assessed the antioxidant potential of NLC-OLE *in vitro*. It is a well-accepted fact that olive polyphenols are excellent reactive oxygen scavengers.[12,13] Our previous studies, demonstrated that OLEsus and NLC-OLE antioxidant activity was cell-type dependent. In this work only NLC-OLE showed antioxidant activity in H_2O_2-activated J774 macrophages (*$p<0.05$). All in all, the *in vitro* results highlighted the importance of OLE encapsulation within NLCs toward an efficient anti-inflammatory and antioxidant effect.

After assessing the *in vitro* potential of NLC-OLE, their therapeutic efficacy was evaluated in an acute DSS colitis mice model with documented similarity to human UC.[29,43] DSS is known to induce weight loss, bloody stool and loose feces in mice. From the clinical score results we confirmed that the administration of DSS successfully induced colitis in mice. However, no formulation was able to reduce the clinical symptoms (Figure 3). The DSS colitis model is a well-stablished *in vivo* model for the study of UC-related innate immune response.[36] During the genesis of active intestinal inflammation, innate response manifests itself as an increased level of leukocyte infiltration in the inflamed mucosa leading to the recrudescence of oxidative stress.[44] MPO, one of the most abundant neutrophil proteins, is commonly used as standard indicator in feces of IBD patients as well as for colitis assessment in IBD animal models.[45] Precisely, it is mostly used in DSS-induced colitis murine models, where extensive neutrophil infiltration occurs during the entire DSS treatment period, even after it is withdrawn.[6,46] At day 7, both OLEsus and NLC-OLE treated DSS groups showed a decrease in MPO activity in comparison with H_2O-treated DSS group (Figure 5). DSS-induced damage is also promoted by several anti/pro-inflammatory cytokines. In this regard, at day 7, mice showed a marked secretion of the pro-inflammatory cytokine TNF-α in colonic tissue which was significantly reduced by NLC-OLE treatment (Figure 5). Contrary to the *in vitro* results, OLE was effective in TNF-α inhibition *in vivo*. This is in line with other study in which the amelioration of acute colitis by OLE in the *in vivo* model was not consistent with its negligible activity in the *in vitro* models of inflammation.[16] The secretion of IL-6, a pleiotropic cytokine mainly localized in the intestinal crypts, was also assessed. Pro-inflammatory as well as wound healing activities have been attributed to IL-6 signalling. Particularly,

IL-6 has shown to protect intestinal epithelial cells from DSS-induced apoptosis.[47] Both OLE and NLC-OLE were able to reduce IL-6 when compared to DSS-control group.

As aforementioned, the increased MPO activity could be correlated with the recrudescence of ROS in the inflamed colonic tissue.[44] Likewise, increased levels of the pro-inflammatory cytokines TNF-α and IL-6 are known to be connected with a higher rate of cellular oxidative stress. Particularly, ROS are known to be induced by IL-6 and TNF-α is known to induce IL-6 secretion through ROS.[33,48] This, together with the *in vitro* proven antioxidant efficacy of NLC-OLE lead us to assume that NLC-OLE could have ameliorated DSS-induced inflammation through its antioxidant activity in the colon.

Aimed to elucidate this, we analyzed the total ROS content in the colon tissue. As expected, DSS-control group presented a significant accumulation of ROS when compared to the healthy-control group (data not shown) and they were significantly reduced by NLC-OLE (*$p<0.05$). Meanwhile, OLE slightly reduced oxidative stress but the differences did not reach statistical significance compared to the control. This, again, highlights the importance of the encapsulation of OLE toward an enhanced pharmacological activity in the murine colitis model.

It is worth noting that no significant therapeutic effect was observed for NLC-Blank treated DSS group in any of the *in vivo* studies, indicating that the nano-sized lipid carrier has no influence on the therapeutic activities of NLC-OLE.

All these results from the *in vivo* experiments were in line with those from the histological assessment of the colitis associated inflammatory injury (Figure 4). DSS-induced colitis (Figure 4A) clearly modified the architecture of the colon tissue, with a reduction of the protective epithelial layer and the number of goblet cells as well as an increased infiltration of immune-related cells. For OLE-treated and NLC-OLE treated DSS groups (Figure 4B and D, respectively) adequate colon structure was observed when compared to the healthy control group (Figure 4C). As expected, NLC-Blank treated group showed a higher infiltration of immune cells (Figure 4E) but the architecture of the crypts was well preserved compared to the control DSS group. Therefore, NLC-OLE demonstrated to maintain the anti-inflammatory potential of OLE and enhanced its ROS scavenging effects after oral administration *in vivo*.

To the extent of our knowledge, this is the first study evaluating the *in vivo* efficacy of OLE loaded NLCs in a murine model of acute colitis. *In vitro*, NLCs inhibited TNF-α production by activated murine

macrophages and the encapsulation of OLE into the lipid core led to an efficient antioxidant activity in stressed macrophages. Our findings from the *in vivo* study showed the ability of orally administered NLC-OLE to alleviate inflammation and oxidative stress in DSS-induced acute colitis as confirmed by the enhanced histological appearance of the colonic samples which was further confirmed by the reduced MPO activity, decreased tissue-associated TNF-α and IL-6 levels and the inhibited ROS-generation in NLC-OLE treated mice colons. The discussed results highlight and justify the combination of olive oil and Precirol formulated within NLCs for the delivery of OLE or other antioxidant/anti-inflamatory phenolic compounds in IBD therapy. On a wider level, future research is also needed to determine the precise mechanism of action and pharmacokinetics of NLC-OLE as well as the rationale for the enhancement of the antioxidant activity of OLE.

5. Acknowledgements

Authors are particularly grateful to the ICTS "NANBIOSIS" and the Drug Formulation Unit (U10) of the CIBER in Bioengineering, Biomaterials and Nanomedicine (CIBER-BBN) at the University of Basque Country (UPV/EHU). A.B. is a research associate from the Belgian F.R.S.-FNRS (Fonds de la Recherché Scientifique).

6. CRediT authorship contribution statement

Amaia Huguet-Casquero: Conceptualization, Investigation, Writing-original draft, Visualization, Formal analysis. **Yining Xu**: Investigation. **Eusebio Gainza**: Conceptualization, Resources, Writing-review & editing, Supervision, Project administration, Funding acquisition. **Jose Luis Pedraz**: Conceptualization, Methodology, Resources, Data curation, Supervision, Writing-review & editing, Funding acquisition. **Ana Beloqui**: Conceptualization, Methodology, Investigation, Resources, Data curation, Writing-review & editing, Supervision, Funding acquisition.

7. Declaration of Competing Interest

The authors declare that they have no known competing financial interests or personal relationships that could have appeared to influence the work reported in this paper.

8. Funding

A.H-C thanks the Spanish Ministry of Economy and Competitiveness for the Industrial Doctorate fellowship grant (DI-15-07513). This work was supported by the University of the Basque Country (UPV/EHU) and the Basque Country Government (Grupos Consolidados, No ref: IT907-16 to J.L.P.). A.B. is recipient of funding from F.R.S.-FNRS (convention T.0013.19). Y.X. is the recipient of a grant from the China Scholarship Council (CSC).

9. References

1 A. Kasser, S. Zeissig and R. Blumberg, *Annu Rev Immunol.,* 2010, **28**, 573:621 (DOI:0.1146/annurev-immunol-030409-101225).

2 A. Stallmach, S. Hagel and T. Bruns, *Best. Pract. Res. Clin. Gastroenterol,* 2010, **24**, 167-182 (DOI:10.1016/j.bpg.2010.01.002).

3 Y. Yang and G. R. Lichtenstein, *Am. J. Gastroenterol.,* 2002, **97**, 803-823 (DOI:10.1016/S0002-9270(02)03952-7).

4 G. Rogler, *Best. Pract. Res. Clin. Gastroenterol,* 2010, **24**, 157-165 (DOI:10.1016/j.bpg.2009.10.011).

5 F. A. Moura, K. Q. de Andrade, J. C. F. dos Santos, O. R. P. Araújo and M. O. F. Goulart, *Redox Biol.,* 2015, **6**, 617-639 (DOI:10.1016/j.redox.2015.10.006).

6 A. Beloqui, R. Coco, P. B. Memvanga, B. Ucakar, A. des Rieux and V. Préat, *Int. J. Pharm.,* 2014, **473**, 203-212 (DOI:10.1016/j.ijpharm.2014.07.009).

7 A. Beloqui, P. B. Memvanga, R. Coco, S. Reimondez-Troitiño, M. Alhouayek, G. G. Muccioli, M. J. Alonso, N. Csaba, M. de la Fuente and V. Préat, *Colloids Surf, B,* 2016, **143**, 327-335 (DOI:10.1016/j.colsurfb.2016.03.038).

8 H. Zatorski, M. Sałaga, M. Zielińska, A. Piechota-Polańczyk, K. Owczarek, R. Kordek, U. Lewandowska, C. Chen and J. Fichna, *Naunyn-Schmiedeberg's Arch. Pharmacol.,* 2015, **388**, 643-651 (DOI:10.1007/s00210-015-1110-9).

9 E. Saldanha, A. Saxena, K. Kaur, F. Kalekhan, P. Venkatesh, R. Fayad, S. Rao, T. George and M. S. Baliga, in *Dietary Interventions in Gastrointestinal Diseases: Foods, Nutrients, and Dietary Supplements*. Academic Press, 2019, p. 277-287. (DOI: 10.1016/B978-0-12-814468-8.00023-5.)

10 M. Marín, R. María Giner, J. -. Ríos and M. Carmen Recio, *J. Ethnopharmacol.,* 2013, **150**, 925-934 (DOI:10.1016/j.jep.2013.09.030).

11 EMA monograph, ed. *Assessment report on Olea europaea L., folium-*, 2017.

12 A. K. Marković, J. Torić, M. Barbarić and C. J. Brala, *Molecules,* 2019, **24** (DOI:10.3390/molecules24102001).

13 L. A. S. Cavaca, I. M. López-Coca, G. Silvero and C. A. M. Afonso, *Stud. Nat. Prod. Chem.,* 2020, **64**, 131-180 (DOI:10.1016/B978-0-12-817903-1.00005-X).

14 E. Giner, M. C. Recio, J. L. Ríos, J. M. Cerdá-Nicolás and R. M. Giner, *Mol. Nutr. Food Res.,* 2016, **60**, 242-255 (DOI:10.1002/mnfr.201500605).

15 E. Giner, M. -. Recio, J. -. Ríos and R. -. Giner, *J. Nat. Prod.,* 2013, **76**, 1113-1120 (DOI:10.1021/np400175b).

16 E. Giner, I. Andújar, M. C. Recio, J. L. Ríos, J. M. Cerdá-Nicolás and R. M. Giner, *J. Agric. Food Chem.,* 2011, **59**, 12882-12892 (DOI:10.1021/jf203715m).

17 G. Corona, X. Tzounis, M. Assunta Dessi, M. Deiana, E. S. Debnam, F. Visioli and J. P. Spencer, *Free Radic. Res.,* 2006, **40**, 647-658.

18 E. González, A. M. Gómez-Caravaca, B. Giménez, R. Cebrián, M. Maqueda, A. Martínez-Férez, A. Segura-Carretero and P. Robert, *Food Chem.,* 2019, **279**, 40-48 (DOI:10.1016/j.foodchem.2018.11.127).

19 P. Lin, W. Qian, X. Wang, L. Cao, S. Li and T. Qian, *Biomed. Chromatogr.,* 2013, **27**, 1162-1167 (DOI:10.1002/bmc.2922).

20 H. Schneider, A. Braun, J. Füllekrug, W. Stremmel and R. Ehehalt, *Int J Mol Sci,* 2010, **11**, 4149-4164 (DOI:10.3390/ijms11104149).

21 E. Collnot, H. Ali and C. Lehr, *J. Control. Release,* 2012, **161**, 235-246 (DOI:10.1016/j.jconrel.2012.01.028).

22 A. Lamprecht, U. Schäfer and C. Lehr, *Pharm. Res.,* 2001, **18**, 788-793 (DOI:10.1023/A:1011032328064).

23 J. Youshia and A. Lamprecht, *Expert Opin. Drug Deliv.,* 2016, **13**, 281-294 (DOI:10.1517/17425247.2016.1114604).

24 A. Huguet-Casquero, M. Moreno-Sastre, T. B. López-Méndez, E. Gainza and J. L. Pedraz, *Pharmaceutics,* 2020, **12**, 429 (DOI:10.3390/pharmaceutics12050429).

25 M. Pastor, M. Moreno-Sastre, A. Esquisabel, E. Sans, M. Viñas, D. Bachiller, V. J. Asensio, Á Del Pozo, E. Gainza and J. L. Pedraz, *Int. J. Pharm.,* 2014, **477**, 485-494.

26 C. A. Fernandes, L. Fievez, A. M. Neyrinck, N. M. Delzenne, F. Bureau and R. Vanbever, *Biochem. Biophys. Res. Commun,* 2012, **420**, 857-861 (DOI:10.1016/j.bbrc.2012.03.088).

27 H. Kitamura, M. Ito, T. Yuasa, C. Kikuguchi, A. Hijikata, M. Takayama, Y. Kimura, R. Yokoyama, T. Kaji and O. Ohara, *Physiol. Genomics,* 2008, **33**, 121-132 (DOI:10.1152/physiolgenomics.00095.2007).

28 A. Aranda, L. Sequedo, L. Tolosa, G. Quintas, E. Burello, J. V. Castell and L. Gombau, *Toxicol. Vitro,* 2013, **27**, 954-963 (DOI:10.1016/j.tiv.2013.01.016).

29 S. Wirtz, V. Popp, M. Kindermann, K. Gerlach, B. Weigmann, S. Fichtner-Feigl and M. F. Neurath, *Nat. Protoc.,* 2017, **12**, 1295-1309 (DOI:10.1038/nprot.2017.044).

30 S. Melgar, A. Karlsson and E. Michaëlsson, *Am. J. Physiol. Gastrointest. Liver Physiol.,* 2005, **288**, G1328-G1338 (DOI:10.1152/ajpgi.00467.2004).

31 M. Alhouayek, D. M. Lambert, N. M. Delzenne, P. D. Cani and G. G. Muccioli, *FASEB J.,* 2011, **25**, 2711-2721 (DOI:10.1096/fj.10-176602).

32 J. E. Krawisz, P. Sharon and W. F. Stenson, *Gastroenterology,* 1984, **87**, 1344-1350 (DOI:https://doi.org/10.1016/0016-5085(84)90202-6).

33 P. Mosińska, M. Salaga and J. Fichna, in *Gastrointestinal Tissue*, ed. J. Gracia-Sancho and J. Salvadó, Academic Press, 2017, p. 53-64.

34 H. Zhu and Y. R. Li, *Exp. Biol. Med.,* 2012, **237**, 474-480 (DOI:10.1258/ebm.2011.011358).

35 S. C. Edgecombe, G. L. Stretch and P. J. Hayball, *J. Nutr.,* 2000, **130**, 2996-3002.

36 A. Beloqui, R. Cococ, M. Alhouayek, M. Á Soliñis, A. Rod́ riguez-Gáscon, G. G. Muccioli and V. Préat, *Int. J. Pharm.,* 2013, **454**, 775-783 (DOI: 10.1016/j.ijpharm.2013.05.017).

37 K. Zai, M. Hirota, T. Yamada, N. Ishihara, T. Mori, A. Kishimura, K. Suzuki, K. Hase and Y. Katayama, *J. Control. Release,* 2018, **286**, 94-102 (DOI: 10.1016/j.jconrel.2018.07.019).

38 A. Beloqui, M. Á Solinís, A. Rodríguez-Gascón, A. J. Almeida and V. Préat, *Nanomed. Nanotechnol. Biol. Med.,* 2016, **12**, 143-161 (DOI: 10.1016/j.nano.2015.09.004).

39 S. Talegaonkar and A. Bhattacharyya, *AAPS PharmSciTech,* 2019, **20**, 121.

40 C. W. How, A. Rasedee and R. Abbasalipourkabir, *IEEE Trans. Nanobiosci.,* 2013, **12**, 72-78 (DOI:10.1109/TNB.2012.2232937).

41 M. L. Castejon, M. Sánchez-Hidalgo, M. Aparicio-Soto, A. González-Benjumea, J. G. Fernández-Bolaños and C. Alarcón-de-la-Lastra, *J. Funct. Foods,* 2019, **58**, 95-104 (DOI:10.1016/j.jff.2019.04.033).

42 L. Serpe, R. Canaparo, M. Daperno, R. Sostegni, G. Martinasso, E. Muntoni, L. Ippolito, N. Vivenza, A. Pera, M. Eandi, M. R. Gasco and G. P. Zara, *Eur. J. Pharm. Sci.,* 2010, **39**, 428-436 (DOI: 10.1016/j.ejps.2010.01.013).

43 S. Wirtz and M. F. Neurath, *Adv. Drug Deliv. Rev.,* 2007, **59**, 1073-1083 (DOI: 10.1016/j.addr.2007.07.003).

44 R. Holma, P. Salmenperä, A. Riutta, I. Virtanen, R. Korpela and H. Vapaatalo, *Eur. J. Pharmacol.,* 2001, **429**, 309-318 (DOI: 10.1016/S0014-2999(01)01330-9).

45 J. L. Mendoza and M. T. Abreu, *Gastroenterol. Clin. Biol.,* 2009, **33 Suppl 3**, S158-173.

46 Y. Yan, V. Kolachala, G. Dalmasso, H. Nguyen, H. Laroui, S. V. Sitaraman and D. Merlin, *PLoS ONE,* 2009, **4** (DOI:10.1371/journal.pone.0006073).

47 K. A. Kuhn, N. A. Manieri, T. -. Liu and T. S. Stappenbeck, *PLoS ONE,* 2014, **9** (DOI:10.1371/journal.pone.0114195).

48 I. Kosmidou, T. Vassilakopoulos, A. Xagorari, S. Zakynthinos, A. Papapetropoulos and C. Roussos, *Am. J. Resp. Cell Mol. Biol.,* 2002, **26**, 587-593 (DOI:10.1165/ajrcmb.26.5.4598).

SUPPLEMENTARY MATERIAL

Materials

Chemicals

Precirol® ATO 5 (Glycerol distearate) was a kind gift from Gattefosé (France). Polysorbate 80 (Tween® 80) was purchased from Panreac Química (Castellar del Vallès, Barcelona, Spain). Organic extra virgin olive oil was donated by Biosasun S.A. (Álava, Spain). D-trehalose anhydrous was purchased from ACROS Organics™ (Geel, Belgium). Oleuropein (purity 80.12%) was kindly donated by Nonaherbs Bio (Tech) (China). Poloxamer 188, potassium dihydrogen phosphate (KH_2PO_4) and ortophosphoric acid (H_3PO_4) were purchased from Merck (Darmstadt, Germany). O-dianisidine hydrochloride, HTAB (hexadecyltrimethylammonium bromide), hydrogen peroxide (30%), sodium dodecyl sulphate (SDS) and polysorbate 20 (Tween 20) were purchased from Sigma-Aldrich (St. Louis, MO, USA). Dextran sodium sulfate (DSS) was purchased from TdB Consultancy (Uppsala, SE). Complete protease inhibitor cocktail tablets were purchased form Roche Diagnostics (Vilvoorde, BE). TRIS-base (purity ≥ 99.9%) was purchased from Carl Roth GmbH (Karlsruhe, Germany). Ultrapure water was obtained from a Milli-Q Water System. Other chemicals were all analytical grade.

Cell culture

J774 murine macrophages were kindly donated by Prof. M.P. Mingeot (UCLouvain, LDRI, BE). Roswell Park Memorial Institute (RPMI) 1640 medium, fetal bovine serum (FBS), penicillin-streptomycin (PEST), Dulbecco's phosphate buffered saline (DPBS) and trypsin-EDTA (0.05%) were purchased from Gibco™ (Invitrogen, UK). Lipopolysaccharide (LPS, *E. coli* O111:B4), 2,7-dichlorofluorescein diacetate (DCFH-DA), hydrogen peroxide (30%) and Cell Counting Kit-8 (CCK-8) were purchased from Sigma-Aldrich (St. Louis, MO, USA).

NLC characterization

Size and zeta potential measurements

The mean particle size (Z-average diameter) and polydispersity index (PDI) of the NLCs were measured by Dynamic Light Scattering (DLS). The zeta potential was determined through Laser Doppler micro-electrophoresis (Malvern® Zetasizer Nano ZS, Model Zen 3600; Malvern instruments Ltd., UK). Prior to the

measurements, nanoparticles were dispersed in Milli-Q water (pH 5.6) at optimal intensity. For the zeta potential measurement, the measured electrophoretic mobility was converted into zeta potential through Smoluchowski approximation. Each assay was performed in triplicate and data are presented as mean ± S.D.

Encapsulation efficiency

The encapsulation efficiency (EE) of oleuropein into NLCs was determined indirectly by measuring the free oleuropein (non-encapsulated oleuropein) in the supernatant obtained after the filtration/centrifugation quantified by a previously validated HPLC method. Considering the initial amount of oleuropein added to each formulation, the EE was calculated as:

$$EE\ (\%) = ((\text{Total amount of OLE} - \text{Amount of free OLE}) / (\text{Total amount of OLE})) \times 100$$

Microscopy analysis

NLC surface properties and morphology were examined under transmission electron microscopy (TEM, Philips JEOL JEM-1400 Plus a 120kV). For this purpose, lyophilized samples were suspended in Milli-Q water at an optimal concentration of 4 mg/ml and sonicated in a water bath for 1 minute. Then, samples were placed on a carbon grid and treated with negative staining uranyl acetate (2%) for particles visualization. Images were captured with a digital camera sCMOS (Hamamatsu, Hawthorne, CA, UK).

BIOSASUN

NanoBioCel